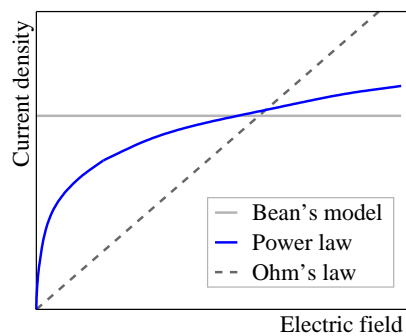





ON NUMERICAL METHODS FOR DIFFUSION OF ELECTRIC FIELDS IN TYPE-II SUPERCONDUCTORS

EDITA JANÍKOVÁ



Promoter: Marián Slodička

October 24, 2008

Ghent University
Faculty of Engineering
Department of Mathematical Analysis
Research Group for Numerical Functional Analysis
and Mathematical Modelling 

Thesis submitted to Ghent University
in candidature for the degree
of Doctor of Philosophy
in mathematics

“Nothing happens unless, first, a dream.”
Carl Sandburg

ACKNOWLEDGEMENTS

This thesis would not have been realized without the support and encouragement of the right people at the right time.

First of all my thanks belong to all professors and teachers that led me through the mysterious world of mathematics and thus enriched my life with many additional and amazing dimensions. Special thanks goes to my promotor Marián Slodička for the time he spent with this thesis and to Fedor Gömöry from the Slovak Academy of Sciences, who widely opened the door into the universe of scientists to me. I also would like to thank professors Jozef Kačur, Luc Dupré, Ján Malý and many others for patient discussions and helpful hints.

I cannot forget all my colleagues from the department of mathematical analysis, that made my research fun and my stay in Belgium enjoyable. I wish there was enough place in this book to thank everybody for everything I appreciated in these four long years. Thank you Viva, Cimo, Valdo and Jano! Thank you, Wouter, for accepting my *sauna-like* room temperature and answering all the questions the best you can. I would like to express great appreciations to Samuel, Hans and Wendy for their organization skills and helpful hand whenever necessary.

I'm glad that my research was sponsored by Ghent University (the BOF grant number 011D01304) as it offered me an amazing opportunity to broaden my horizons by making Belgium a part of my life and participation on number of international scientific events possible.

Many of my thanks belong to my family and especially to my parents for the care, love and support they provide me with anytime I need it. I'm happy to have Bianca for her blind love and many mischiefs that enhance my life.

Joško, thank you for your a bit less blind love but also much less gnawn sweaters. I can hardly express how much I'm grateful for everything you have done for me.

All my sportmates in Belgium deserve a big hug for welcoming me as an effective football player and leaving me in original state ;)

Last but not least, I want to thank all my friends back at home for staying in touch, despite the distance.

Edita Janíková

CONTENTS

Acknowledgements	iii
1 Introduction	1
1.1 Superconductivity	1
1.1.1 The two types of superconductivity	3
1.2 Macroscopic models of superconductivity	4
1.3 Problem formulation	5
1.3.1 Related problems	9
1.4 Overview of the thesis	10
2 Samenvatting (in Dutch)	13
3 Notation and function spaces	19
3.1 Notation and basic definitions	19
3.2 Function spaces for problems in electromagnetism	22
4 Whitney's edge elements	26
4.1 Informal overview	26
4.2 Galerkin method	29
4.3 Finite elements in general	30
4.4 Whitney's edge elements	31
4.5 Approximation properties	36

5	Time-discretization	38
5.1	Discretization scheme	40
5.2	Stability	42
5.3	Convergence	45
5.4	Convergence by the div-curl lemma	49
5.4.1	New steady-state div-curl lemma	49
5.4.2	New time-dependent div-curl lemma	51
5.4.3	Convergence	53
5.5	Error estimates	58
5.6	Numerical experiments	59
5.7	Conclusions	67
6	Fixed-point method	68
6.1	Iteration scheme in the Lipschitz continuous case	69
6.1.1	Basic inequalities	71
6.1.2	Error estimates and convergence	74
6.2	Iteration scheme in the non-Lipschitz continuous case	76
6.2.1	Stability	77
6.2.2	Error estimates and convergence	78
6.3	Numerical experiments	79
6.3.1	Lipschitz continuous case	79
6.3.2	Non-Lipschitz continuous case	82
6.4	Conclusions	84
7	Relaxation method	86
7.1	Existence and uniqueness	88
7.2	The properties of the Jacobian of the vector field \mathbf{J}	88
7.3	A priori estimates	89
7.4	Convergence	94
7.5	Choice of the linearization matrix	98
7.6	Conclusions	98
8	Full discretization	100
8.1	Full discretization in the Lipschitz continuous case	101
8.1.1	Computational scheme	101
8.1.2	Auxiliary problem	102
8.1.3	Convergence to the auxiliary problem	102
8.1.4	Error estimates and convergence	103
8.1.5	Numerical experiments	106

8.2	Full discretization in the non-Lipschitz continuous case	110
8.2.1	Computational scheme	110
8.2.2	Auxiliary problem	112
8.2.3	Convergence to the auxiliary problem	112
8.2.4	Error estimates and convergence	113
8.2.5	Numerical experiments	117
8.3	Conclusions	121
Appendix		122
A.	Basic algebraic inequalities	122
B.	Newton's method	123
List of Figures		124
List of Tables		126
Index		128
Bibliography		130

1 INTRODUCTION

This thesis is devoted to the study of the diffusion of the electric field in type-II superconductors in low-frequency electromagnetism. The necessity for accurate numerical methods in this research domain is increasing along with the growing number and importance of industrial applications of type-II superconductors. Due to the more and more complicated structures of superconducting devices, accurate macroscopic models and their rigorous mathematical analysis are needed.

The basic information on superconductors together with the development of a mathematical model follows in the next sections. At the end of this chapter, the overview of the thesis is given.

1.1 Superconductivity

Superconductors are materials having ability to conduct electric current with zero resistance under specific physical conditions. Each superconductor is characterized by at least three parameters: the *critical temperature* T_c , the *critical current* I_c and the *critical (magnetic) field* H_c . The resistivity of the superconductor is suddenly lost when it is cooled below T_c . Figure 1.1 shows how the resistivity depends on the temperature in a non-superconducting and in a superconducting metal. The superconductor exhibits zero resistivity only if the amplitude of the transport current stays below I_c and the external magnetic field does not exceed H_c .

How can one recognize a superconductor? Superconductivity was discovered by H. Kamerlingh Onnes in 1911 when he studied the resistivity of metals at low

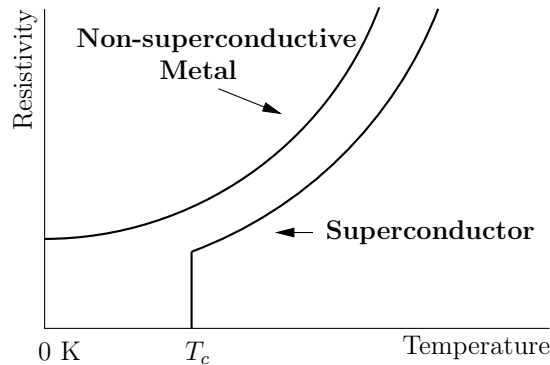


Figure 1.1: For a non-superconducting metal (such as copper or gold) the resistivity approaches a finite value at zero temperature. For a superconductor (such as lead or mercury) all signs of resistivity disappear suddenly below a certain temperature T_c .

temperatures. He noted that some materials entered a state of zero resistivity at a critical temperature [42]. One of the consequences of zero resistivity is the following experiment. Suppose initially a small sample of material held at temperature $T > T_c$ and placed in a zero external magnetic field. We first cool it down to a temperature below T_c while keeping the field zero. Later, we turn on the external field with magnitude less than the critical magnetic field H_c . The field inside the sample remains zero. The reason is, that Maxwell's equations (see e.g. page 5) combined with the zero electric field condition $\mathbf{E} = \mathbf{0}$ induce that the magnetic field remains constant in time at all points inside the superconductor ($\partial_t \mathbf{B} = \mathbf{0}$). Thus by applying the external field to the sample being already superconducting, the state with zero magnetic field everywhere inside the sample is conserved.

However nowadays, the fundamental proof that the superconductivity occurs in a given material is the expulsion of a weak external magnetic field also called the *Meissner–Ochsenfeld effect*. Consider the previous experiment but now process the steps in a different order. Still suppose the initial temperature of the sample above T_c and first turn on the external field. The magnetic field easily penetrates the sample. Now, the sample is cooled down below T_c . The magnetic field is expelled and the same state is obtained as if first cooling and then

applying the magnetic field would have been done. This fact cannot be deduced from zero resistivity hence this is a new and separate physical phenomenon associated with superconductors.

Another feature commonly studied in connection with superconductors is hysteresis—the persistent memory. From many extensive works within this field we refer to a short but handy introduction in the book by Mayergoyz [51] and to the thesis of Sjöström [60]. The latter also explains how the model used in this thesis exhibits hysteresis. Hence, the study of this complex phenomenon stays beyond the scope of our work.

1.1.1 The two types of superconductivity

Superconductors are usually divided into two groups: type-I and type-II superconductors. They behave similarly for very weak external magnetic field, but as the field becomes stronger it turns out, that either one of two possibilities can occur.

In the type-I superconductors (mainly pure metals), the field \mathbf{B} remains zero inside the material until suddenly, as the critical field H_c is reached, the superconductivity is destroyed.

In the type-II superconductors (mainly alloys), the presence of the mixed state during the transition from a normal to a superconducting state can be observed. The type-II superconductors have two different critical fields, denoted H_{c1} , the *lower critical field*, and H_{c2} the *upper critical field*. For small values of applied magnetic field \mathbf{H} the Meissner–Ochsenfeld effect leads to the zero magnetic flux density in the sample, i.e. $\mathbf{B} = \mathbf{0}$. But once the field exceeds H_{c1} , the magnetic flux starts to enter the superconductor and hence \mathbf{B} is non zero. Upon increasing the field further the magnetic flux density gradually increases, until finally at H_{c2} the superconductivity is destroyed.

The high-temperature superconductors form an appealing subgroup of type-II superconductors for their high critical temperature. However, the highest T_c attained at ambient pressure has been 138 K.

The mechanisms which cause superconductivity, are not the same for the two types of superconductors. Moreover the mechanism of the type-II superconductivity is still not completely understood. Our numerical study is based exclusively on this latter type. To learn more about superconductors we refer the reader to the catching work of Annett [3].

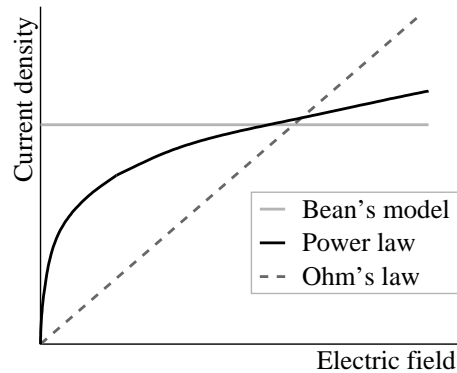


Figure 1.2: The current-voltage characteristic: for a non-superconducting metal defined by the Ohm's law, for a superconductor defined by Bean's critical-state model or the power law.

1.2 Several macroscopic models of superconductivity and contemporary results

The discovery of a family of high-temperature superconductors in 1986 [9] newly stimulated the interest in research of superconductivity as a new phenomenon not yet explained by the current theory. Furthermore, the superconducting state persisting up to temperatures higher than 90 K became economically more interesting and therefore more commercial applications became feasible. Since then the superconducting devices developed to more and more complicated structures. This has led to the study of macroscopic models of superconductivity. From several monographs dealing with the background of macroscopic models of superconductivity, we recommend the works of Chapman [16, 17]. To take a general view from mesoscopic to macroscopic models, we refer to [18].

Bean's critical-state model [8] was one of the first macroscopic models of superconductivity. Figure 1.2 shows how the current density in this model depends on the electric field. Motivated by the abrupt change from zero to a large resistance between the pinned and flux flow regimes, the model imposes that a current either flows at the critical level J_c or not at all. There are many papers written on this topic. Barnes et al. [5] suggested a numerical method solving the current and field distributions in 2D model of type-II super-

conductor effected by surrounding media. The model based on the variational inequality was studied for example by Bossavit [11] and Prigozhin [56]. Unfortunately, Bean's critical-state model is not fully applicable to superconductors with smooth current-voltage characteristics.

The power law constitutive relation $\mathbf{E} = E_c(\mathbf{J}/J_c)^n$ is another macroscopic model which is widely employed. It was first introduced by Rhyner [58] and is frequently used in engineering applications (for 2D problems see e.g. [13], for 3D cases refer to [31, 50]). This model was firstly derived with the intention to model the soft transition of the current density. Later it has been justified by arguments of flux creep [14]. In two dimensions and under specific assumptions the analytical solution can be found to the problem of distribution of the electric field in type-II superconductors [32]. One can also find a lot of articles focusing on the numerical analysis in this field (in 2D), but there are very few of them discussing the 3D cases. A common approach is to take advantage of the symmetries of the geometry in order to reduce the problem to two dimensions [13]. Few authors consider general 3D geometries. Yin et al. [73] studied the well-posedness of the 3D problem formulated in the unknown \mathbf{H} . Elliott et al. [25] formulated the problem also in terms of the magnetic field but as an evolutionary variational inequality. They defined a finite element approximation and proved its convergence. Discretizing the problem in the time variable yielded an unconstrained optimization problem. The problem was then discretized in space by using curl-conforming Whitney's elements on a tetrahedral mesh. The authors carried out a numerical analysis for both the extended Bean's model (see e.g. [11]) and the power law. Some authors formulate the eddy current problem in terms of electric field. Slodička [61] studied the nonlinear diffusion in type-II superconductors in 3D using the method of monotone operators. He proposed the discretization in time and proved its convergence.

1.3 Problem formulation

Suppose that the superconducting material occupies an open bounded domain $\Omega \subset \mathbb{R}^3$, with a Lipschitz continuous boundary Γ . The symbol $\boldsymbol{\nu}$ stands for the outward unit normal vector to Γ .

To derive a precise mathematical model of type-II superconductors, we use the eddy current version of Maxwell's equations

$$\begin{aligned} \nabla \times \mathbf{H} &= \mathbf{J}, & (\text{Ampère's law}) \\ \partial_t \mathbf{B} + \nabla \times \mathbf{E} &= \mathbf{0}, & (\text{Faraday's law}) \end{aligned} \quad (1.1)$$

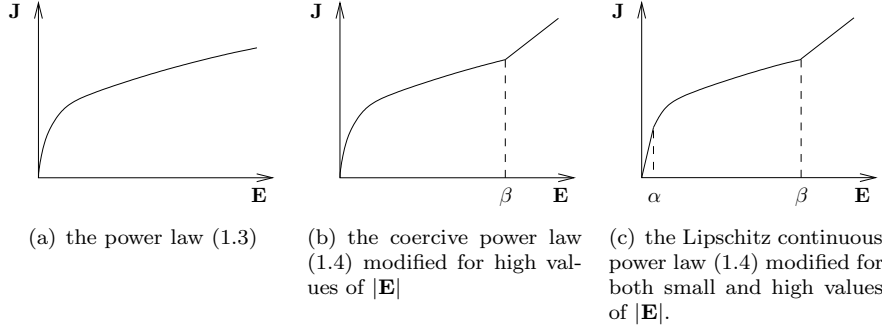


Figure 1.3: The sketch of the dependence of the current density \mathbf{J} on the electric field \mathbf{E} used in our model.

where \mathbf{H} is the magnetic field, \mathbf{J} the current density, \mathbf{B} the magnetic induction and \mathbf{E} the electric field.

The nonlinear resistive property of type-II superconductors will be based on the power law, usually written in the following form

$$\mathbf{E} = E_c \left(\frac{|\mathbf{J}|}{J_c} \right)^{n-1} \frac{\mathbf{J}}{J_c}, \quad (1.2)$$

where the parameters J_c and n are identified from the direct current measurements (for AC measurements see e.g. [71]). The conventional criterion of $E_c = 1\mu\text{V}/\text{cm}$ should be employed. The parameter n is the measure of sharpness of the resistive transition. If $n = 1$, the relation (1.2) leads to the linear Ohm's law. If $n \rightarrow \infty$, the solution to the power law formulation converges to the solution to Bean's critical-state formulation (for the proof in 2D see [6], in 3D refer to [73]). The power n usually varies between 7 and 1000 depending on the superconducting material. Further, we suppose that E_c and J_c are constant and thus, for the sake of simplicity of mathematical analysis, they will be omitted.

As we will use the formulation in terms of electric field, the power law has to be inverted. Thus

$$\mathbf{J} = \mathbf{J}(\mathbf{E}) = |\mathbf{E}|^{-1/p} \mathbf{E}. \quad (1.3)$$

The parameter $p \in (1; 1.2)$ as $p = \frac{n}{n-1}$.

The power law works very well for currents up to the critical current density, J_c , which is not the case for all applications. When the norm of the applied current density \mathbf{J}_{tot} is considerably higher than J_c , the power law is no longer convenient due to the unbounded exponential increase of the electric field. Duron et al. [24] suggested an artificial formula to solve this problem but we decided to cut-off and linearly extend the power law, as shown on Figure 1.3b. We obtain the following relation

$$\mathbf{J}(\mathbf{E}) = \begin{cases} |\mathbf{E}|^{-1/p} \mathbf{E}, & 0 \leq |\mathbf{E}| \leq \beta, \\ \beta^{-1/p} \mathbf{E}, & \beta < |\mathbf{E}|. \end{cases} \quad (1.4)$$

The parameter β is fixed such that $\beta^{1-1/p} > J_c$.

It is in fact rather difficult to predict what is happening in the superconductor when the electric current is very small. Therefore it is from the mathematical point of view very convenient to work with the following modification of the power law

$$\mathbf{J}(\mathbf{E}) = \begin{cases} \alpha^{-1/p} \mathbf{E}, & 0 \leq |\mathbf{E}| < \alpha, \\ |\mathbf{E}|^{-1/p} \mathbf{E}, & \alpha \leq |\mathbf{E}| \leq \beta, \\ \beta^{-1/p} \mathbf{E}, & \beta < |\mathbf{E}|, \end{cases} \quad (1.5)$$

where $\alpha, \beta > 0$ are fixed parameters. Later, in Chapter 6, Lemma 6.5, we will prove, that the previously defined vector field \mathbf{J} is Lipschitz continuous, i.e. there exists a positive constant δ such that the relation

$$|\mathbf{J}(\mathbf{s}) - \mathbf{J}(\mathbf{t})| \leq \delta |\mathbf{s} - \mathbf{t}|$$

is valid for all $\mathbf{s}, \mathbf{t} \in \mathbb{R}^3$. Therefore, we refer to this instance as to the Lipschitz continuous case.¹ This model is from mathematical point of view very simple - as it is not degenerate near $\mathbf{E} = \mathbf{0}$.

It is, however, interesting to study all three cases, i.e. the model based on any of three presented modifications of the power law (1.3)–(1.5). They differ considerably not only in mathematical methods that can be employed, but also in computational costs. Hence, depending on a particular problem setting and requirements, the appropriate model can be chosen.

Type-II superconductors are characterized by two critical field values - H_{c1} and H_{c2} . The first critical field value H_{c1} at which magnetic flux starts penetrating the superconducting sample is extremely low. For $H > H_{c1}$, which is

¹Analogously, when the constitutive relation (1.4) is used, we will speak about the non-Lipschitz continuous case.

the case for most practical applications,

$$\mathbf{B} = \mu_0 \mathbf{H} \quad (1.6)$$

is a good approximation of the \mathbf{B} – \mathbf{H} relation. The combination of (1.3) and (1.6) with Maxwell's equations constitutes a tool to compute the electromagnetic behaviour of a superconductor of arbitrary shape with arbitrary applied magnetic field and arbitrary transport current [60]. Therefore we employ (1.6) as a second constitutive equation in our models. As μ_0 is a constant, we will neglect it in our further study.

Combining previous relations, we finally obtain the following evolutionary nonlinear and degenerate partial differential equation (PDE)

$$\partial_t(\mathbf{J}(\mathbf{E})) + \nabla \times \nabla \times \mathbf{E} = \mathbf{0} \quad \text{in } \Omega \times [0, T], \quad (1.7)$$

along with the boundary conditions

$$\nabla \times \mathbf{E} \times \boldsymbol{\nu} = \mathbf{G}_1 \quad \text{on } \Gamma \times [0, T] \quad (1.8)$$

or

$$\mathbf{E} \times \boldsymbol{\nu} = \mathbf{G}_2 \quad \text{on } \Gamma \times [0, T] \quad (1.9)$$

and the initial condition

$$\mathbf{E}(0) = \mathbf{E}_0 \quad \text{in } \Omega. \quad (1.10)$$

The boundary condition (1.8) describes the temporal variations of external magnetic field. The usual boundary condition to express the external variations of magnetic field is

$$\boldsymbol{\nu} \times \mathbf{H} = \boldsymbol{\nu} \times \mathbf{h}_{ext} \quad \text{on } \Gamma. \quad (1.11)$$

From (1.6) and Faraday's law we have that

$$\boldsymbol{\nu} \times \mu_0 \partial_t \mathbf{H} = \nabla \times \mathbf{E} \times \boldsymbol{\nu}. \quad (1.12)$$

Thus the boundary conditions (1.11) and (1.8) are related by (1.12).

Further, the vector fields \mathbf{G}_1 and \mathbf{G}_2 will be taken uniformly equal to zero in order to simplify the analysis of the problem. Thus one of the following homogeneous boundary conditions is considered

$$\nabla \times \mathbf{E} \times \boldsymbol{\nu} = \mathbf{0} \quad \text{on } \Gamma \times [0, T] \quad (1.13)$$

or

$$\mathbf{E} \times \boldsymbol{\nu} = \mathbf{0} \quad \text{on } \Gamma \times [0, T]. \quad (1.14)$$

The mathematical proofs would otherwise become a little more cumbersome than necessary. If the boundary value \mathbf{G}_1 is smooth enough, in the sense that there exists \mathbf{E} such that $\nabla \times \mathbf{E} \times \boldsymbol{\nu} = \mathbf{G}_1$ and \mathbf{G}_1 can be extended to the whole domain Ω , the problem can be “shifted” (analogously for \mathbf{G}_2). It will be, however, a nice task to find out, precisely how regular \mathbf{G}_1 or \mathbf{G}_2 must be, in order to be able to get appropriate results. This problem is closely coupled to the problem of the trace regularity in the considered function spaces.

Due to the nonlinear nature of (1.7) a special numerical approach is needed.

The variational formulation of the problem setting (1.7), (1.10), (1.13) or (1.7), (1.10), (1.14) reads as follows: Find \mathbf{E} such that for almost every $t \in (0, T)$ holds that $\mathbf{E}(t) \in \mathbf{M}$ and

$$\begin{aligned} \langle \partial_t \mathbf{J}(\mathbf{E}), \boldsymbol{\varphi} \rangle + (\nabla \times \mathbf{E}, \nabla \times \boldsymbol{\varphi}) &= 0 \quad \forall \boldsymbol{\varphi} \in \mathbf{M}, \\ \mathbf{E}(0) &= \mathbf{E}_0. \end{aligned} \quad (1.15)$$

Here \mathbf{M} denotes an appropriate space of functions. Its precise form depends on the definition of the nonlinear function \mathbf{J} and on the choice of the boundary condition. The space \mathbf{M} will be specified for each problem separately. More details on the properties of used function spaces can be found in Chapter 3.

The goal of this thesis is to design a numerical scheme for solving (1.15).

1.3.1 Related problems

Considering mathematical methods, the problems of the diffusion of electric field are close to the nonlinear problems in porous media. The former involves the curl-operator, the latter the gradient. From many articles in this field, the articles of Jäger and Kačur [34–36], Kačur [44–46], Kačur and Luckhaus [47], and Slodička [62, 63] served as a helpful source of ideas and mathematical tools during my research.

If one considers the permanent magnets or other ferromagnetic materials with linear electric behaviour (\mathbf{E} – \mathbf{J} relation) but nonlinear magnetic response (\mathbf{B} – \mathbf{H} relation), the following nonlinear PDE arises

$$\mathbf{A} + \nabla \times \mathbf{M}(\nabla \times \mathbf{A}) = \mathbf{F},$$

where \mathbf{A} denotes the magnetic vector potential and \mathbf{M} is the reluctivity of the magnetic material [10]. On the other hand, the formulation in the magnetic field \mathbf{H} can lead to the linear PDE with nonlinear boundary condition [33]. From mathematical point of view, similar problems arise in these models and therefore similar methods of solving are required. I have learned some useful techniques

from the article of Heise [33], where the complete mathematical analysis of a 2D nonlinear problem involving ferromagnetic medium is given together with error estimates of employed finite element method. In this field authors also prefer to employ geometrical symmetries in order to obtain a two dimensional model despite the suitability of the results for general geometries. The related form of the nonlinearities considered should allow smooth conversion of the general 3D results presented in this thesis to the mentioned models.

1.4 Overview of the thesis

This thesis is devoted to the study of a nonlinear degenerate transient eddy current problem involving superconducting materials of the second type. Most of the results were already published in international journals.

Previously, the mathematical model has been derived employing the power law constitutive relation between electric field and current density. In the thesis three different versions of the problem (1.15) are studied: the easiest problem involving only the Lipschitz continuous nonlinearity (1.5), the non-Lipschitz but coercive model based on the modified power law (1.4) and the most complex problem where the degenerate² power law (1.3) is used to define the vector field \mathbf{J} . Different stages of the analysis were therefore worked out for different versions of the \mathbf{E} - \mathbf{J} constitutive relation. The eddy current problem with unmodified power law (1.3) is studied only in Chapter 5. The modifications (1.4) and (1.5) are considered in zigzag along the thesis. A comprehensive outline of this evolution can be seen on Figure 1.4. In addition, the notes in *cursive* are stated at the beginning of each chapter or section in order to emphasize, which modification of power law is considered in the forthcoming part of the text.

Due to the degeneracy of the problem based on the power law (1.3), special function spaces have to be introduced. Their properties are studied in Chapter 3. Basic information on the finite element method suitable for discretization of Maxwell's equations is given in Chapter 4. An informal overview is followed by general definitions and properties of Whitney's edge elements. The most important approximation properties of Whitney's finite elements are stated at the end of the chapter.

In Chapter 5, we extend the results of Slodička [61]. We study convergence of the backward Euler method applied to the problem (1.15) under assumption that the nonlinear term is defined by the relation (1.3). We deduce that the

²By degenerate, we mean the unbounded derivative and lack of the coercivity of the vector field \mathbf{J} .

method converges. We carry out the error estimates (Theorem 5.12) and present the numerical experiments. Our results are compared with the results obtained by the backward Euler method employed to the model formulated by the means of the magnetic field in place of the electric one (**H**-formulation, see Section 5.6). Our results seem to be more computationally demanding and less accurate but more stable and thus more reliable. These results have been published in [66].

Chapter 6 is devoted to the steady-state problem. Once we have proposed the discretization in time in Chapter 5, the problem (1.7)–(1.10) can be transformed to the time-independent problem. We propose a linear iteration scheme to solve this 3D stationary problem of the electromagnetic diffusion. Convergence of the method, error estimates and numerical examples are carried out. The method is stable and efficient. It is based on the fixed-point principle, which constrains its speed. These results have been published in [37] and [38].

The convergence of the relaxation method inspired by the articles of Kačur [44, 46] is studied in Chapter 7. Some new theoretical results are presented as preliminaries to the future work in this field. These results will be presented on the international conference ICNAAM 2008.

In the last chapter, we propose two fully discrete methods to solve the problem (1.7)–(1.10) equipped with the constitutive relations (1.4) and (1.5) respectively. We show the well-posedness of the problem, prove the existence of a weak solution for each time step as well as its stability. The convergence of the methods is proven on basis of the error estimates (Theorems 8.2 and 8.8). These results have been presented on the international conference ACOMEN 2008 [39].

Numerical examples

The numerical examples in the thesis are rather academical in order to check the performance of the methods and verify the theoretical results. For more practical oriented calculations more stable and robust numerical software has to be developed. This was not the aim of my research. The computations are based on the software ALBERT, the ancestor of ALBERTA [59]. The Whitney elements for the approximation of electric field were implemented by Bañas and Cimrák [7, 21].

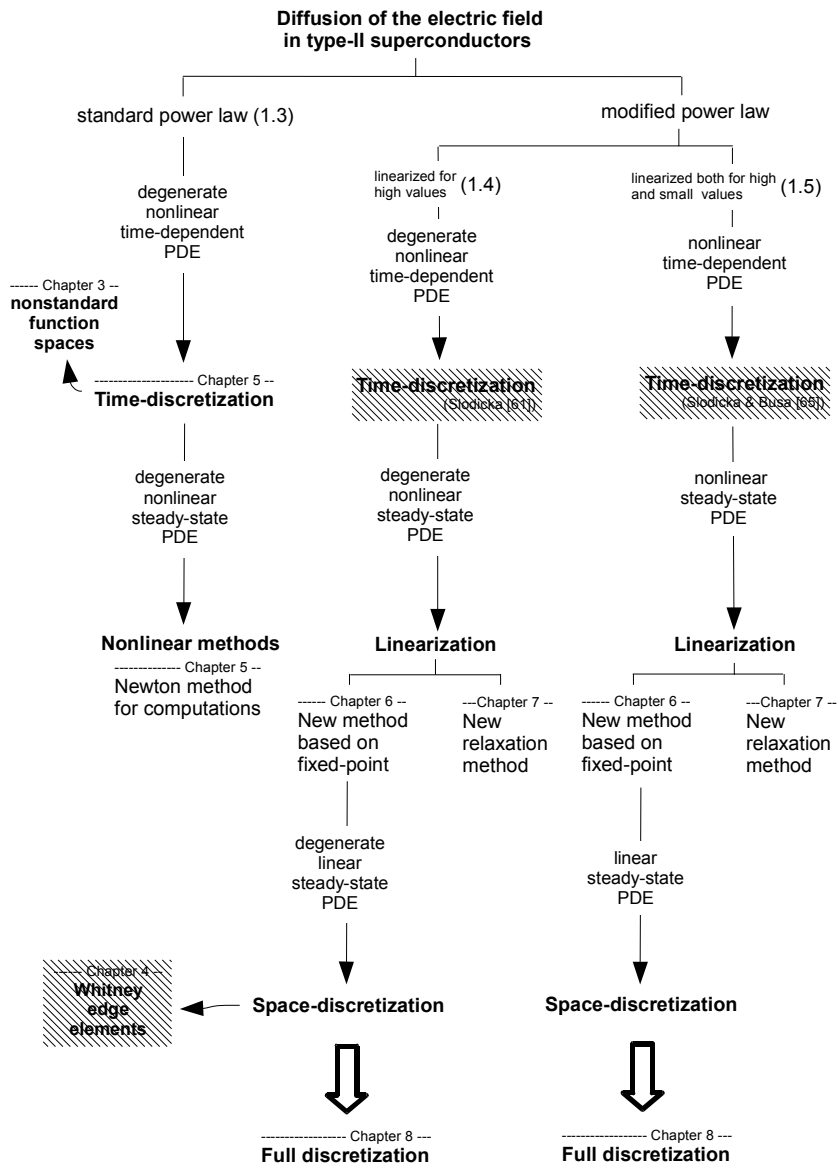


Figure 1.4: Overview of results. Hatched areas represent the work of other authors.

2 SAMENVATTING

De doctoraatsthesis handelt over diffusieverschijnselen voor de elektrische veldsterkte in type II supergeleiders. Dit is een specifiek ‘eddy current’-probleem in elektromagnetisme. De noodzaak voor nauwkeurige numerieke methoden in dit onderzoeksdomein neemt toe omwille van het groeiend aantal industriële toepassingen die van type II supergeleiders gebruik maken.

Inleiding

Supergeleiders zijn materialen die onder specifieke fysische voorwaarden elektrische stroom weerstandsloos geleiden. Elke supergeleider wordt gekarakteriseerd door ten minste drie parameters: de *kritische temperatuur* T_c , de *kritische elektrische stroom* I_c en het *kritisch (magnetisch) veld* H_c . De supergeleiding gaat verloren wanneer de temperatuur hoger wordt dan de kritische temperatuur T_c . Fig. 1.1 toont de temperatuursafhankelijkheid van de weerstand van een supergeleider. De weerstand van de supergeleider is verwaarloosbaar klein wanneer de elektrische stroom door de geleider kleiner blijft dan de kritische waarde I_c en het extern magnetisch veld de waarde H_c niet overschrijdt.

Supergeleiders worden onderverdeeld in twee klassen: type I en type II supergeleiders. Beide klassen gedragen zich heel gelijkaardig bij kleine externe magnetische velden, maar bij de type II supergeleiders is er een uitgesproken overgangsfase tussen normale geleiding en supergeleiding. De numerieke studie van dit doctoraatswerk is uitsluitend gebaseerd op type II supergeleiders.

Modellering

Als gevolg van de steeds toenemende complexiteit van elektromagnetische systemen die gebruik maken van supergeleiding, is er een nood aan nauwkeurige macroscopische modellen en een strenge wiskundige analyse ervan. De relatie tussen het elektrisch veld \mathbf{E} en de stroomdichtheid \mathbf{J} wordt gewoonlijk beschreven via de constitutieve wet $\mathbf{E} = E_c(\mathbf{J}/J_c)^n$. Deze wet werd voor het eerst voorgesteld door Rhyner in [58]. In een tweedimensionale ruimte en onder specifieke voorwaarden, kan het elektrisch veld in type II supergeleiders analytisch neergeschreven worden, zie [32]. Bovendien is er in de literatuur reeds uitvoerig aandacht besteed aan een 2D numerieke analyse van de verdeling van de elektrische veldsterkte in supergeleiders. Een 3D numerieke analyse is in veel beperktere mate beschreven. In dit doctoraatswerk hebben we dan ook specifiek aandacht voor de numerieke analyse van een 3D model.

Voor het bekomen van een nauwkeurig wiskundig model voor type II supergeleiders gebruiken we de ‘eddy current’-formulering van de Maxwell vergelijkingen (1.1), met \mathbf{H} de magnetische veldsterkte, \mathbf{J} de elektrische stroomdichtheid, \mathbf{B} de magnetische inductie en \mathbf{E} de elektrische veldsterkte.

In de thesis bestuderen we drie verschillende versies van probleem (1.15). Mathematisch is het meest ingewikkelde model gebaseerd op de machtswet (1.3), die goed werkt in het geval de stroomdichtheid kleiner is dan de kritische stroomdichtheid J_c . De afgeleide van het vectorveld \mathbf{J} , gedefinieerd door (1.3), wordt oneindig in $\mathbf{E} = \mathbf{0}$ en is bijgevolg een uitdaging voor numerieke analyse. Bovendien is het gebruik van de machtswet moeilijker door de exponentiële toename van de elektrische veldsterkte wanneer de grootte van de stroomdichtheid \mathbf{J}_{tot} aanzienlijk groter wordt dan J_c . We besloten daarom de machtswet (1.3) enkel te gebruiken bij voldoende lage waarden van de stroomdichtheid en dit te combineren met een lineaire extrapolatie voor hoge stroomdichtheden, zoals getoond in Figuur 1.3b. De gewijzigde machtswet (1.4) vormt de basis van een tweede model in deze thesis. Het vectorveld \mathbf{J} gedefinieerd door (1.4) heeft nog steeds een oneindige afgeleide in $\mathbf{E} = \mathbf{0}$, maar het is coërcief wat ons toelaat te werken in gekende functieruimten.

Gezien de complexiteit van de berekeningen van diffusieverschijnselen in een supergeleider, bij kleine elektrische stroomdichtheden, is het vanuit wiskundig oogpunt interessant een gewijzigde machtswet te beschouwen, namelijk (1.5). In Hoofdstuk 6, Lemma 6.5, bewijzen we dat het vectorveld \mathbf{J} gedefinieerd door (1.5) Lipschitz continu is. Daarom is dit model, wat wiskundige analyse betreft, het eenvoudigste.

Toch is het interessant de drie gevallen, d.w.z. het model gebaseerd op elk

van de drie voorgestelde wijzigingen aan de machtswet, te bestuderen. Deze verschillen sterk en dat niet alleen naar de bruikbare wiskundige methodes, maar ook naar rekenkost. Afhankelijk van de specifieke probleemstelling en vereisten kan dus een geschikt model gekozen worden. Het ‘eddy current’-probleem met ongewijzigde machtswet (1.3) bestuderen we enkel in Hoofdstuk 5. De aanpassingen (1.4) en (1.5) komen afwisselend voor in de thesis. Figuur 1.4 geeft een overzicht van deze evolutie.

Als tweede constitutieve wet in onze modellen, gebruiken we een lineaire relatie (1.6) tussen de magnetische veldsterkte \mathbf{H} en de magnetische inductie \mathbf{B} .

Wanneer we alle voorgaande relaties combineren, komen we uiteindelijk tot volgende niet-lineaire partiële differentiaalvergelijking:

$$\partial_t(\mathbf{J}(\mathbf{E})) + \nabla \times \nabla \times \mathbf{E} = \mathbf{0} \quad \text{in } \Omega \times [0, T], \quad (2.1)$$

samen met één van de volgende randvoorwaarden

$$\nabla \times \mathbf{E} \times \boldsymbol{\nu} = \mathbf{G}_1 \quad \text{op } \Gamma \times [0, T] \quad (2.2)$$

of

$$\mathbf{E} \times \boldsymbol{\nu} = \mathbf{G}_2 \quad \text{op } \Gamma \times [0, T] \quad (2.3)$$

en de beginvoorwaarde

$$\mathbf{E}(0) = \mathbf{E}_0. \quad (2.4)$$

Kortom, we behandelen hier een niet-lineaire tijdsafhankelijke partiële differentiaalvergelijking met lineaire randvoorwaarden.

De basisprincipes van supergeleiding, samen met een meer gedetailleerde beschrijving van het wiskundig model worden gegeven in Hoofdstuk 1.

Vorbereidingen

Omwille van de afwezigheid van ellipticiteit van (2.1) bij gebruik van de machtswet (1.3), zijn aangepaste numerieke benaderingen nodig en dienen niet-standaard functieruimten ingevoerd te worden. Hun eigenschappen worden bestudeerd in Hoofdstuk 3. In dit hoofdstuk voeren we notaties in en bewijzen we enkele eigenschappen van de nieuwe functieruimten, zoals bijvoorbeeld hun wederkerigheid (Lemma 3.2, Opmerking 3.3).

Op Hoofdstuk 4 na behandelt deze thesis enkel onze eigen resultaten. Hoofdstuk 4 is een overzicht van reeds bestaande theorieën. Dit hoofdstuk behandelt de definitie en eigenschappen van zogenaamde Whitney elementen. Deze standaard eindige elementen zijn één van de eenvoudigste eindige elementen

die kunnen gebruikt worden voor discretisatie van de Maxwell vergelijkingen. De belangrijkste benaderingseigenschappen van Whitney eindige elementen zijn vermeld op het einde van het hoofdstuk. Dit hoofdstuk is geschreven als korte en eenvoudige introductie voor hen die starten in dit onderzoeksdomein.

Eens de functieruimten gedefinieerd zijn en de theorie van discretisatie beschreven is, kunnen we overstappen op numerieke schema's. Het niet-lineaire tijdsafhankelijk probleem (2.1)-(2.4) dient gelineariseerd te worden en gediscrètiseerd in ruimte en tijd.

Tijdsdiscretisatie

De achterwaartse Euler methode is een standaard numerieke methode voor discretisatie in de tijd. Slodička [61] heeft de convergentie van de methode voor het probleem (2.1)-(2.4) aangetoond wanneer de constitutieve wet (1.4) wordt gebruikt. In Hoofdstuk 5 bestuderen we de convergentie van de achterwaartse Euler methode voor het 'eddy current'-probleem (2.1)-(2.4) in combinatie met de ongewijzigde machtsfunctie (1.3). Hierbij wordt de ruimte van de testfuncties \mathbf{V}_0 gedefinieerd zoals in Hoofdstuk 3 en is de wederkerigheid cruciaal in de verdere analyse. Dit hoofdstuk is gebaseerd op het artikel [66] en de presentatie op de conferentie NumAn 2008 [40]. Eerst beschrijven we de tijdsdiscretisatie en tonen de consistentie aan. Dan leiden we foutenschattingen af en tonen de convergentie van de achterwaartse Euler methode aan. In deel 5.4 bewijzen we opnieuw de convergentie door gebruik te maken van het Murat en Tartar's div-curl lemma. De nieuwe versie van dit krachtig lemma is beschreven en bewezen in Lemmata 5.8 en 5.9. De foutenschattingen zijn afgeleid in Deel 5.5. Tenslotte zijn de numerieke experimenten beschreven. We vergelijken de numerieke resultaten met deze van de achterwaartse Euler methode die gebruikt werd voor de beschrijving van de diffusie van het magnetisch veld in type II supergeleiders (deel 5.6). Onze methode blijkt meer rekenintensief en minder nauwkeurig, maar is stabiel en dus meer betrouwbaar.

'Fixed-point' methode

Hoofdstuk 6 handelt over het stationaire probleem. Na tijdsdiscretisatie herleidt de tijdsafhankelijke niet-lineaire partiële differentiaalvergelijking (2.1) zich tot het niet-lineair probleem van de vorm:

$$\mathbf{J}(\mathbf{E}) + \nabla \times \nabla \times \mathbf{E} = \mathbf{F}. \quad (2.5)$$

Aangezien de vergelijking (2.5) niet-lineair is, is de volgende stap linearisatie.

In [37] en [38] hebben we voor het probleem (2.5) een nieuw linearisatieschema, gebaseerd op de fixed-point methode, voorgesteld. In [37] hebben we gewerkt met een eenvoudige variant van de machtswet: we hebben namelijk \mathbf{J} gedefinieerd door (6.2). In [38] beschouwden we een veralgemening van deze eenvoudige formulering. Hoofdstuk 6 is gebaseerd op het artikel [38]. Vooreerst ontwikkelen en analyseren we een nieuw linearisatieschema voor het model gebaseerd op de Lipschitz continue niet-lineariteit \mathbf{J} (1.5). Daarna bestuderen we het linearisatieschema voor het niet-Lipschitz continu geval.

De ‘cutt-off’ van \mathbf{J} voor grote waarden van de elektrische veldsterkte vormt een cruciale stap bij het bewijzen van de convergentie van het voorgestelde linearisatieschema. Aangezien beide methoden gebaseerd zijn op het fixed-point principe, kan men verwachten dat deze traag zijn. Nochtans, een zorgvuldige combinatie van de schema’s leidt tot een robuuste en efficiënte numerieke methode om het probleem (2.5) op te lossen.

De figuren bij de numerieke experimenten hebben alle hetzelfde karakter. Aanvankelijk dalen ze snel, om vervolgens relatief constant te blijven. Dit is een gevolg van het feit dat met toenemend aantal iteraties de initieel dominante linearisatiefout geleidelijk aan ondergeschikt wordt aan de discretisatiefout. Aangezien de nauwkeurigheid van de linearisatieschema’s ongeveer gelijk is aan de discretisatiefout, kan het verbeterd worden door de keuze van een dichter rooster. Toename van de rekentijd en geheugengebruik dienen echter in rekening gebracht te worden.

Relaxatiemethode

In Hoofdstuk 7 werden we geïnspireerd door de relaxatiemethoden ingevoerd door Kačur in [44] en [46]. De niet-lineariteit en de tijdsafgeleide in de partiële differentiaalvergelijking (2.1) worden benaderd door een matrix die weinig verschilt van de Jacobi matrix van het vectorveld \mathbf{J} . Een aantal nieuwe theoretische resultaten worden voorgesteld als aanzet tot verder onderzoek in dit veld.

Volledige discretisatie

In het laatste hoofdstuk combineren we voorgaande deelresultaten in een complete aanpak, waarbij discretisatie in tijd en ruimte, alsook linearisatie aan bod komen. Met andere woorden, we stellen een volledig discrete lineaire numerieke methode voor om het probleem (2.1)-(2.4) op te lossen. We tonen de consistentie van het probleem aan, bewijzen het bestaan van een oplossing voor elke tijdstap en tonen eveneens de stabiliteit aan. De convergentie van de methode

wordt bewezen. In het laatste deel leiden we de foutenschatting af (Theorema 5.12). In de bewijzen worden de monotoniteitseigenschappen samen met het Minty-Browder argument gebruikt.

De achterwaartse Euler methode is gebruikt voor de tijdsdiscretisatie. Voor de linearisatie en ruimtediscretisatie ontwikkelen we een lineair numeriek schema gebaseerd op de ‘fixed point’ methode en Whitney elementen. We leiden foutenschattingen af die de convergentie van het voorgestelde volledig discreet, lineair numeriek schema garanderen en leggen het verband tussen de fout en de keuze van de discretisatieparameters.

Hoofdstuk 8 bestaat uit twee delen. In het eerste deel bestuderen we het probleem (2.1)-(2.4) met de constitutieve wet (1.5). In het tweede deel wordt het probleem (1.15) samen met de constitutieve wet (1.4) geanalyseerd. In beide delen stellen we een lineair numeriek schema voor en tonen we aan dat het schema goed gedefinieerd is. Dan leiden we foutenschattingen af, waarmee de convergentie bewezen wordt. De efficiëntie van de methode en de werkelijke convergentiesnelheid worden geïllustreerd aan de hand van numerieke voorbeelden op het eind van elk deel. Enkele resultaten van dit hoofdstuk werden voorgesteld op de conferentie ACOMEN 2008 [39]. De convergentie van de benaderingsschema's lijken zelfs sneller te zijn dan theoretisch voorspeld. De numerieke experimenten kunnen echter beïnvloed worden door de keuze van de exacte oplossing. Daarom dienen meer uitgebreide numerieke experimenten uitgewerkt te worden, vooraleer men de foutenschattingen tracht te verbeteren. Aangezien de methode gebaseerd is op het ‘fixed-point’ principe, is de methode niet snel. Verschillende honderden interne iteraties dienen uitgevoerd te worden vooraleer het stopcriterium voldaan is. Het ‘fixed-point’ principe garandeert echter robustheid en stabiliteit van de methode.

Berekeningen

De numerieke voorbeelden om de performantie van de methoden en de theoretische resultaten te verifiëren zijn eerder academisch. Voor meer praktisch gerichte berekeningen dient een robuuste softwarecode ontwikkeld te worden. Dit was niet het doel van het doctoraatsonderzoek. De gebruikte computercode is gebaseerd op ALBERT, de voorganger van ALBERTA [59]. De Whitney elementen voor de benadering van de elektrische veldsterkte werd geïmplementeerd door Bañas en Cimrak [7, 21].

3 NOTATION AND FUNCTION SPACES

This chapter is devoted to the notation, definitions of basic function spaces as well as to the definitions and properties of advanced function spaces essential for the later study.

3.1 Notation and basic definitions

Throughout the thesis, the domain $\Omega \subset \mathbb{R}^3$ is a bounded domain with Lipschitz continuous boundary Γ , if not specified otherwise. The vector $\boldsymbol{\tau}$ denotes a unit tangent vector to the boundary Γ and $\boldsymbol{\nu}$ stands for a unit normal vector to the boundary.

The symbol $\delta_{i,j}$ denotes Kronecker's delta,

$$\delta_{i,j} = \begin{cases} 1, & i = j, \\ 0, & i \neq j. \end{cases}$$

The space of continuous functions on Ω will be denoted by $C(\Omega)$ and the space of k -times continuously differentiable functions on Ω by $C^k(\Omega)$. By $C_0^k(\Omega)$ we mean the set of functions belonging to $C^k(\Omega)$ with compact support in Ω . We use $C^k(\overline{\Omega})$ to denote the set of functions in $C^k(\Omega)$ having bounded and uniformly continuous derivatives up to order k in $\overline{\Omega}$.

Let X be a normed space. The set of all continuous linear functionals defined on X is a normed Banach space denoted by X^* and called a *dual space* to X . The norm in the dual space is defined as follows

$$\|f\|_{X^*} = \sup_{x \in X} \frac{|f(x)|}{\|x\|_X}. \quad (3.1)$$

The standard notation as well as the explanation of some symbols and definitions related to function spaces can be found in [49].

We will focus on the vector fields, that is vector functions of a vector variable in \mathbb{R}^3 . For vectors and spaces of vector functions **bold** letters will be used.

The space of distributions denoted by $\mathbf{C}_0^\infty(\Omega)^*$ is the dual space of $\mathbf{C}_0^\infty(\Omega)$ in the sense that a linear functional $T : \mathbf{C}_0^\infty(\Omega) \rightarrow \mathbb{C}$ is contained in $\mathbf{C}_0^\infty(\Omega)^*$ if for every compact set $K \subset \Omega$ there exist constants C and k such that

$$|T(\varphi)| \leq C \sum_{|\alpha| \leq k} \sup_K |D^\alpha \varphi| \quad \text{for all } \varphi \in \mathbf{C}_0^\infty(\Omega).$$

The Lebesgue space $\mathbf{L}_m(\Omega)$ ($m \geq 1$) is understood in a standard way as the set of functions with bounded $\mathbf{L}_m(\Omega)$ -norm, i.e.

$$\|\mathbf{u}\|_m =: \left(\int_\Omega |\mathbf{u}(\mathbf{x})|^m \, d\mathbf{x} \right)^{1/m} < \infty.$$

In place of $\|\cdot\|_2$, the simpler $\|\cdot\|$ will be used. For more complicated spaces, the whole space appears in the subscript of the norm.

By $\mathbf{x} \cdot \mathbf{y}$, the usual scalar product of vectors \mathbf{x}, \mathbf{y} in \mathbb{R}^n is meant.

The symbol (\cdot, \cdot) denotes the scalar product in $\mathbf{L}_2(\Omega)$:

$$(\mathbf{u}, \mathbf{v}) = \int_\Omega \mathbf{u}(\mathbf{x}) \cdot \mathbf{v}(\mathbf{x}) \, d\mathbf{x}. \quad (3.2)$$

The last integral is well defined even if \mathbf{u}, \mathbf{v} do not both belong to $\mathbf{L}_2(\Omega)$. Based on Hölder's inequality, it is enough that $\mathbf{u} \in \mathbf{L}_p(\Omega)$ and $\mathbf{v} \in \mathbf{L}_q(\Omega)$, where $p, q > 1$ are dual (conjugate) exponents, that is

$$p^{-1} + q^{-1} = 1.$$

More generally, the integral in (3.2) can be interpreted as a duality relation, i.e. $\mathbf{u} \in \mathbf{U}$ and $\mathbf{v} \in \mathbf{U}^*$. Then, the notation $\langle \mathbf{u}, \mathbf{v} \rangle$ is used in place of (\mathbf{u}, \mathbf{v}) .

The standard notation $\mathbf{W}^{k,p}(\Omega)$ is used for the spaces of functions defined almost everywhere in Ω possessing derivatives up to the order k in $\mathbf{L}_p(\Omega)$. The spaces $\mathbf{W}^{k,p}(\Omega)$ are usually referred to as Sobolev spaces.

The theory of Lebesgue and Sobolev spaces can be found in [1].

A mapping $\mathbf{F} : \mathbf{X} \rightarrow \mathbf{Y}$ is said to be *Lipschitz continuous* if there exists a constant $C \geq 0$ such that for all \mathbf{x} and \mathbf{y} from the domain of definition of \mathbf{F} ,

$$\|\mathbf{F}(\mathbf{x}) - \mathbf{F}(\mathbf{y})\|_{\mathbf{Y}} \leq C \|\mathbf{x} - \mathbf{y}\|_{\mathbf{X}}$$

holds.

We say that a mapping \mathbf{F} from a real normed space \mathbf{X} to \mathbf{X}^* is *coercive* if

$$\langle \mathbf{F}(\mathbf{x}), \mathbf{x} \rangle \geq c(\|\mathbf{x}\|_{\mathbf{X}}) \|\mathbf{x}\|_{\mathbf{X}} \quad \forall \mathbf{x} \in \mathbf{X},$$

where $c(t)$ is a real-valued function of a nonnegative t such that $c(t) \rightarrow \infty$ as $t \rightarrow \infty$.

If $\mathbf{X} = \mathbb{R}^n$ then the previous definition can be rewritten as

$$\frac{\mathbf{F}(\mathbf{x}) \cdot \mathbf{x}}{\|\mathbf{x}\|_{\mathbb{R}^n}} \rightarrow \infty \quad \text{as } \|\mathbf{x}\|_{\mathbb{R}^n} \rightarrow \infty.$$

The bilinear form $a : \mathbf{X} \times \mathbf{X} \rightarrow \mathbb{R}$ is called *coercive* or \mathbf{X} -*elliptic* if there exists a constant $C > 0$ such that

$$a(\mathbf{x}, \mathbf{x}) \geq C \|\mathbf{x}\|_{\mathbf{X}} \quad \forall \mathbf{x} \in \mathbf{X}.$$

A mapping \mathbf{F} from a real normed space \mathbf{X} to its dual \mathbf{X}^* is said to be *monotone* if

$$\langle \mathbf{F}(\mathbf{x}) - \mathbf{F}(\mathbf{y}), \mathbf{x} - \mathbf{y} \rangle \geq 0 \quad (3.3)$$

for \mathbf{x} and \mathbf{y} from the domain of definition of the mapping \mathbf{F} ; it is said to be *strictly monotone* if equality in (3.3) can hold only if $\mathbf{x} = \mathbf{y}$.

Let \mathbf{X} be a normed linear space and $\{\mathbf{x}_n\}$ a sequence in \mathbf{X} .

We say that $\{\mathbf{x}_n\}$ *converges strongly* (or only converges) to $\mathbf{x} \in \mathbf{X}$ and write it as

$$\mathbf{x}_n \rightarrow \mathbf{x},$$

if $\lim_{n \rightarrow \infty} \|\mathbf{x}_n - \mathbf{x}\|_{\mathbf{X}} = 0$.

We say that $\{\mathbf{x}_n\}$ converges *weakly* to $\mathbf{x} \in \mathbf{X}$ and write it as

$$\mathbf{x}_n \rightharpoonup \mathbf{x},$$

if $\lim_{n \rightarrow \infty} \phi(\mathbf{x}_n) = \phi(\mathbf{x})$ for every $\phi \in \mathbf{X}^*$.

For each weakly convergent sequence $\mathbf{x}_n \rightharpoonup \mathbf{x}$ in a Hilbert space \mathbf{H} holds that

$$\lim_{n \rightarrow \infty} \|\mathbf{x}_n\|_{\mathbf{H}} \geq \|\mathbf{x}\|_{\mathbf{H}}. \quad (3.4)$$

3.2 Function spaces for problems in electromagnetism

The *curl*-operator on a three dimensional vector function $\mathbf{v} \in \mathbf{C}_0^\infty(\Omega)^*$, where $\mathbf{v} = (v_1, v_2, v_3)$, is defined by

$$\nabla \times \mathbf{v} = (\partial_2 v_3 - \partial_3 v_2, \partial_3 v_1 - \partial_1 v_3, \partial_1 v_2 - \partial_2 v_1),$$

where the derivatives are understood in the sense of distributions.

The set of all functions with well defined curl

$$\mathbf{H}(\mathbf{curl}; \Omega) := \{\mathbf{v} \in \mathbf{L}_2(\Omega) \mid \nabla \times \mathbf{v} \in \mathbf{L}_2(\Omega)\},$$

equipped with the graph norm

$$\|\mathbf{v}\|_{\mathbf{H}(\mathbf{curl}; \Omega)} = \left(\|\mathbf{v}\|^2 + \|\nabla \times \mathbf{v}\|^2 \right)^{1/2}, \quad (3.5)$$

forms a Hilbert space.

The space $\mathbf{H}_0(\mathbf{curl}; \Omega)$ is defined as the closure of $\mathbf{C}_0^\infty(\Omega)$ functions in the norm (3.5) or alternatively by use of the following theorem:

Theorem 3.1 *If $\Omega \subset \mathbb{R}^3$ is a bounded Lipschitz domain and the function $\mathbf{u} \in \mathbf{H}(\mathbf{curl}; \Omega)$ is such that for every $\boldsymbol{\varphi} \in \mathbf{C}^\infty(\overline{\Omega})$ holds*

$$(\nabla \times \mathbf{u}, \boldsymbol{\varphi}) - (\mathbf{u}, \nabla \times \boldsymbol{\varphi}) = 0,$$

then $\mathbf{u} \in \mathbf{H}_0(\mathbf{curl}; \Omega)$.

Thanks to the previous property of the functions from $\mathbf{H}_0(\mathbf{curl}; \Omega)$ one can prove that $\mathbf{H}(\mathbf{curl}; \Omega)$ is the closure of $\mathbf{C}^\infty(\overline{\Omega})$ in the $\mathbf{H}(\mathbf{curl}; \Omega)$ norm (see e.g. [30]).

For physical reasons we expect the tangential trace of the electric field to be well defined in some sense. The tangential trace, $\gamma_t(\mathbf{v}) = \boldsymbol{\nu} \times \mathbf{v}|_\Gamma$ of the function from $\mathbf{H}(\mathbf{curl}; \Omega)$ exists in the dual space to the $\mathbf{W}^{1/2,2}(\Gamma)$ also denoted by $\mathbf{H}^{-1/2}(\Gamma)$. In addition for any $\mathbf{u} \in \mathbf{H}^1(\Omega)$ and any $\mathbf{v} \in \mathbf{H}(\mathbf{curl}; \Omega)$ following Green's formula holds

$$(\nabla \times \mathbf{v}, \mathbf{u}) - (\mathbf{v}, \nabla \times \mathbf{u}) = \langle \gamma_t(\mathbf{v}), \mathbf{u} \rangle_\Gamma \quad (3.6)$$

for any Lipschitz domain Ω .

When Γ is sufficiently regular (cf. [69]), a formula similar to (3.6) has been derived for $\langle \cdot, \cdot \rangle_\Gamma$ the duality product between $\mathbf{H}^{-1/2}(\operatorname{div}_\Gamma, \Gamma)$ and $\mathbf{H}^{-1/2}(\operatorname{curl}_\Gamma, \Gamma)$ and both fields \mathbf{u} and \mathbf{v} belonging to $\mathbf{H}(\mathbf{curl}; \Omega)$. The precise definition of the above spaces as well as the proof of the formula can be found in [15] and references therein.

Hence, the space $\mathbf{H}_0(\mathbf{curl}; \Omega)$ is a set of functions from $\mathbf{H}(\mathbf{curl}; \Omega)$ with zero tangential trace on Γ .

Analogously to $\mathbf{H}(\mathbf{curl}; \Omega)$ and $\mathbf{H}_0(\mathbf{curl}; \Omega)$, we will define function spaces \mathbf{V} and \mathbf{V}_0 which have a bit less regularity than the previously defined $\mathbf{H}(\mathbf{curl}; \Omega)$ but will play a significant role in Chapter 5.

By \mathbf{V} we denote the space of 3D vector functions from $\mathbf{L}_{2-1/p}(\Omega)$ with curl in $\mathbf{L}_2(\Omega)$, i.e.

$$\mathbf{V} = \{\mathbf{v} \in \mathbf{L}_{2-1/p}(\Omega) \mid \nabla \times \mathbf{v} \in \mathbf{L}_2(\Omega)\}, \quad p > 1 \quad (3.7)$$

endowed with the graph norm

$$\|\mathbf{u}\|_{\mathbf{V}} := \|\mathbf{u}\|_{2-1/p} + \|\nabla \times \mathbf{u}\|. \quad (3.8)$$

Now, let us define \mathbf{V}_0 as the closure of the space of smooth functions $\mathbf{C}_0^\infty(\Omega)$ in the norm of \mathbf{V} .

We denote by \mathbf{V}_0^* the dual space to \mathbf{V}_0 .

In some situations [20], the following generalization of the space $\mathbf{H}(\mathbf{curl}; \Omega)$ is also useful:

$$\mathbf{H}^\alpha(\mathbf{curl}; \Omega) = \{\mathbf{v} \in W^{\alpha,2}(\Omega) \mid \nabla \times \mathbf{v} \in W^{\alpha,2}(\Omega)\} \text{ for some } \alpha > 0, \alpha \in \mathbb{R}$$

with the norm $\|\mathbf{v}\|_{\mathbf{H}^\alpha(\mathbf{curl}; \Omega)} = \left(\|\mathbf{v}\|_{W^{\alpha,2}(\Omega)}^2 + \|\nabla \times \mathbf{v}\|_{W^{\alpha,2}(\Omega)}^2 \right)^{1/2}$.

Properties of \mathbf{V} and \mathbf{V}_0

The properties of \mathbf{V} , such as existence of the tangential trace and density results, cannot be proven in similar way as those of more standard space $\mathbf{H}(\mathbf{curl}; \Omega)$ [53] because the space \mathbf{V} is not a Hilbert space. Therefore special techniques have to be employed. The trace theorems and Green's formula are inevitable in order to prove the correspondence between strong and weak formulation of the problem defined in \mathbf{V}_0 . We will leave this problem open for the future work which will certainly capture its audience among mathematicians dealing with functional analysis. So far, we have succeeded to prove the following properties of the spaces \mathbf{V} and \mathbf{V}_0 :

Lemma 3.2 (reflexivity) *The vector space \mathbf{V} is a reflexive Banach space.*

Proof Directly from the definition of the space \mathbf{V} and its norm follows that the space \mathbf{V} is a Banach space.

Let us define a vector space \mathbf{X} as a product of usual Sobolev spaces,

$$\mathbf{X} = \mathbf{L}_{2-1/p}(\Omega) \times \mathbf{L}_2(\Omega).$$

It is a reflexive Banach space as the product of finite number of reflexive Banach spaces [49, Theorem 0.16.5].

Let us now introduce its subset

$$\tilde{\mathbf{V}} = \{(\mathbf{v}, \nabla \times \mathbf{v}) \in \mathbf{X}\}.$$

Let $\{(\mathbf{v}_n, \nabla \times \mathbf{v}_n)\}$ be an arbitrary Cauchy sequence in $\tilde{\mathbf{V}}$. Then $\{\mathbf{v}_n\}$ is a Cauchy sequence in $\mathbf{L}_{2-1/p}(\Omega)$, therefore there exists $\mathbf{v} \in \mathbf{L}_{2-1/p}(\Omega)$ such that $\mathbf{v}_n \rightarrow \mathbf{v}$ in $\mathbf{L}_{2-1/p}(\Omega)$. Similarly, there exists $\mathbf{f} \in \mathbf{L}_2(\Omega)$ such that $\nabla \times \mathbf{v}_n \rightarrow \mathbf{f}$ in $\mathbf{L}_2(\Omega)$. From the definition of the curl-operator in the distributional sense, we directly obtain that $\mathbf{f} = \nabla \times \mathbf{v}$ in the sense of functionals on $\mathbf{C}_0^\infty(\Omega)$. Using the density of $\mathbf{C}_0^\infty(\Omega)$ in $\mathbf{L}_2(\Omega)$ and the Hahn-Banach theorem, $\nabla \times \mathbf{v}$ can be extended (in a unique way) to the whole space $\mathbf{L}_2(\Omega)$. As $\mathbf{f} \in \mathbf{L}_2(\Omega)$ we get that $\mathbf{f} = \nabla \times \mathbf{v}$ in $\mathbf{L}_2(\Omega)$. Thus $(\mathbf{v}, \mathbf{f}) \in \tilde{\mathbf{V}}$. Consequently the set $\tilde{\mathbf{V}}$ is a closed subset of \mathbf{X} and following [49, Theorem 0.16.4] it is a reflexive space.

As \mathbf{V} is isomorphic to $\tilde{\mathbf{V}}$, the space \mathbf{V} is also a reflexive Banach space [49, Theorem 0.16.6]. \square

Remark 3.3 *The proof of the reflexivity of the space \mathbf{V}_0 is now straightforward as it is a closed subspace of a reflexive Banach space.*

Following lemma tells us more about the dual space to the space \mathbf{V}_0 .

Lemma 3.4 (dual space) *Let Ω be a convex bounded Lipschitz domain in \mathbb{R}^3 (or smooth bounded domain in \mathbb{R}^3). The dual space \mathbf{V}_0^* to the space \mathbf{V}_0 is the subset of the dual space \mathbf{H}^{-1} to the space $\mathbf{H}_0^1(\Omega)$.*

Proof Take arbitrary $\mathbf{z} \in \mathbf{H}_0^1(\Omega)$. Using Theorem 3.47 and Remark 3.48 from [53] we get that there exists some positive constant C , such that

$$\|\mathbf{z}\|_{\mathbf{H}_0^1} \leq C \left(\|\mathbf{z}\| + \|\nabla \times \mathbf{z}\| + \|\nabla \cdot \mathbf{z}\| + \|\mathbf{z} \times \mathbf{n}\|_{\mathbf{L}_2(\Gamma)} \right). \quad (3.9)$$

So $\nabla \times \mathbf{z} \in \mathbf{L}_2(\Omega)$. Using the Sobolev embedding theorem (cf. [1]) in three dimensions, we obtain that $\mathbf{H}_0^1(\Omega) \hookrightarrow \mathbf{L}_6(\Omega) \hookrightarrow \mathbf{L}_{2-1/p}(\Omega)$, thus $\mathbf{z} \in \mathbf{L}_{2-1/p}(\Omega)$. As the set of all smooth functions is dense in $\mathbf{H}_0^1(\Omega)$, and (3.9) is valid, we deduce that $\mathbf{z} \in \mathbf{V}_0$. So $\mathbf{H}_0^1(\Omega) \subset \mathbf{V}_0$ what directly implies, that $\mathbf{V}_0^* \subset \mathbf{H}^{-1}$. \square

4 WHITNEY'S EDGE ELEMENTS

There are many books and papers dealing with the finite element approximation in general or specially in $\mathbf{H}(\mathbf{curl}; \Omega)$. I will not try to compete with them in methodology and mathematical rigorousness. My intention is to give my point of view on the concept of Whitney's finite elements and its advantages, hoping that it will inspire some future young researchers. To those who are familiar with the concept of finite elements we recommend to skip the next subsection and jump directly to Section 4.2 where we start to deal with finite elements with a touch of mathematical rigorousness.

The precise definitions of finite elements and interpolation operators are of importance when implementing the computational schemes. Approximation properties of the finite element space are essential for the theoretical analysis of the error estimation. The rigorous definition of finite elements in general follows in Section 4.3. The precise definition of Whitney's finite elements will be given in Section 4.4 and its most important approximation properties are listed in Section 4.5.

4.1 Informal overview

I realized how exciting the theory of finite elements is after I got to know that Whitney—whose name is mostly used among mathematicians in connection with curl-conforming finite elements—has discovered them by accident. His domain of interest was geometric integration theory and differential geometry. Thus his research was done in this area without thinking of an application in approximation of $\mathbf{H}(\mathbf{curl}; \Omega)$ by finite elements. In 1957, Whitney [72] was work-

ing on the interactions between algebraic topology and the theory of integration while he discovered Whitney's forms. Only in 1980 Nédélec [55] introduced the same functions but now as the lowest order basis functions for $\mathbf{H}(\mathbf{curl}; \Omega)$ -conforming finite elements, that is Whitney's elements. Some of the potentially unknown terms are clarified in the following text.

As we discussed in Chapter 3, $\mathbf{H}(\mathbf{curl}; \Omega)$ is a natural function space where the solution to the eddy current problem should be found. But this is an infinite dimensional space, what can lead to some troubles when we want to solve the problem. If we do not know the exact solution—and this is usually the case—we will try to solve the problem using computers. But how to implement the infinite dimensional space of functions? Answer to this question provides the method of finite elements (FEM) introduced by Galerkin in 1915.

The FEM consists of finding the finite dimensional subspace of the infinite dimensional function space and showing that a solution of the finite dimensional projection of the problem leads to an approximate solution which is *good enough*—means *near enough* to the precise solution of the problem. Successive construction of better and better subspaces should lead to better and better approximation of the solution.

How does one construct such a finite element space? A theoretical mathematician can suppose, that there *exists* such a space and does not bother himself with finding it precisely. But if one really wants to find the solution, a precise description of the finite dimensional space has to be given, so that the computations can be implemented. That is why Nédélec started to discuss this subject.

The finite dimensional subspace has to have some properties in order to approximate the problem *good enough*. The most important one is that it is a subspace, otherwise the things go complicated. This is called $\mathbf{H}(\mathbf{curl}; \Omega)$ -conformity, i.e. the finite dimensional space generated by given basis functions is a subspace of $\mathbf{H}(\mathbf{curl}; \Omega)$. Nédélec found out the property that assures that a finite element will be $\mathbf{H}(\mathbf{curl}; \Omega)$ -conforming and he showed that Whitney's elements are $\mathbf{H}(\mathbf{curl}; \Omega)$ -conforming.

Let us suppose that we are working in the domain $I \subset \mathbb{R}$, an interval. A very rough approximation of an arbitrary function f will be an approximation by a linear function. This will be, of course, too rough. So what about piecewise linear? It can do a much better job. Nevertheless, piecewise linear functions are quite difficult to manage. Where should we cut it in pieces? Moreover, there are too many piecewise linear functions defined on an interval. Therefore we have to give a structure to these *pieces*. And that is how we invented a *mesh*.

We divide the interval I into several, n , smaller intervals, I_j , $j = 1, \dots, n$,

of the same length or of the different, it does not make big difference. The small intervals and its boundary points—nodes—form the mesh together. Now, the approximation of the function f has to be linear in each I_j separately but can change the direction in the nodes. The space of all such functions will be further denoted by X_n . Of course, the functions in X_n are not all piecewise linear functions defined on the interval I . However, if we choose I_j *small enough*, we have chance to obtain a good approximation of the function f .

Since X_n is obviously finite dimensional it has a finite basis. How to choose an appropriate basis? One can for example define the *aspects* of the functions which are of interest to him. For example the values of the functions in the nodes. Or the values in the boundary points of the interval I and the values of the integrals through I_j for each j . We call these aspects *degrees of freedom* of the finite element space. If one defines enough aspects—such that specifying the value of each aspect determines a function from X_n doubtlessly—we call this set of aspects a *unisolvant* set of degrees of freedom. Such degrees of freedom can be used to define a set of basis functions of X_n . For example the functions from X_n which are equal to 1 in one of the nodal points and 0 in all the others. These finite elements are also called *Lagrange's elements*.

For more complicated domains - for example domains in more dimensions - it is no more straightforward to define a mesh. We can divide a plain domain D into triangles, rectangles or other geometric shapes. We can even combine triangles and rectangles. In addition our domain can have a curved boundary and we have to find out what to do with its curved edges. Crowley, Silvester and Hurwitz [22] solved this complex problem by the introduction of a reference element (interval of length 1, rectangle of side 1, etc.) and its subsequent projection on all other elements.

Let us summarize. From what was said before we know that a *finite element* is a triple consisting of the geometric domain (interval, triangle, rectangle), the space of functions (polynomials) defined on this domain, and the degrees of freedom (values in nodes, or integral over the domain). First, a reference finite element is defined, which is afterwards 'cloned' and used to cover the whole considered domain by a mesh and a global space of finite elements. But first a projection to an arbitrary (similar enough) finite element is specified, which has to be smooth enough and has to preserve all important properties of the reference finite element. Once the projection is given, we can map the reference finite element to any other. We consider again the whole domain D . We construct a mesh such that the reference element (or several types) can be mapped onto each small subdomain of D . The global space consisting of the union of all small finite elements forms the approximation space X_n .

Once the finite dimensional approximation space is defined, it will be useful to have some instrument to *project* arbitrary functions¹ onto X_n . The orthogonal projection—through scalar product—is the first one that crosses ones mind. But it has not all important properties we need. Therefore the specific *interpolation operator* is associated to each finite element space. It is defined using degrees of freedom of the finite element. The interpolation $r(f)$ of the function f is the function from X_n which has the same degrees of freedom as the function f —the same values in nodal points or the same integrals over I_j 's. As the specification of all degrees of freedom determines uniquely a function from X_n , the interpolation operator r is correctly defined. It is a natural choice of the mapping from whole space X to the approximation space X_n as the degrees of freedom are the features of the functions we are interested in. By using an orthogonal or another kind of projection we can lose the information about these important features.

4.2 Galerkin method

The finite element theory is based on the Galerkin method and Cea's lemma [19].

Consider a Hilbert space W , a bilinear form $a : W \times W \rightarrow \mathbb{R}$ and a linear bounded functional $f \in W^*$. Let $u \in W$ be a solution to the equation

$$a(u, \phi) = \langle f, \phi \rangle \quad \forall \phi \in W. \quad (4.1)$$

The Lax–Milgram lemma [28, p.78] states that if the bilinear form a is W -coercive and continuous then there exists a unique u solving (4.1).

Let W^h be any finite dimensional subspace of W . Let u^h , also called the *Galerkin approximation* of u , be a solution to the equation

$$a(u^h, \phi^h) = \langle f, \phi^h \rangle \quad \forall \phi^h \in W^h. \quad (4.2)$$

If a is coercive and continuous, the existence and uniqueness of the solution to the problem (4.2) follow again from the Lax–Milgram lemma.

In the light of C ea's lemma, the approximation error of the Galerkin approximation depends mainly on the choice of the approximation space W^h .

Lemma 4.1 (C ea's lemma) *Let W, W^h be Hilbert spaces such that $W^h \subset W$. Let a be a continuous coercive bilinear form on W . Let u and u^h solve (4.1)*

¹Or at least a set of functions which are dense in X .

and (4.2) respectively. Then there exists a positive constant C independent of the approximation parameter h such that

$$\|u - u^h\|_W \leq C \inf_{\phi \in W^h} \|u - \phi\|_W.$$

Let us consider a system $\{W^h\}_h$ of finite dimensional subspaces of the space W . The following lemma gives a sufficient condition for convergence of the Galerkin approximations u^h to the solution u of (4.1).

Lemma 4.2 *Let the assumptions of Céa's lemma be satisfied. Let \mathcal{W} be a dense subspace of W and consider a system of mappings $r^h : \mathcal{W} \rightarrow W^h$ with the property*

$$\|\phi - r^h \phi\|_W \xrightarrow{h \rightarrow 0} 0 \quad \forall \phi \in \mathcal{W}.$$

Then the sequence of Galerkin approximations u^h converges to the exact solution u of (4.1), that is

$$\lim_{h \rightarrow 0} \|u - u^h\|_W = 0.$$

Once we have the basic knowledge of the Galerkin method, we can proceed to the rigorous definition of finite elements.

4.3 Finite elements in general

The mathematical concept of finite element as a triple was introduced by Ciarlet [19]. In Section 4.1 we have seen the sketch of his approach. In this section we give explicit definitions. Following Ciarlet, a *finite element* is a triple consisting of a geometric domain, T , a space of functions on T , P_T , and a set of linear functionals on P_T , Σ_T , also called *degrees of freedom* of the finite element.

The finite element is said to be *unisolvant* if the degrees of freedom Σ_T are chosen in such a way that specifying a value for each degree of freedom uniquely determines a function in P_T . Thus in a unisolvant finite element, we can construct the basis of P_T using degrees of freedom Σ_T .

We call r an *interpolation operator* if for each sufficiently smooth function f defined on T a uniquely determined interpolant $r(f) \in P_T$ is given such that for all $\sigma \in \Sigma_T$ holds $\sigma(r(f) - f) = 0$.

Our plan is to define some global finite element space. Suppose there is a global domain D which is divided into smaller geometric domains all resembling

some reference element T . Techniques of mapping the reference finite element onto a general element allow us to construct a global finite element space as a union of all small finite elements. The global space of functions P is constructed as union of local P_T extended by 0 to other elements. Global degrees of freedom are similarly union of local degrees of freedom.

Let X be a space of functions. The finite element (T, P_T, Σ_T) is said to be *X-conforming* if the corresponding global finite element space is a subspace of X .

4.4 Whitney's edge elements

The most suitable first order finite elements for the discretization of the electric field in Maxwell's equations are Whitney's edge finite elements. In the literature also appearing as edge elements, vector covariant elements or curl-conforming elements of Nédélec. There are many authors dealing with this issue and at least two different approaches. The classical functional approach can be found for example in the book by Monk [53]. It will be employed throughout this section. The other approach using differential forms was adopted by many authors for its more general and more flexible nature, but it is also much more difficult to master. We refer the reader interested in this theory to an extensive paper by Hiptmair [57] or to the book by Bossavit [12].

To define Whitney's finite elements rigorously, we have to define T , P_T and Σ_T from the previous section. We suppose that the global domain $\Omega \subset \mathbb{R}^3$ is a bounded polygonal domain with boundary Γ . By dividing Ω into tetrahedra we construct a tetrahedral mesh, denoted by \mathcal{M} . The geometric domain T from the previous section is then a tetrahedron. In order to obtain a suitable mesh, it has to obey some geometric laws.

The set of all tetrahedra will be denoted by \mathcal{T} . Each tetrahedron comprises 4 faces, 6 edges and 4 vertices. These simplices will be considered as part of the mesh too. The mesh \mathcal{M} is well-defined if any two of tetrahedra intersect along a common face, edge or node, but no other way.²

We denote by h_T the diameter of the smallest sphere containing \overline{T} and by ρ_T the diameter of the largest sphere contained in \overline{T} . The mesh \mathcal{M} is called *regular* if there are constants $C > 0$ and $h > 0$ such that

$$h_T/\rho_T \leq C \quad \forall T \in \mathcal{T}, \quad (4.3)$$

²Such mesh is also referred as a conforming mesh because it usually assures conformity of the space of finite elements.

and

$$h = \max_{T \in \mathcal{T}} \{h_T\}. \quad (4.4)$$

The method of Galerkin is based on solving the problem on the family of meshes with h tending to zero. In virtue of this fact the mesh \mathcal{M} is often denoted by \mathcal{M}_h to be able to recognize several meshes with different characteristic h . The family of meshes is said to be *regular* if there is a constant $C > 0$ independent of h satisfying (4.3).

Let us proceed to the definition of the space of functions P_T . This is usually a space of polynomials. We will discuss only the case of polynomials of degree one. It is also possible to define P_T as a space of higher order polynomials. For details see [30] or [53]. The space P_T is defined as follows

$$P_T := \{\mathbf{p}(\mathbf{x}) = \mathbf{a} \times \mathbf{x} + \mathbf{c} \mid \mathbf{a}, \mathbf{c} \in \mathbb{R}^3, \mathbf{x} \in T\}. \quad (4.5)$$

Next, the degrees of freedom have to be defined. Let T be a tetrahedron with edges denoted by e_i , $i = 1, \dots, 6$ and let \mathbf{u} be a function in $\mathbf{W}^{1,s}(T)$ for some $s > 2$. Then

$$\Sigma_T := \{M_{e_i}, i = 1, \dots, 6\},$$

where

$$M_{e_i}(\mathbf{u}) := \int_{e_i} \mathbf{u} \cdot \boldsymbol{\tau}_{e_i} \, ds.$$

The vector $\boldsymbol{\tau}_{e_i}$ is a unit vector in direction of e_i .

The Whitney edge element is unisolvent. For the proof see e.g. [30].

Remark 4.3 *In the above definition, we suppose quite high regularity of the function \mathbf{u} so that the integral over the edge in the definition of M_{e_i} makes sense.*

The interpolation operator r_h is defined by

$$M_{e_i}(\mathbf{u} - r_h \mathbf{u}) = 0 \quad \text{for all } i = 1, \dots, 6. \quad (4.6)$$

The most important approximation properties of r_h are to be found in the next section.

Remark 4.4 *In virtue of the previous remark we realize that the interpolation operator r_h does not make sense for all functions from $\mathbf{H}(\mathbf{curl}; \Omega)$. To date, the best characterization of the functions for which the interpolant is defined is given in [4]. As the operator r_h is defined on the dense subset of $\mathbf{H}(\mathbf{curl}; \Omega)$, this small deficiency is no real handicap of the edge elements (check Lemma 4.2).*

Once the edge elements are specified, the *basis functions* can be determined. These are defined on each tetrahedron as vector fields $\mathbf{w}_{e_i} \in P_T$, $i = 1, \dots, 6$ such that $M_{e_i}(\mathbf{w}_{e_j}) = \delta_{i,j}$ for all $i, j = 1, \dots, 6$. Clearly, this definition does not show if the set $\{\mathbf{w}_{e_i}\}_{i=1}^6$ forms the basis of P_T , neither how one can construct \mathbf{w}_{e_i} exactly. Fortunately, we know the way, but first some auxiliary functions have to be introduced.

Let us deal with one separate tetrahedron. We denote its vertices by numbers 0, 1, 2, 3. By w_k we denote the linear functions having value 1 in the vertex k and 0 in all other vertices of the tetrahedron. For each k there exists only one w_k and it has the form $w_k(\mathbf{x}) = \nabla w_k \cdot \mathbf{x} + c_k$, where ∇w_k denotes the gradient of the function w_k and $c_k \in \mathbb{R}$ is a constant.

Let e be the edge connecting vertices 0 and 1. Then the *edge function* associated with the edge e has the following form

$$\mathbf{w}_e = w_0 \nabla w_1 - w_1 \nabla w_0. \quad (4.7)$$

In order to prove that the two previously given definitions of function \mathbf{w}_e coincide, we work out a deeper analysis of the properties of w_k and ∇w_k .

First of all, the function w_0 equals 1 in vertex 0 and 0 in vertex 1. In addition w_0 is linear on the edge between 0 and 1. The function w_1 is 'reverse' to w_0 on the edge $e = \{01\}$, thus $w_0 + w_1 = 1$ in all points of the edge e .

Next, we denote by h_0 the height of the tetrahedron in the vertex 0, by A the orthogonal projection of vertex 0 to the plain given by remaining vertices 1, 2, 3 and by \mathbf{h}_0 the vector connecting the points A and 0. As the function w_0 is linear, its gradient is a vector with constant norm and direction in the whole tetrahedron. In addition, $w_0 = 0$ in the plain 1, 2, 3 and therefore ∇w_0 has to be perpendicular to this plain, i.e. ∇w_0 and \mathbf{h}_0 have the same direction. Using the mean value theorem we obtain that

$$(\nabla w_0, \mathbf{h}_0) = w_0(0) - w_0(A) = 1,$$

thus we obtain the following relation for the norm of the gradient of the function w_0

$$|\nabla w_0| = h_0^{-1}.$$

Similarly, $|\nabla w_1| = h_1^{-1}$ and the vectors \mathbf{h}_1 and ∇w_1 are co-linear.

Now, we can proceed to the evaluation of $M_e(\mathbf{w}_e)$.

$$\begin{aligned} M_e(\mathbf{w}_e) &= \int_e \mathbf{w}_e \cdot \boldsymbol{\tau}_e \, ds = \int_e w_0 \nabla w_1 \cdot \boldsymbol{\tau}_e \, ds - \int_e w_1 \nabla w_0 \cdot \boldsymbol{\tau}_e \, ds \\ &= \nabla w_1 \cdot \boldsymbol{\tau}_e \int_e w_0 \, ds - \nabla w_0 \cdot \boldsymbol{\tau}_e \int_e w_1 \, ds. \end{aligned}$$

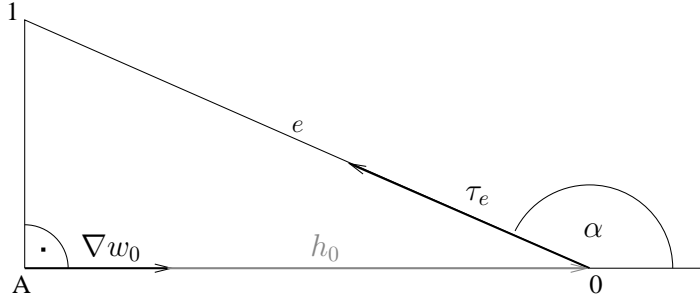


Figure 4.1: How to compute the scalar product $\nabla w_0 \cdot \tau_e$.

We denote by α the angle between the vectors ∇w_0 and τ_e . Then

$$\nabla w_0 \cdot \tau_e = |\nabla w_0| |\tau_e| \cos \alpha = h_0^{-1} \cos \alpha = -|e|^{-1},$$

where $|e|$ denotes the length of the edge e . For the last equality check Figure 4.1. The second scalar product can be evaluated similarly, $\nabla w_1 \cdot \tau_e = |\nabla w_1| \cos \beta = |e|^{-1}$. Finally, we get

$$M_e(\mathbf{w}_e) = |e|^{-1} \int_e w_0 + w_1 \, ds = 1.$$

Further we need to check if $M_{e'}(\mathbf{w}_e) = 0$ for $e' \neq e$. Let us do it for the edge $e' = \{02\}$. On this edge $w_1 = 0$ and its gradient ∇w_1 is perpendicular to this edge. Therefore $M_{02}(\mathbf{w}_e) = 0$. Similarly, we obtain 0 for all other edges of the tetrahedron.

Next, we have to check if \mathbf{w}_e defined by (4.7) belongs to the previously defined space P_T and if the set of all \mathbf{w}_e 's forms its basis. We have to find \mathbf{a} and \mathbf{c} such that $\mathbf{w}_e = \mathbf{a} \times \mathbf{x} + \mathbf{c}$. Using basic vector identities and the definition of w_k , we successively obtain

$$\begin{aligned} (\nabla w_0 \times \nabla w_1) \times \mathbf{x} &= (\mathbf{x} \cdot \nabla w_0) \nabla w_1 - (\mathbf{x} \cdot \nabla w_1) \nabla w_0 \\ &= (w_0 - c_0) \nabla w_1 - (w_1 - c_1) \nabla w_0 \\ &= \mathbf{w}_e + c_0 \nabla w_1 - c_1 \nabla w_0. \end{aligned}$$

Thus $\mathbf{a} = \nabla w_0 \times \nabla w_1$ and $\mathbf{c} = c_1 \nabla w_0 - c_0 \nabla w_1$.

Finally, we will prove that the \mathbf{w}_e 's given by (4.7) (and fulfilling $M_{e_i}(\mathbf{w}_{e_j}) = \delta_{i,j}$) form a basis of P_T . The number of basis functions agrees with the dimension of the space P_T : $\dim P_T = 6 = \text{number of edges of a tetrahedron}$, thus it is sufficient to prove the linear independence of the \mathbf{w}_e 's. This will be done by contradiction. Let us suppose that the set $B = \{\mathbf{w}_e, \forall e \in T\}$ is linearly dependent. It means that there exists the edge e_0 such that \mathbf{w}_{e_0} can be written as linear combination of remaining elements of B . Without loss of generality, let e_0 be the edge between vertices 0 and 1, i.e. $\mathbf{w}_{e_0} = \mathbf{w}_{01}$. We suppose that there exist $\alpha_1, \dots, \alpha_5 \in \mathbb{R}$ such that

$$\mathbf{w}_{01} = \alpha_1 \mathbf{w}_{02} + \alpha_2 \mathbf{w}_{03} + \alpha_3 \mathbf{w}_{12} + \alpha_4 \mathbf{w}_{13} + \alpha_5 \mathbf{w}_{23} \quad (4.8)$$

for all points of the tetrahedron T . Employing relation (4.8) in the vertex 0 leads to the linear dependence of the vectors $\nabla \mathbf{w}_1$, $\nabla \mathbf{w}_2$ and $\nabla \mathbf{w}_3$ and therefore of the vectors \mathbf{h}_1 , \mathbf{h}_2 and \mathbf{h}_3 . But this is not possible in a nondegenerate tetrahedron. Why? Let us try to construct a tetrahedron under supposition that \mathbf{h}_1 , \mathbf{h}_2 and \mathbf{h}_3 lie in one plane denoted by P . A plane A_1 , perpendicular to \mathbf{h}_1 , intersects with the plane A_2 , perpendicular to \mathbf{h}_2 , in a line p_{12} perpendicular to both \mathbf{h}_1 and \mathbf{h}_2 . If not, we cannot construct a tetrahedron because A_1 and A_2 are planes of the faces of the tetrahedron and therefore they have to intersect—each two faces of a nondegenerate tetrahedron intersect. The line p_{12} is also perpendicular to \mathbf{h}_3 as $\mathbf{h}_3 \subset P$. When we construct A_3 , the plane perpendicular to \mathbf{h}_3 , we realize that also intersections $p_{23} = A_3 \cap A_2$ and $p_{13} = A_3 \cap A_1$ are perpendicular to the plane P . But it means that these intersections which are in fact edges of the sought tetrahedron are all parallel which is not possible because in a nondegenerate tetrahedron each three edges intersect. To conclude, the functions \mathbf{w}_e form the basis of the space P_T defined on a nondegenerate tetrahedron T .

After finally having all necessary components, we define the approximation space of Whitney's edge elements by

$$\mathbf{W}_h = \{\mathbf{p}(\mathbf{x}) : \mathbf{p}(\mathbf{x})|_T \in P_T, \quad \forall T \in \mathcal{T}\}. \quad (4.9)$$

We are still in arrears with one very important property of Whitney's edge elements and it is their $\mathbf{H}(\mathbf{curl}; \Omega)$ -conformity. The exact proof can be found in [30] or [53]. It is based on the fact, that if \mathbf{f}_1 belongs to $\mathbf{H}(\mathbf{curl}; T)$ and \mathbf{f}_2 to $\mathbf{H}(\mathbf{curl}; T')$ for two distinct tetrahedra T and T' having common face Σ , then if $\mathbf{f}_1 \times \boldsymbol{\nu} = \mathbf{f}_2 \times \boldsymbol{\nu}$, the function

$$\mathbf{f} = \begin{cases} \mathbf{f}_1 & \text{on } T, \\ \mathbf{f}_2 & \text{on } T' \end{cases}$$

belongs to $\mathbf{H}(\mathbf{curl}; T \cup T' \cup \Sigma)$. The Whitney elements have this property.

For more detailed overview with pictures and list of interesting properties of Whitney's edge elements as well as of Whitney's nodal, facial and tetrahedral elements, we refer to [21].

4.5 Approximation properties

In all theorems in this section we suppose that \mathcal{M}_h is a regular family of meshes on $\bar{\Omega}$ and r_h is the interpolant defined by (4.6).

The following classical approximation result can be found e.g. in [29].

Theorem 4.5 *For any $\mathbf{u} \in \mathbf{W}^{2,2}(\Omega)$ holds $\|\mathbf{u} - r_h \mathbf{u}\| \leq Ch^2 |\mathbf{u}|_2$.*

The following general approximation results for functions with higher regularity were published in the paper by Monk [52].

Theorem 4.6 *Let $\mathbf{u} \in \mathbf{W}^{1,s}(\Omega)$, $s > 2$. Then:*

1. *There is a constant $C = C(s)$ such that*

$$\|\mathbf{u} - r_h \mathbf{u}\| + h \|\mathbf{u} - r_h \mathbf{u}\|_{\mathbf{H}(\mathbf{curl}; \Omega)} \leq Ch \|\mathbf{u}\|_{\mathbf{W}^{1,s}(\Omega)}.$$

2. *If, in addition $\mathbf{u} \in \mathbf{W}^{2,2}(\Omega)$, then*

$$\|\mathbf{u} - r_h \mathbf{u}\| + h \|\mathbf{u} - r_h \mathbf{u}\|_{\mathbf{H}(\mathbf{curl}; \Omega)} \leq Ch^2 \|\mathbf{u}\|_{\mathbf{W}^{2,2}(\Omega)}.$$

In [20], Ciarlet Jr. and Zou have improved previous results by requiring lower regularity.

Theorem 4.7 *For all $\mathbf{u} \in \mathbf{H}^s(\mathbf{curl}; \Omega)$, $1/2 < s \leq 1$ holds*

$$\|\mathbf{u} - r_h \mathbf{u}\| \leq Ch^s \|\mathbf{u}\|_{\mathbf{H}^s(\mathbf{curl}; \Omega)}.$$

The paper by Hiptmair [57] states the following result based on the commuting property of a *De Rham* diagram, which describes important relations between Whitney's edge elements, analogous elements defined for nodes, faces and tetrahedra and the infinite dimensional spaces they are approximating [21, 23].

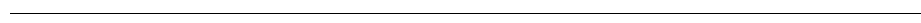
Theorem 4.8 *For all $\mathbf{u} \in \mathbf{H}^s(\mathbf{curl}; \Omega)$, for $s \in [0, 1] \cup \mathbb{N}$ holds*

$$\|\nabla \times (\mathbf{u} - r_h \mathbf{u})\| \leq Ch^{\min\{s, 2\}} |\nabla \times \mathbf{u}|_{\mathbf{W}^{s,2}(\Omega)}.$$

The last approximation property can be found in [30].

Theorem 4.9 *For all $\mathbf{u} \in \mathbf{W}^{2,2}(\Omega)$ holds that*

$$\|\mathbf{u} - r_h \mathbf{u}\|_{\mathbf{H}(\text{curl}; \Omega)} \leq Ch \left(|\mathbf{u}|_{\mathbf{L}_1(\Omega)} + |\mathbf{u}|_{\mathbf{L}_2(\Omega)} \right).$$



5 TIME-DISCRETIZATION

The nonlinearity (1.3) is used.

The backward Euler method is a standard numerical tool for discretization in time. Slodička [61] has proven the convergence of the method for problem (1.7), (1.8) and (1.10) when the constitutive relation (1.4) is used. In this chapter, we study the convergence of the backward Euler method in the case of eddy current problem (1.15) equipped with the unmodified power law constitutive relation (1.3). In these circumstances, the space \mathbf{V}_0 as defined in Chapter 3 is a natural choice of the space of test functions.¹

This chapter is based on the article [66] and my presentation on the Conference in Numerical Analysis—NumAn 2008 [40]. The chapter is organized as follows. After rigorous definition of the problem and proof of the uniqueness of its solution, we propose the time-discretization scheme as known from the backward Euler method. We show the well-posedness of the scheme in Lemma 5.2. Next, the a priori estimates are derived and the convergence of the method is shown. In Section 5.4, we prove again the convergence by use of Murat and Tartar’s div-curl lemma. The new versions of this powerful lemma are stated and proven in Lemmas 5.8 and 5.9. The error estimates are derived in Section 5.5. The numerical experiments are presented in Section 5.6.

If the nonlinear vector field \mathbf{J} is given by (1.3), the variational formulation (1.15) reads as follows: Find $\mathbf{E} \in \mathbf{V}_0$ such that, for any $\boldsymbol{\varphi} \in \mathbf{V}_0$

$$\begin{aligned} (\partial_t \mathbf{J}(\mathbf{E}), \boldsymbol{\varphi}) + (\nabla \times \mathbf{E}, \nabla \times \boldsymbol{\varphi}) &= 0 && \text{a.e. in } [0, T], \\ \mathbf{E}(0) &= \mathbf{E}_0 && \text{a.e. in } \Omega. \end{aligned} \quad (5.1)$$

¹As an equivalent Green’s formula (3.6) for the functions belonging to \mathbf{V}_0 is not yet derived, the compatibility between the weak and strong formulation of the problem cannot yet be proven.

Let us define an auxiliary real-valued function j as

$$j(s) = s^{-1/p} \quad \text{for } s > 0. \quad (5.2)$$

Then $\mathbf{J}(\mathbf{E}) = j(|\mathbf{E}|)\mathbf{E}$, for all $\mathbf{E} \in \mathbb{R}^3$.

Further in the text the following notation is used

$$q = \frac{2p-1}{p-1}.$$

It means that q is the dual (conjugate) exponent to $2 - 1/p$.

The following theorem proves the uniqueness of a weak solution to (5.1) in appropriate spaces.

Lemma 5.1 *There exists at most one solution to (5.1) satisfying the following relations: $\mathbf{E} \in L_{2-1/p}((0, T), \mathbf{L}_{2-1/p}(\Omega))$, $\nabla \times \mathbf{E} \in L_2((0, T), \mathbf{L}_2(\Omega))$ and $\partial_t \mathbf{J}(\mathbf{E}) \in L_q((0, T), \mathbf{L}_q(\Omega))$.*

Proof Suppose there exist two different solutions \mathbf{E}_1 and \mathbf{E}_2 to the problem (5.1), then

$$(\mathbf{J}(\mathbf{E}_1(t)) - \mathbf{J}(\mathbf{E}_2(t)), \boldsymbol{\varphi}) + \int_0^t (\nabla \times (\mathbf{E}_1 - \mathbf{E}_2), \nabla \times \boldsymbol{\varphi}) = 0.$$

Setting $\boldsymbol{\varphi} = \mathbf{E}_1 - \mathbf{E}_2$ and integrating in time over $[0, T]$, the second term reads as

$$\int_0^T \left(\int_0^t \nabla \times (\mathbf{E}_1 - \mathbf{E}_2), \nabla \times (\mathbf{E}_1 - \mathbf{E}_2)(t) \right) = \frac{1}{2} \left\| \int_0^T \nabla \times (\mathbf{E}_1 - \mathbf{E}_2) \right\|^2.$$

Hence, we can write

$$\int_0^T (\mathbf{J}(\mathbf{E}_1) - \mathbf{J}(\mathbf{E}_2), \mathbf{E}_1 - \mathbf{E}_2) + \frac{1}{2} \left\| \int_0^T \nabla \times (\mathbf{E}_1 - \mathbf{E}_2) \right\|^2 = 0. \quad (5.3)$$

From the Cauchy-Schwartz inequality, we obtain that

$$(\mathbf{J}(\mathbf{E}_1) - \mathbf{J}(\mathbf{E}_2), \mathbf{E}_1 - \mathbf{E}_2) \geq \int_{\Omega} \left(|\mathbf{E}_1|^{1-1/p} - |\mathbf{E}_2|^{1-1/p} \right) (|\mathbf{E}_1| - |\mathbf{E}_2|). \quad (5.4)$$

For all positive real numbers α, β and all non-negative real numbers x and y , the following relation is valid²

$$(\alpha + \beta)^2(x^\alpha - y^\alpha)(x^\beta - y^\beta) \geq 4\alpha\beta \left(x^{\frac{\alpha+\beta}{2}} - y^{\frac{\alpha+\beta}{2}} \right)^2. \quad (5.5)$$

This, together with (5.3) and (5.4), implies

$$0 \geq \int_0^T (\mathbf{J}(\mathbf{E}_1) - \mathbf{J}(\mathbf{E}_2), \mathbf{E}_1 - \mathbf{E}_2) \geq C \int_0^T \int_\Omega \left(|\mathbf{E}_1|^{1-1/(2p)} - |\mathbf{E}_2|^{1-1/(2p)} \right)^2.$$

Hence, we deduce that $|\mathbf{E}_1| = |\mathbf{E}_2|$ a.e. in $\Omega \times (0, T)$. The substitution of this equality into (5.3) gives

$$\int_0^T \int_\Omega |\mathbf{E}_1|^{-1/p} |\mathbf{E}_1 - \mathbf{E}_2|^2 + \frac{1}{2} \left\| \int_0^T \nabla \times (\mathbf{E}_1 - \mathbf{E}_2) \right\|^2 = 0,$$

which yields that $\mathbf{E}_1 = \mathbf{E}_2$ a.e. in $\Omega \times (0, T)$. \square

5.1 Discretization scheme

Let us consider a finite time interval $[0, T]$. The time-discretization is based on the backward Euler method. We use an equidistant partitioning with time step $\tau = T/n$, for any $n \in \mathbb{N}$, so we divide the time interval $[0, T]$ into n equidistant subintervals $[t_{i-1}, t_i]$, where $t_i = i\tau$. For any function z we introduce the notation

$$z_i = z(t_i), \quad \delta z_i = \frac{z_i - z_{i-1}}{\tau}.$$

We suggest the following nonlinear recursive approximation scheme for $i = 1, \dots, n$:

$$\begin{aligned} (\delta(j(|\mathbf{e}_i|)\mathbf{e}_i), \boldsymbol{\varphi}) + (\nabla \times \mathbf{e}_i, \nabla \times \boldsymbol{\varphi}) &= 0 \quad \forall \boldsymbol{\varphi} \in \mathbf{V}_0 \\ \mathbf{e}_0 &= \mathbf{E}_0. \end{aligned} \quad (5.6)$$

Lemma 5.2 *Assume $\mathbf{E}_0 \in \mathbf{V}_0$. Then there exists a uniquely determined $\mathbf{e}_i \in \mathbf{V}_0$ solving (5.6) for any $i = 1, \dots, n$.*

²Its proof is straightforward and it is left to the reader.

Proof The left-hand side of (5.6) can be considered as a nonlinear operator $\mathcal{J} : \mathbf{V}_0 \rightarrow \mathbf{V}_0^*$ defined as $\mathcal{J}(\lambda) = j(|\lambda|)\lambda + \tau \nabla \times \nabla \times \lambda$. Since

$$\frac{\langle \mathcal{J}(\lambda), \lambda \rangle}{\|\lambda\|_{\mathbf{V}_0}} = \frac{\|\lambda\|_{2-1/p}^{2-1/p} + \tau \|\nabla \times \lambda\|^2}{\|\lambda\|_{2-1/p} + \|\nabla \times \lambda\|} \rightarrow \infty \quad \text{as} \quad \|\lambda\|_{\mathbf{V}_0} \rightarrow \infty,$$

the operator \mathcal{J} is coercive. The Gâteaux differential of \mathcal{J} in point \mathbf{x} and direction \mathbf{h} is

$$D\mathcal{J}(\mathbf{x}, \mathbf{h}) = -\frac{1}{p} |\mathbf{x}|^{-2-1/p} (\mathbf{h} \cdot \mathbf{x}) \mathbf{x} + |\mathbf{x}|^{-1/p} \mathbf{h} + \tau \nabla \times \nabla \times \mathbf{h}.$$

The monotonicity of the operator \mathcal{J} can be shown using the generalized Lagrange formula (see [70, Chapter 1]), i.e. there exists some $\theta \in (0, 1)$ such that

$$\begin{aligned} (\mathcal{J}(\mathbf{x} + \mathbf{h}) - \mathcal{J}(\mathbf{x}), \mathbf{h}) &= (D\mathcal{J}(\mathbf{x} + \theta \mathbf{h}), \mathbf{h}) \\ &= \int_{\Omega} |\mathbf{x} + \theta \mathbf{h}|^{-1/p} |\mathbf{h}|^2 + \tau \|\nabla \times \mathbf{h}\|^2 \\ &\quad - \frac{1}{p} |\mathbf{x} + \theta \mathbf{h}|^{-2-1/p} (\mathbf{h} \cdot (\mathbf{x} + \theta \mathbf{h}))^2 \\ &\geq (1 - 1/p) \int_{\Omega} |\mathbf{x} + \theta \mathbf{h}|^{-1/p} |\mathbf{h}|^2 + \tau \|\nabla \times \mathbf{h}\|^2 \\ &\geq 0. \end{aligned} \tag{5.7}$$

Moreover we deduce that

$$(\mathcal{J}(\mathbf{x} + \mathbf{h}) - \mathcal{J}(\mathbf{x}), \mathbf{h}) = 0 \quad \implies \quad \mathbf{h} = \mathbf{0} \quad \text{a.e. in } \Omega, \tag{5.8}$$

which implies the strict monotonicity of \mathcal{J} .

One can easily check that \mathcal{J} is demicontinuous (see [70, Definition 1.8]). Therefore, according to the theory of monotone operators (see [70, Theorem 18.2, Remark 18.2]), the problem (5.6) admits a unique weak solution $\mathbf{e}_i \in \mathbf{V}_0$. \square

The previous lemma is very simple and elegant, but it is also very theoretical as it concerns infinite dimensional spaces. When one solves the problem numerically, the infinite dimensional spaces are usually approximated by finite dimensional ones (as will be studied in Chapter 8). Let us now suppose, that there exists a Schauder basis $\{\mathbf{v}_k\}$ of the space \mathbf{V}_0 and that the space \mathbf{V}_0 can be approximated by finite dimensional subspaces $\mathbf{V}_{0,k}$ generated by the first k

basis functions \mathbf{v}_k . If there exists a bounded projector $P_{\mathbf{V}_{0,k}} : \mathbf{V}_0 \longrightarrow \mathbf{V}_{0,k}$ such that

$$\lim_{k \rightarrow \infty} \|\phi - P_{\mathbf{V}_{0,k}} \phi\|_{\mathbf{V}} = 0 \quad \forall \phi \in \mathbf{V}_0,$$

the solution to the problem (5.6) can be constructed as the limit of a sequence of solutions to the equivalent finite dimensional problems

$$(j(|\mathbf{e}_{i,k}|)\mathbf{e}_{i,k}, \boldsymbol{\varphi}) + \tau (\nabla \times \mathbf{e}_{i,k}, \nabla \times \boldsymbol{\varphi}) = (j(|\mathbf{e}_{i-1}|)\mathbf{e}_{i-1}, \boldsymbol{\varphi}) \quad \forall \boldsymbol{\varphi} \in \mathbf{V}_{0,k}.$$

The rigorous proof of the convergence is very similar to the proof of Theorem 5.7, therefore it will be omitted.

5.2 Stability

Next, we derive suitable a priori estimates for \mathbf{e}_i for each time step $i = 1, \dots, n$. We proceed in several steps, starting with a technical lemma.

Lemma 5.3 *Let $g : \mathbb{R} \rightarrow \mathbb{R}$ be a non-negative continuous function such that $G(s) := g(s)s$ is monotonically increasing. Let Φ_G be the primitive function of G . Then for any $\mathbf{x}, \mathbf{y} \in \mathbb{R}^3$ we have*

$$\Phi_G(|\mathbf{y}|) - \Phi_G(|\mathbf{x}|) \leq g(|\mathbf{y}|)\mathbf{y} \cdot (\mathbf{y} - \mathbf{x}).$$

Proof We use the mean-value theorem to deduce that there exists θ between $|\mathbf{x}|$ and $|\mathbf{y}|$ such that

$$\begin{aligned} \Phi_G(|\mathbf{y}|) - \Phi_G(|\mathbf{x}|) &= \int_{|\mathbf{x}|}^{|\mathbf{y}|} g(s)s \, ds \\ &= g(\theta)\theta(|\mathbf{y}| - |\mathbf{x}|). \end{aligned}$$

If $|\mathbf{y}| \geq |\mathbf{x}|$ then

$$\begin{aligned} g(\theta)\theta(|\mathbf{y}| - |\mathbf{x}|) &\leq g(|\mathbf{y}|)|\mathbf{y}|(|\mathbf{y}| - |\mathbf{x}|) \\ &= g(|\mathbf{y}|)(|\mathbf{y}|^2 - |\mathbf{y}||\mathbf{x}|) \\ &\leq g(|\mathbf{y}|)\mathbf{y} \cdot (\mathbf{y} - \mathbf{x}). \end{aligned}$$

But the same is valid also if $|\mathbf{y}| \leq |\mathbf{x}|$ and thus the proof is completed. \square

Lemma 5.3 can be used to get basic energy estimates for \mathbf{e}_i with very low regularity of \mathbf{E}_0 .

Lemma 5.4 *Assume $\mathbf{E}_0 \in \mathbf{L}_{2-1/p}(\Omega)$. Then*

$$\frac{p-1}{2p-1} \|\mathbf{e}_j\|_{2-1/p}^{2-1/p} + \sum_{i=1}^j \|\nabla \times \mathbf{e}_i\|^2 \tau \leq \frac{p-1}{2p-1} \|\mathbf{E}_0\|_{2-1/p}^{2-1/p}$$

holds for all $j = 1, \dots, n$.

Proof We set $\varphi = \mathbf{e}_i$ in (5.6), sum the result up for $i = 1, \dots, j$ and we get

$$\sum_{i=1}^j (\mathbf{J}(\mathbf{e}_i) - \mathbf{J}(\mathbf{e}_{i-1}), \mathbf{e}_i) + \sum_{i=1}^j \|\nabla \times \mathbf{e}_i\|^2 \tau = 0. \quad (5.9)$$

In Lemma 5.3 we set $g(t) = t^{\frac{1}{p-1}}$. Then

$$\Phi_G(s) = \int_0^s t^{1+1/(p-1)} dt = \int_0^s t^{p/(p-1)} dt = \frac{s^q}{q}.$$

Next we set $\mathbf{y} = \mathbf{J}(\mathbf{e}_i)$ and $\mathbf{x} = \mathbf{J}(\mathbf{e}_{i-1})$ in Lemma 5.3. Then

$$\frac{1}{q} \left[\|\mathbf{e}_i\|_{2-1/p}^{2-1/p} - \|\mathbf{e}_{i-1}\|_{2-1/p}^{2-1/p} \right] \leq (\mathbf{J}(\mathbf{e}_i) - \mathbf{J}(\mathbf{e}_{i-1}), \mathbf{e}_i).$$

Using this last inequality in (5.9) we obtain

$$\frac{1}{q} \sum_{i=1}^j \left[\|\mathbf{e}_i\|_{2-1/p}^{2-1/p} - \|\mathbf{e}_{i-1}\|_{2-1/p}^{2-1/p} \right] + \sum_{i=1}^j \|\nabla \times \mathbf{e}_i\|^2 \tau \leq 0,$$

from which we easily conclude the proof. \square

For more regular \mathbf{E}_0 , the following stability result can be obtained.

Lemma 5.5 *Assume $\mathbf{E}_0 \in \mathbf{V}_0$. Then*

$$\|\nabla \times \mathbf{e}_j\|^2 + \sum_{i=1}^j \|\nabla \times (\mathbf{e}_i - \mathbf{e}_{i-1})\|^2 \leq \|\nabla \times \mathbf{E}_0\|^2$$

holds for any $j = 1, \dots, n$.

Proof Setting $\varphi = \mathbf{e}_i - \mathbf{e}_{i-1}$ in (5.6) and summing up for $i = 1, \dots, j$ we get

$$\sum_{i=1}^j (\delta \mathbf{J}(\mathbf{e}_i), \delta \mathbf{e}_i) \tau + \sum_{i=1}^j (\nabla \times \mathbf{e}_i, \nabla \times (\mathbf{e}_i - \mathbf{e}_{i-1})) = 0.$$

The monotonicity of $\mathbf{J}(\mathbf{e})$, together with the algebraic identity

$$\sum_{j=1}^n a_j(a_j - a_{j-1}) = \frac{1}{2} \left[a_n^2 - a_0^2 + \sum_{j=1}^n (a_j - a_{j-1})^2 \right], \quad (5.10)$$

implies

$$\|\nabla \times \mathbf{e}_j\|^2 + \sum_{i=1}^j \|\nabla \times (\mathbf{e}_i - \mathbf{e}_{i-1})\|^2 \leq \|\nabla \times \mathbf{E}_0\|^2,$$

which concludes the proof. \square

Using Lemmas 5.4 and 5.5, the following a priori estimates for $\delta\mathbf{J}(\mathbf{e}_i)$ can be derived.

Lemma 5.6 (i) *Assume that $\mathbf{E}_0 \in \mathbf{L}_{2-1/p}(\Omega)$. Then there exists a positive C such that*

$$\sum_{i=1}^n \|\delta\mathbf{J}(\mathbf{e}_i)\|_{\mathbf{V}_0^*}^2 \tau \leq C.$$

(ii) *Assume that $\mathbf{E}_0 \in \mathbf{V}_0$. Then there exists a positive C such that*

$$\|\delta\mathbf{J}(\mathbf{e}_i)\|_{\mathbf{V}_0^*} \leq C$$

for any $i = 1, \dots, n$.

Proof We remind the definition of the norm in \mathbf{V}_0^*

$$\|\mathbf{z}\|_{\mathbf{V}_0^*} = \sup_{\boldsymbol{\varphi} \in \mathbf{V}_0} \frac{|(\mathbf{z}, \boldsymbol{\varphi})|}{\|\boldsymbol{\varphi}\|_{\mathbf{V}}}.$$

Further we can write for any $\boldsymbol{\varphi} \in \mathbf{V}_0$

$$(\delta\mathbf{J}(\mathbf{e}_i), \boldsymbol{\varphi}) = -(\nabla \times \mathbf{e}_i, \nabla \times \boldsymbol{\varphi}).$$

Applying the Cauchy inequality we see that

$$|(\delta\mathbf{J}(\mathbf{e}_i), \boldsymbol{\varphi})| \leq \|\nabla \times \mathbf{e}_i\| \|\nabla \times \boldsymbol{\varphi}\|$$

and

$$\|\delta\mathbf{J}(\mathbf{e}_i)\|_{\mathbf{V}_0^*} = \sup_{\boldsymbol{\varphi} \in \mathbf{V}_0} \frac{|(\delta\mathbf{J}(\mathbf{e}_i), \boldsymbol{\varphi})|}{\|\boldsymbol{\varphi}\|_{\mathbf{V}}} \leq \|\nabla \times \mathbf{e}_i\|.$$

The rest of the proof readily follows from Lemmas 5.4 and 5.5. \square

5.3 Convergence

We introduce the vector fields \mathbf{e}_n and \mathbf{j}_n , piecewise linear in time, given by

$$\begin{aligned}\mathbf{e}_n(0) &= \mathbf{E}_0, \\ \mathbf{e}_n(t) &= \mathbf{e}_{i-1} + (t - t_{i-1})\delta\mathbf{e}_i \quad \text{for } t \in (t_{i-1}, t_i], \quad i = 1, \dots, n\end{aligned}$$

and

$$\begin{aligned}\mathbf{j}_n(0) &= \mathbf{J}(\mathbf{E}_0), \\ \mathbf{j}_n(t) &= \mathbf{J}(\mathbf{e}_{i-1}) + (t - t_{i-1})\delta\mathbf{J}(\mathbf{e}_i) \quad \text{for } t \in (t_{i-1}, t_i], \quad i = 1, \dots, n.\end{aligned}$$

Next, we define the step vector field $\bar{\mathbf{e}}_n$

$$\bar{\mathbf{e}}_n(0) = \mathbf{E}_0, \quad \bar{\mathbf{e}}_n(t) = \mathbf{e}_i \quad \text{for } t \in (t_{i-1}, t_i], \quad i = 1, \dots, n.$$

Using the new notation we rewrite (5.6) as

$$(\partial_t \mathbf{j}_n, \boldsymbol{\varphi}) + (\nabla \times \bar{\mathbf{e}}_n, \nabla \times \boldsymbol{\varphi}) = 0 \quad \forall \boldsymbol{\varphi} \in \mathbf{V}_0. \quad (5.11)$$

Now, we are in a position to prove the convergence of an approximate solution to a weak solution of (5.1).

Theorem 5.7 *Suppose $\mathbf{E}_0 \in \mathbf{V}_0$. Then there exists a vector field \mathbf{e} such that*

- (i) $\bar{\mathbf{e}}_n \rightharpoonup \mathbf{e}$ in $L_{2-1/p}((0, T), \mathbf{L}_{2-1/p}(\Omega))$
- (ii) $\nabla \times \bar{\mathbf{e}}_n \rightharpoonup \nabla \times \mathbf{e}$ in $L_2((0, T), \mathbf{L}_2(\Omega))$
- (iii) $\mathbf{J}(\bar{\mathbf{e}}_n) \rightharpoonup \mathbf{J}(\mathbf{e})$ in $L_q((0, T), \mathbf{L}_q(\Omega))$
- (iv) \mathbf{e} is a weak solution of (5.1).

The convergence is meant in the sense of subsequences, i.e. it is valid for a subsequence, which is denoted again by the same symbol as the whole sequence.

Proof The proof is worked out in several steps.

(i) and (ii)

The spaces $L_{2-1/p}((0, T), \mathbf{L}_{2-1/p}(\Omega))$ and $L_2((0, T), \mathbf{L}_2(\Omega))$ are reflexive. The sequences $\{\bar{\mathbf{e}}_n\}$ and $\{\nabla \times \bar{\mathbf{e}}_n\}$ are bounded thanks to the stability results from Lemmas 5.4 and 5.5. So we can use Theorem 1 from [74, p.126] and we obtain that there exist $\mathbf{e} \in L_{2-1/p}((0, T), \mathbf{L}_{2-1/p}(\Omega))$ and $\mathbf{z} \in L_2((0, T), \mathbf{L}_2(\Omega))$ such

that $\bar{\mathbf{e}}_n \rightharpoonup \mathbf{e}$ in $L_{2-1/p}((0, T), \mathbf{L}_{2-1/p}(\Omega))$ and $\nabla \times \bar{\mathbf{e}}_n \rightharpoonup \mathbf{z}$ in $L_2((0, T), \mathbf{L}_2(\Omega))$. Further, for any $\varphi \in \mathbf{C}_0^\infty(\Omega)$ we have

$$\begin{aligned} \int_0^T (\nabla \times \bar{\mathbf{e}}_n, \varphi) &= \int_0^T (\bar{\mathbf{e}}_n, \nabla \times \varphi) \\ \int_0^T (\mathbf{z}, \varphi) &\stackrel{\downarrow}{=} \int_0^T (\mathbf{e}, \nabla \times \varphi) = \int_0^T (\nabla \times \mathbf{e}, \varphi). \end{aligned}$$

According to the Hahn-Banach theorem we conclude that $\mathbf{z} = \nabla \times \mathbf{e}$.

(iii)

Lemma 5.4, together with the identity

$$\int_{\Omega} |\bar{\mathbf{e}}_n|^{2-1/p} = \int_{\Omega} |\mathbf{J}(\bar{\mathbf{e}}_n)|^q,$$

implies

$$\mathbf{J}(\bar{\mathbf{e}}_n) \rightharpoonup \mathbf{w}, \quad \text{in } L_q((0, T), \mathbf{L}_q(\Omega)).$$

We integrate (5.11) twice over the time and we pass to the limit (for a subsequence) as $n \rightarrow \infty$. We obtain

$$\int_0^t (\mathbf{w}, \varphi) + \int_0^t \left(\int_0^s \nabla \times \mathbf{e}, \nabla \times \varphi \right) = \int_0^t (\mathbf{J}(\mathbf{E}_0), \varphi) \quad (5.12)$$

for any $\varphi \in \mathbf{V}_0$ and $t, s \in [0, T]$.

Now, we would like to show that $\mathbf{w} = \mathbf{J}(\mathbf{e})$. We use the monotone structure of the non-linear operator $\mathbf{J}(\mathbf{e})$ and the Minty-Browder trick (cf. [26, Section 0.1] or [27, Section 5.A.3.]). We have

$$\int_0^T (\mathbf{J}(\bar{\mathbf{e}}_n) - \mathbf{J}(\mathbf{u}), \bar{\mathbf{e}}_n - \mathbf{u}) \geq 0, \quad (5.13)$$

which is valid for any $\mathbf{u} \in L_{2-1/p}((0, T), \mathbf{L}_{2-1/p}(\Omega))$.

The following holds

$$\mathbf{j}_n(t) = \mathbf{J}(\bar{\mathbf{e}}_n(t)) + (t - t_{i-1} - \tau) \partial_t \mathbf{j}_n(t). \quad (5.14)$$

Thus,

$$\int_0^T (\mathbf{j}_n, \bar{\mathbf{e}}_n) = \int_0^T (\mathbf{J}(\bar{\mathbf{e}}_n), \bar{\mathbf{e}}_n) + \int_0^T (t - t_{i-1} - \tau) (\partial_t \mathbf{j}_n, \bar{\mathbf{e}}_n).$$

According to Lemma 5.6 we obtain

$$\lim_{n \rightarrow \infty} \int_0^T (\mathbf{j}_n, \bar{\mathbf{e}}_n) = \lim_{n \rightarrow \infty} \int_0^T (\mathbf{J}(\bar{\mathbf{e}}_n), \bar{\mathbf{e}}_n).$$

Next, using the previous identity and the property (3.4) of the weak-convergent sequences, we successively deduce that

$$\begin{aligned} \lim_{n \rightarrow \infty} \int_0^T (\mathbf{J}(\bar{\mathbf{e}}_n), \bar{\mathbf{e}}_n) &= \lim_{n \rightarrow \infty} \int_0^T (\mathbf{j}_n, \bar{\mathbf{e}}_n) \\ &\stackrel{(5.11)}{=} \lim_{n \rightarrow \infty} \left[\int_0^T (\mathbf{J}(\mathbf{E}_0), \bar{\mathbf{e}}_n) - \int_0^T \left(\int_0^t \nabla \times \bar{\mathbf{e}}_n, \nabla \times \bar{\mathbf{e}}_n \right) \right] \\ &= \int_0^T (\mathbf{J}(\mathbf{E}_0), \mathbf{e}) - \frac{1}{2} \lim_{n \rightarrow \infty} \left\| \int_0^T \nabla \times \bar{\mathbf{e}}_n \right\|^2 \\ &\leq \int_0^T (\mathbf{J}(\mathbf{E}_0), \mathbf{e}) - \frac{1}{2} \left\| \int_0^T \nabla \times \mathbf{e} \right\|^2 \\ &= \int_0^T (\mathbf{J}(\mathbf{E}_0), \mathbf{e}) - \int_0^T \left(\int_0^t \nabla \times \mathbf{e}, \nabla \times \mathbf{e} \right) \\ &\stackrel{(5.12)}{=} \int_0^T (\mathbf{w}, \mathbf{e}). \end{aligned}$$

Passing to the limit for $n \rightarrow \infty$ in (5.13) we get

$$\int_0^T (\mathbf{w} - \mathbf{J}(\mathbf{u}), \mathbf{e} - \mathbf{u}) \geq 0.$$

By substituting $\mathbf{u} = \mathbf{e} + \varepsilon \mathbf{v}$ for any \mathbf{v} and $\varepsilon > 0$ we obtain

$$\int_0^T (\mathbf{w} - \mathbf{J}(\mathbf{e} + \varepsilon \mathbf{v}), \mathbf{v}) \leq 0.$$

Considering the limit case $\varepsilon \rightarrow 0$ we see that

$$\int_0^T (\mathbf{w} - \mathbf{J}(\mathbf{e}), \mathbf{v}) \leq 0.$$

Finally we put $\mathbf{v} = \mathbf{w} - \mathbf{J}(\mathbf{e})$ and we can deduce that

$$\mathbf{w} = \mathbf{J}(\mathbf{e}) \quad \text{a.e. in } \Omega \times (0, T).$$

(iv)

According to (5.14) and Lemma 5.6 we can write that

$$\lim_{n \rightarrow \infty} \int_0^t (\mathbf{j}_n, \varphi) = \lim_{n \rightarrow \infty} \int_0^t (\mathbf{J}(\bar{\mathbf{e}}_n), \varphi) = \int_0^t (\mathbf{J}(\mathbf{e}), \varphi).$$

A priori estimates imply the equicontinuity and equiboundedness of $\mathbf{j}_n(t)$, i.e.

$$\begin{aligned} (\mathbf{j}_n(t), \varphi) - (\mathbf{j}_n(s), \varphi) &= \int_s^t (\partial_t \mathbf{j}_n, \varphi) \leq \int_s^t \|\partial_t \mathbf{j}_n\|_{\mathbf{V}_0^*} \|\varphi\|_{\mathbf{V}_0} \\ &\leq C|t - s| \|\varphi\|_{\mathbf{V}_0} \end{aligned}$$

and

$$|(\mathbf{j}_n(t), \varphi)| \leq C \|\varphi\|_{\mathbf{V}_0}.$$

Therefore, from [49, Theorem 1.6.9] for any $t \in (0, T)$ and $\varphi \in \mathbf{V}_0$ holds that $(\mathbf{j}_n(t), \varphi) \rightarrow (\mathbf{J}(\mathbf{e}(t)), \varphi)$.

Now, let us integrate (5.11) over $(0, t)$ for any $t \in (0, T)$. We have

$$(\mathbf{j}_n(t), \varphi) + \int_0^t (\nabla \times \bar{\mathbf{e}}_n, \nabla \times \varphi) = (\mathbf{J}(\mathbf{E}_0), \varphi) \quad \forall \varphi \in \mathbf{V}_0. \quad (5.15)$$

Passing to the limit for $n \rightarrow \infty$ we arrive at

$$(\mathbf{J}(\mathbf{e}(t)), \varphi) + \int_0^t (\nabla \times \mathbf{e}, \nabla \times \varphi) = (\mathbf{J}(\mathbf{E}_0), \varphi) \quad \forall \varphi \in \mathbf{V}_0. \quad (5.16)$$

We remind that $\mathbf{J}(\mathbf{e}(t))$ exists in all points of $[0, T]$ and it has a derivative a.e. in $[0, T]$. This follows from the relation

$$\begin{aligned} (\mathbf{j}_n(t), \varphi) - (\mathbf{j}_n(0), \varphi) &= \int_0^t (\partial_t \mathbf{j}_n, \varphi) \\ \downarrow & \qquad \qquad \qquad \downarrow \\ (\mathbf{J}(\mathbf{e}(t)), \varphi) - (\mathbf{J}(\mathbf{E}_0), \varphi) &= \int_0^t (\mathbf{z}, \varphi) \end{aligned},$$

which means that $\mathbf{z} = \partial_t \mathbf{J}(\mathbf{e}) \in L_q((0, T), \mathbf{L}_q(\Omega))$.

Now, we differentiate the identity (5.16) with respect to the time variable to conclude the proof. \square

The convergence of the approximate solution was proven in Theorem 5.7 only for a subsequence of $\{\bar{\mathbf{e}}_n\}$. If we now take into account Lemma 5.1, we obtain the convergence of the whole sequence $\{\bar{\mathbf{e}}_n\}$ to the unique weak solution of (5.1) in corresponding spaces.

5.4 Proof of the convergence using a new version of Murat and Tartar's div-curl lemma

In this section, the convergence of the approximation scheme (5.6) is studied using a new version of Murat and Tartar's div-curl lemma [54,68] also known as compensated compactness criterion. It leads to the convergence of the backward Euler method to the solution to the problem (5.1) in the interior of the domain Ω .

First, two new variations of the div-curl lemma are stated and proven. These results will be presented on the conference NumAn 2008 [40]. In Section 5.4.3, we employ the lemmas to prove the convergence of the approximation scheme (5.6).

5.4.1 New steady-state div-curl lemma

Lemma 5.8 is a generalization of the famous steady-state div-curl lemma to the more specific function spaces.

Lemma 5.8 *Let $\Omega \subset \mathbb{R}^3$ be open, bounded and $\Omega \in C^2$. Let $p \in (1, 2]$. Assume that $\{\mathbf{v}_k\}_{k=1}^\infty$ is a sequence in $\mathbf{L}_q(\Omega)$ and $\{\mathbf{w}_k\}_{k=1}^\infty$ is a sequence in \mathbf{V}_0 such that*

$$(i) \quad \|\mathbf{w}_k\|_{2-1/p} + \|\nabla \times \mathbf{w}_k\| \leq C,$$

$$(ii) \quad \|\mathbf{v}_k\|_q + \|\nabla \cdot \mathbf{v}_k\|_q \leq C.$$

Suppose further

$$\mathbf{v}_k \rightharpoonup \mathbf{v} \quad \text{in } \mathbf{L}_q(\Omega)$$

and

$$\mathbf{w}_k \rightharpoonup \mathbf{w} \quad \text{in } \mathbf{V}_0.$$

Then

$$\lim_{k \rightarrow \infty} \langle \Phi \mathbf{w}_k, \mathbf{v}_k \rangle = \langle \Phi \mathbf{w}, \mathbf{v} \rangle$$

for any $\Phi \in C_0^\infty(\overline{\Omega})$.

Proof Consider for each $k = 1, 2, \dots$ the vector field \mathbf{u}_k solving

$$\begin{aligned} -\Delta \mathbf{u}_k &= \mathbf{v}_k && \text{in } \Omega, \\ \mathbf{u}_k &= \mathbf{0} && \text{on } \Gamma. \end{aligned} \tag{5.17}$$

As $q > 2$ (since $p > 1$), $\mathbf{v}_k \in \mathbf{L}_q(\Omega)$ implies $\mathbf{v}_k \in \mathbf{L}_2(\Omega)$ and from the Lax–Milgram theorem, we get that there exists unique $\mathbf{u}_k \in \mathbf{W}_0^{1,2}(\Omega)$ —solution to

the equation (5.17). From [28, Theorem 8.12], we obtain that \mathbf{u}_k belongs to $\mathbf{W}_0^{2,2}(\Omega)$. In addition, we can use higher regularity of \mathbf{v}_k . We invoke [41, Theorem 9.2.1.] and we deduce, that

$$\mathbf{u}_k \in \mathbf{W}_0^{2,q}(\Omega). \quad (5.18)$$

From Rellich-Kondrachov theorem [1, Theorem 6.2] and the fact that $q > 2$, we deduce that

$$\mathbf{W}_0^{2,q}(\Omega) \hookrightarrow \mathbf{W}^{1,q}(\Omega') \quad (5.19)$$

for any bounded subdomain $\Omega' \subset \Omega$. This, together with the relation (5.18), implies the relative compactness of the sequence $\{\mathbf{u}_k\}$ in $\mathbf{W}^{1,q}(\Omega')$. Therefore there exists a subsequence of the sequence $\{\mathbf{u}_k\}$ (denoted again by the same symbol) strongly converging to some element of the space $\mathbf{W}^{1,q}(\Omega')$, i.e.

$$\mathbf{u}_k \rightarrow \mathbf{u} \text{ in } \mathbf{W}^{1,q}(\Omega') \quad (5.20)$$

and thus

$$\nabla \times \mathbf{u}_k \rightarrow \nabla \times \mathbf{u} \text{ in } \mathbf{L}^q(\Omega'), \quad (5.21)$$

where $\mathbf{u} \in \mathbf{W}_0^{2,2}(\Omega)$ solves

$$\begin{aligned} -\Delta \mathbf{u} &= \mathbf{v} && \text{in } \Omega, \\ \mathbf{u} &= \mathbf{0} && \text{on } \Gamma. \end{aligned} \quad (5.22)$$

The last has been obtained from (5.17) by passing to the limit for $k \rightarrow \infty$. We can derive as well, that $\mathbf{u} \in \mathbf{W}_0^{2,q}(\Omega)$.

One can also see that the function \mathbf{z}_k given by $\mathbf{z}_k = \nabla \cdot \mathbf{u}_k$ solves

$$\begin{aligned} -\Delta \mathbf{z}_k &= \nabla \cdot \mathbf{v}_k && \text{in } \Omega, \\ \mathbf{z}_k &= \nabla \cdot \mathbf{u}_k && \text{on } \Gamma. \end{aligned} \quad (5.23)$$

As $\mathbf{u}_k \in \mathbf{W}^{2,2}(\Omega)$, it holds that $\nabla \cdot \mathbf{u}_k \in \mathbf{W}^{1,2}(\Omega) \hookrightarrow \mathbf{L}^4(\Gamma)$ and the boundary condition is well-posed.

Similar reasoning as for the solution to the equation (5.17) leads to the following regularity of the solution \mathbf{z}_k to the equation (5.23): $\mathbf{z}_k \in \mathbf{W}^{1,2}(\Omega)$, $\mathbf{z}_k \in \mathbf{W}^{2,2}(\Omega)$ and $\mathbf{z}_k \in \mathbf{W}^{2,q}(\Omega)$. Further, according to (5.19), the relative compactness of the sequence $\{\nabla \cdot \mathbf{u}_k\}$ in $\mathbf{W}^{1,q}(\Omega')$ is obtained. Therefore, upon passing to the subsequence if necessary, we have

$$\nabla \cdot \mathbf{u}_k \rightarrow \nabla \cdot \mathbf{u} \text{ in } \mathbf{W}^{1,q}(\Omega') \quad (5.24)$$

and thus

$$\nabla(\nabla \cdot \mathbf{u}_k) \rightarrow \nabla(\nabla \cdot \mathbf{u}) \text{ in } \mathbf{L}^q(\Omega'). \quad (5.25)$$

Now, using the identity

$$-\Delta \mathbf{M} = \nabla \times (\nabla \times \mathbf{M}) - \nabla(\nabla \cdot \mathbf{M}),$$

which is valid for any vector \mathbf{M} , we can write for arbitrary $\Phi \in C_0^\infty(\overline{\Omega})$

$$\begin{aligned} \langle \Phi \mathbf{w}_k, \mathbf{v}_k \rangle &= \langle \Phi \mathbf{w}_k, -\Delta \mathbf{u}_k \rangle \\ &= \langle \Phi \mathbf{w}_k, \nabla \times \nabla \times \mathbf{u}_k \rangle - \langle \Phi \mathbf{w}_k, \nabla(\nabla \cdot \mathbf{u}_k) \rangle \\ &= \langle \nabla \times (\Phi \mathbf{w}_k), \nabla \times \mathbf{u}_k \rangle - \langle \Phi \mathbf{w}_k, \nabla(\nabla \cdot \mathbf{u}_k) \rangle \\ &= \langle \Phi \nabla \times \mathbf{w}_k, \nabla \times \mathbf{u}_k \rangle + \langle \nabla \Phi \times \mathbf{w}_k, \nabla \times \mathbf{u}_k \rangle \\ &\quad - \langle \Phi \mathbf{w}_k, \nabla(\nabla \cdot \mathbf{u}_k) \rangle. \end{aligned}$$

According to (5.20), (5.21), (5.24) and (5.25) we obtain

$$\begin{aligned} \langle \Phi \mathbf{w}_k, \mathbf{v}_k \rangle &\rightarrow \langle \Phi \nabla \times \mathbf{w}, \nabla \times \mathbf{u} \rangle + \langle \nabla \Phi \times \mathbf{w}, \nabla \times \mathbf{u} \rangle \\ &\quad - \langle \Phi \mathbf{w}, \nabla(\nabla \cdot \mathbf{u}) \rangle \\ &= \langle \nabla \times (\Phi \mathbf{w}), \nabla \times \mathbf{u} \rangle - \langle \Phi \mathbf{w}, \nabla(\nabla \cdot \mathbf{u}) \rangle \\ &= \langle \Phi \mathbf{w}, \nabla \times \nabla \times \mathbf{u} \rangle - \langle \Phi \mathbf{w}, \nabla(\nabla \cdot \mathbf{u}) \rangle \\ &= \langle \Phi \mathbf{w}, -\Delta \mathbf{u} \rangle \\ &= \langle \Phi \mathbf{w}, \mathbf{v} \rangle, \end{aligned}$$

which concludes the proof. \square

5.4.2 New time-dependent div-curl lemma

In the next variation of the div-curl lemma, the time variable is also involved. Similar result (in different spaces) can be found in [64].

Lemma 5.9 *Let $\Omega \subset \mathbb{R}^3$ be open, bounded and $\Omega \in C^2$. Let $p \in (1, 2]$. Let $\{\mathbf{v}_n\}_{n=1}^\infty$ be a sequence in $L_2((0, T), \mathbf{L}_q(\Omega))$ and $\{\mathbf{w}_n\}_{n=1}^\infty$ a sequence in $L_2((0, T), \mathbf{V}_0)$ such that*

$$(i) \int_0^T \left[\|\mathbf{w}_n\|_{2-1/p}^2 + \|\nabla \times \mathbf{w}_n\|^2 \right] \leq C,$$

$$(ii) \int_0^T \left[\|\mathbf{v}_n\|_q^2 + \|\nabla \cdot \mathbf{v}_n\|_q^2 + \|\partial_t \mathbf{v}_n\|_{\mathbf{V}_0^*}^2 \right] \leq C.$$

Suppose further

$$\mathbf{v}_n \rightharpoonup \mathbf{v} \quad \text{in } L_2((0, T), \mathbf{L}_q(\Omega))$$

and

$$\mathbf{w}_n \rightharpoonup \mathbf{w} \quad \text{in } L_2((0, T), \mathbf{V}_0).$$

Then

$$\lim_{n \rightarrow \infty} \int_0^T \langle \Phi \mathbf{w}_n, \mathbf{v}_n \rangle = \int_0^T \langle \Phi \mathbf{w}, \mathbf{v} \rangle$$

for any $\Phi \in C_0^\infty(\overline{\Omega})$.

Proof The proof is similar to the proof of Lemma 5.8. However, the important steps will be repeated in order to avoid confusion.

Consider for each $n = 1, 2, \dots$ the vector field \mathbf{u}_n solving

$$\begin{aligned} -\Delta \mathbf{u}_n &= \mathbf{v}_n && \text{in } \Omega, \\ \mathbf{u}_n &= \mathbf{0} && \text{on } \Gamma. \end{aligned} \quad (5.26)$$

As $q > 2$ (since $p > 1$), $\mathbf{v}_n \in \mathbf{L}_q(\Omega)$ implies $\mathbf{v}_n \in \mathbf{L}_2(\Omega)$ and from the Lax–Milgram theorem we get that there exists unique $\mathbf{u}_n \in \mathbf{W}_0^{1,2}(\Omega)$ —solution to the equation (5.17). From [28, Theorem 8.12] we obtain that \mathbf{u}_n belongs to $\mathbf{W}^{2,2}(\Omega)$. In addition, we can use higher regularity of \mathbf{v}_n . We invoke [41, Theorem 9.2.1.] and we deduce that $\mathbf{u}_n \in \mathbf{W}^{2,q}(\Omega)$. This is valid with t as a parameter, so

$$\mathbf{u}_n \in L_2((0, T), \mathbf{W}^{2,q}(\Omega)). \quad (5.27)$$

Equation (5.26) can be differentiated with respect to the time variable and we get

$$\begin{aligned} -\Delta \partial_t \mathbf{u}_n &= \partial_t \mathbf{v}_n && \text{in } \Omega, \\ \partial_t \mathbf{u}_n &= \mathbf{0} && \text{on } \Gamma. \end{aligned} \quad (5.28)$$

Using Lemma 3.4, $\partial_t \mathbf{v}_n \in \mathbf{V}_0^*$ implies $\partial_t \mathbf{v}_n \in \mathbf{H}^{-1}$ and from the Lax–Milgram theorem, we get that there exists unique $\partial_t \mathbf{u}_n \in \mathbf{H}_0^1(\Omega)$ —solution to the equation (5.28). We conclude that

$$\partial_t \mathbf{u}_n \in L_2((0, T), \mathbf{H}^1(\Omega)). \quad (5.29)$$

The relations (5.27), (5.29) and [43, Lemma 1.3.8], together with the fact that

$$\mathbf{W}^{2,q}(\Omega) \hookrightarrow \mathbf{W}^{1,q}(\Omega') \hookrightarrow \mathbf{H}^1(\Omega')$$

for any bounded subdomain $\Omega' \subset \Omega$, implies the relative compactness of the sequence $\{\mathbf{u}_n\}$ in $L_2((0, T), \mathbf{W}^{1,q}(\Omega'))$. This means that there exists a subsequence of the sequence $\{\mathbf{u}_n\}$ strongly converging to some element of the space $L_2((0, T), \mathbf{W}^{1,q}(\Omega'))$, i.e.

$$\mathbf{u}_n \rightarrow \mathbf{u} \text{ in } L_2((0, T), \mathbf{W}^{1,q}(\Omega')), \quad (5.30)$$

where $\mathbf{u} \in L_2((0, T), \mathbf{W}^{2,2}(\Omega))$ solves

$$\begin{aligned} -\Delta \mathbf{u} &= \mathbf{v} && \text{in } \Omega, \\ \mathbf{u} &= \mathbf{0} && \text{on } \Gamma. \end{aligned} \quad (5.31)$$

The last has been obtained from (5.26) by passing to the limit for $k \rightarrow \infty$. We can derive as well, that $\mathbf{u} \in L_2((0, T), \mathbf{W}^{2,q}(\Omega))$.

One can also see that $\mathbf{z}_n = \nabla \cdot \mathbf{u}_n$ solves

$$\begin{aligned} -\Delta \mathbf{z}_n &= \nabla \cdot \mathbf{v}_n && \text{in } \Omega, \\ \mathbf{z}_n &= \nabla \cdot \mathbf{u}_n && \text{on } \Gamma. \end{aligned} \quad (5.32)$$

As $\mathbf{u}_n \in \mathbf{W}^{2,2}(\Omega)$, so $\nabla \cdot \mathbf{u}_n \in \mathbf{W}^{1,2}(\Omega) \hookrightarrow \mathbf{L}_4(\Gamma)$ and the boundary condition is well-posed.

Similarly as before for the solution to the equation (5.26), we get that $\mathbf{z}_n \in L_2((0, T), \mathbf{W}^{1,2}(\Omega))$, $\mathbf{z}_n \in L_2((0, T), \mathbf{W}^{2,2}(\Omega))$ and $\mathbf{z}_n \in L_2((0, T), \mathbf{W}^{2,q}(\Omega))$. From the relation (5.29), we deduce that $\partial_t \nabla \cdot \mathbf{u}_n \in L_2((0, T), \mathbf{L}_2(\Omega))$. This, together with the embedding

$$\mathbf{W}^{2,q} \hookrightarrow \mathbf{W}^{1,q} \hookrightarrow \mathbf{L}_2(\Omega),$$

gives the relative compactness of the sequence $\{\nabla \cdot \mathbf{u}_n\}$ in $L_2((0, T), \mathbf{W}^{1,q}(\Omega'))$. Therefore, upon passing to the subsequence if necessary, we have

$$\nabla \cdot \mathbf{u}_n \rightarrow \nabla \cdot \mathbf{u} \text{ in } L_2((0, T), \mathbf{W}^{1,q}(\Omega')). \quad (5.33)$$

The rest of the proof is almost identical with the one of Lemma 5.8. \square

5.4.3 Convergence

The following lemma assures the stability of $\nabla \cdot \mathbf{J}(\mathbf{e}_{i,k})$ in $\mathbf{L}_q(\Omega)$, which is important in order to satisfy the assumptions of Lemma 5.9.

Lemma 5.10 *Assume that $\mathbf{E}_0 \in \mathbf{C}_0^\infty(\Omega)$ and that there exists $C > 0$ such that $\|\nabla \cdot \mathbf{J}(\mathbf{E}_0)\|_q \leq C$. Let \mathbf{e}_i be the solution to (5.6). Then*

$$\|\nabla \cdot (\mathbf{J}(\mathbf{e}_i))\|_q \leq C$$

for any $i = 1, \dots, n$.

Proof If $\Phi \in \mathbf{C}_0^\infty(\bar{\Omega})$ then $\nabla\Phi \in \mathbf{C}_0^\infty(\bar{\Omega}) \subset \mathbf{V}_0$. Therefore, we can set $\varphi = \nabla\Phi$ into (5.6) and since $\nabla \times \nabla\Phi = \mathbf{0}$, we recursively obtain

$$\langle \mathbf{J}(\mathbf{e}_i), \nabla\Phi \rangle = \langle \mathbf{J}(\mathbf{E}_0), \nabla\Phi \rangle.$$

Using Green's formula, we get

$$\langle \nabla \cdot \mathbf{J}(\mathbf{e}_i), \Phi \rangle = \langle \nabla \cdot \mathbf{J}(\mathbf{E}_0), \Phi \rangle.$$

This last equality is valid for all $\Phi \in \mathbf{C}_0^\infty(\bar{\Omega})$. Using the density of $\mathbf{C}_0^\infty(\bar{\Omega})$ in $\mathbf{L}_{2-1/p}(\Omega)$ [49] and the assumption on the $\nabla \cdot \mathbf{J}(\mathbf{E}_0)$, we can deduce that $\nabla \cdot \mathbf{J}(\mathbf{e}_i) = \nabla \cdot \mathbf{J}(\mathbf{E}_0)$ in $\mathbf{L}_q(\Omega)$. The statement of the lemma follows directly from this last equality. \square

Now, we can proceed to the proof of the convergence of the sequence of approximate solutions $\{\bar{\mathbf{e}}_n\}$. The following theorem holds for a subsequence, which is denoted again by the same symbol as the whole sequence.

Theorem 5.11 *Let the assumptions of Lemma 5.10 be fulfilled. Then the following holds:*

- (i) $\bar{\mathbf{e}}_n \rightharpoonup \mathbf{E}$ in $L_2((0, T), \mathbf{L}_{2-1/p}(\Omega))$,
- (ii) $\bar{\mathbf{e}}_n \rightharpoonup \mathbf{E}$ in $L_2((0, T), \mathbf{V}_0)$,
- (iii) $\bar{\mathbf{j}}_n - \mathbf{j}_n \rightarrow \mathbf{0}$ in $L_2((0, T), \mathbf{V}_0^*)$,
- (iv) $\mathbf{j}_n \rightharpoonup \mathbf{J}(\mathbf{E})$ in $L_2((0, T), \mathbf{L}_q(\Omega))$,
- (v) $\langle \mathbf{j}_n(t), \varphi \rangle \rightarrow \langle \mathbf{J}(\mathbf{E}(t)), \varphi \rangle$ for all $t \in [0, T]$ and $\varphi \in \mathbf{C}_0^\infty(\Omega)$,
- (vi) \mathbf{E} is a weak solution to (1.15).

Proof (i) and (ii) – as in the proof of Theorem 5.7.

(iii)

The norm in $L_2((0, T), \mathbf{V}_0^*)$ is defined as follows

$$\|u\|_{L_2((0, T), \mathbf{V}_0^*)} := \left(\int_0^T \|u\|_{\mathbf{V}_0^*}^2 \right)^{1/2}.$$

Using the stability result for $\delta\mathbf{J}(\mathbf{e}_i)$ we deduce

$$\begin{aligned} |\langle \bar{\mathbf{j}}_n - \mathbf{j}_n, \boldsymbol{\varphi} \rangle| &\leq C\tau \|\delta\mathbf{J}(\mathbf{e}_i)\|_{\mathbf{V}_0^*} \|\boldsymbol{\varphi}\|_{\mathbf{V}} \\ &\leq C\tau \|\boldsymbol{\varphi}\|_{\mathbf{V}}. \end{aligned}$$

The rest of the proof is straightforward.

(iv)

Let $\Phi \in \mathbf{C}_0^\infty(\Omega)$ be nonnegative. Using the monotonicity of the operator \mathbf{J} we can write

$$\int_0^T \langle \mathbf{J}(\bar{\mathbf{e}}_n) - \mathbf{J}(\mathbf{u}), \Phi(\bar{\mathbf{e}}_n - \mathbf{u}) \rangle \geq 0 \quad (5.34)$$

for any $\mathbf{u} \in L_2((0, T), \mathbf{L}_{2-1/p}(\Omega))$. Now, we will examine the asymptotic behaviour of each part of this duality separately. First, we have

$$\begin{aligned} \int_0^T \langle \mathbf{J}(\bar{\mathbf{e}}_n), \Phi \bar{\mathbf{e}}_n \rangle &= \int_0^T \langle \bar{\mathbf{j}}_n, \Phi \bar{\mathbf{e}}_n \rangle \\ &= \int_0^T \langle \bar{\mathbf{j}}_n - \mathbf{j}_n, \Phi \bar{\mathbf{e}}_n \rangle + \int_0^T \langle \mathbf{j}_n, \Phi \bar{\mathbf{e}}_n \rangle. \end{aligned}$$

Therefore, using (iii) and Lemmas 5.4 and 5.5 we obtain

$$\lim_{n \rightarrow \infty} \int_0^T \langle \mathbf{J}(\bar{\mathbf{e}}_n), \Phi \bar{\mathbf{e}}_n \rangle = \lim_{n \rightarrow \infty} \int_0^T \langle \mathbf{j}_n, \Phi \bar{\mathbf{e}}_n \rangle.$$

Next, using Lemmas 5.4, 5.5 and 5.10 we see that the assumptions of the time-dependent div-curl lemma are fulfilled for $\mathbf{w}_n = \bar{\mathbf{e}}_n$ and $\mathbf{v}_n = \mathbf{j}_n$. We can write

$$\int_0^T \langle \mathbf{j}_n, \Phi \bar{\mathbf{e}}_n \rangle \rightarrow \int_0^T \langle \mathbf{a}, \Phi \mathbf{E} \rangle,$$

where

$$\mathbf{j}_n \rightharpoonup \mathbf{a} \text{ in } L_2((0, T), \mathbf{L}_q(\Omega)). \quad (5.35)$$

This limit exists for some subsequence, as the sequence $\{\mathbf{j}_n\}$ is bounded in the reflexive space $L_2((0, T), \mathbf{L}_q(\Omega))$.

Further, the space $L_2((0, T), \mathbf{C}_0^\infty(\Omega))$ is dense in $L_2((0, T), \mathbf{L}_{2-1/p}(\Omega))$. Thus, for any $\varepsilon > 0$ there exists $\mathbf{u}_\varepsilon \in L_2((0, T), \mathbf{C}_0^\infty(\Omega))$ such that

$$\|\mathbf{u} - \mathbf{u}_\varepsilon\|_{L_2((0, T), \mathbf{L}_{2-1/p}(\Omega))} \leq \varepsilon.$$

Then we have

$$\begin{aligned} \int_0^T \langle \mathbf{J}(\bar{\mathbf{e}}_n) - \mathbf{a}, \Phi \mathbf{u} \rangle &= \int_0^T \langle \bar{\mathbf{j}}_n - \mathbf{j}_n, \Phi \mathbf{u}_\varepsilon \rangle \\ &+ \int_0^T \langle \bar{\mathbf{j}}_n - \mathbf{j}_n, \Phi(\mathbf{u} - \mathbf{u}_\varepsilon) \rangle \\ &+ \int_0^T \langle \mathbf{j}_n - \mathbf{a}, \Phi \mathbf{u} \rangle \end{aligned}$$

and

$$\begin{aligned} \left| \int_0^T \langle \mathbf{J}(\bar{\mathbf{e}}_n) - \mathbf{a}, \Phi \mathbf{u} \rangle \right| &\leq \|\Phi\|_{L_\infty(\Omega)} \int_0^T \|\bar{\mathbf{j}}_n - \mathbf{j}_n\|_{\mathbf{W}^*} \|\mathbf{u}_\varepsilon\|_{\mathbf{W}} \\ &+ \|\Phi\|_{L_\infty(\Omega)} \int_0^T \|\bar{\mathbf{j}}_n - \mathbf{j}_n\|_{\mathbf{L}_q(\Omega)} \|\mathbf{u} - \mathbf{u}_\varepsilon\|_{\mathbf{L}_{2-1/p}(\Omega)} \\ &+ \|\Phi\|_{L_\infty(\Omega)} \int_0^T \|\mathbf{j}_n - \mathbf{a}\|_{\mathbf{L}_q(\Omega)} \|\mathbf{u}\|_{\mathbf{L}_{2-1/p}(\Omega)}. \end{aligned}$$

Using **(iii)** we deduce

$$\lim_{n \rightarrow \infty} \left| \int_0^T \langle \mathbf{J}(\bar{\mathbf{e}}_n) - \mathbf{a}, \Phi \mathbf{u} \rangle \right| \leq C\varepsilon \|\Phi\|_{L_\infty(\Omega)}.$$

Passing to the limit for $\varepsilon \rightarrow 0$ we obtain

$$\int_0^T \langle \mathbf{J}(\bar{\mathbf{e}}_n), \Phi \mathbf{u} \rangle \rightarrow \int_0^T \langle \mathbf{a}, \Phi \mathbf{u} \rangle.$$

Finally, from **(i)** we have that

$$\int_0^T \langle \mathbf{J}(\mathbf{u}), \Phi \bar{\mathbf{e}}_n \rangle \rightarrow \int_0^T \langle \mathbf{J}(\mathbf{u}), \Phi \mathbf{E} \rangle.$$

Therefore, we can pass to the limit in (5.34) and we obtain

$$\int_0^T \langle \mathbf{a} - \mathbf{J}(\mathbf{u}), \Phi(\mathbf{E} - \mathbf{u}) \rangle \geq 0, \quad (5.36)$$

which is valid for any $\mathbf{u} \in L_2((0, T), \mathbf{L}_{2-1/p}(\Omega))$.

Now, we set $\mathbf{u} = \mathbf{E} + \varepsilon \mathbf{z}$ for any $\mathbf{z} \in L_2((0, T), \mathbf{L}_{2-1/p}(\Omega))$ and $\varepsilon > 0$. We get

$$\int_0^T \langle \mathbf{a} - \mathbf{J}(\mathbf{E} + \varepsilon \mathbf{z}), \Phi \mathbf{z} \rangle \leq 0.$$

Passing with $\varepsilon \rightarrow 0$ and setting

$$\mathbf{z} = \mathbf{a} - \mathbf{J}(\mathbf{E}) \in L_2((0, T), \mathbf{L}_q(\Omega)) \supset L_2((0, T), \mathbf{L}_{2-1/p}(\Omega))$$

we deduce

$$\int_0^T \int_{\Omega} \Phi |\mathbf{a} - \mathbf{J}(\mathbf{E})|^2 \leq 0, \quad \forall \Phi \in C_0^\infty(\bar{\Omega}), \Phi \geq 0,$$

from which we see that $\mathbf{a} = \mathbf{J}(\mathbf{E})$ a.e. in Ω . This, together with (5.35), completes the proof.

(v)

Let us take an arbitrary but fixed $\varphi \in \mathbf{C}_0^\infty(\Omega)$.

From Lemma 5.6, the derivative $\partial_t \mathbf{j}_n$ is bounded in $L_2((0, T), \mathbf{V}_0^*)$. As this is a Banach space, the generalized Lagrange formula is applicable, i.e.

$$\langle \mathbf{j}_n(t), \varphi \rangle - \langle \mathbf{j}_n(0), \varphi \rangle = \int_0^t \langle \partial_t \mathbf{j}_n, \varphi \rangle. \quad (5.37)$$

From Lemma 3.4, $\partial_t \mathbf{j}_n$ is bounded in $L_2((0, T), \mathbf{H}^{-1})$, thus there exists a weakly converging subsequence. Its limit will be denoted by \mathbf{z} .

Thanks to the nature of the functions $\bar{\mathbf{e}}_n, \bar{\mathbf{j}}_n$ and \mathbf{j}_n the convergence in the previous parts of this theorem can be taken on any subinterval $(0, t)$ in place of the whole interval $(0, T)$. So when we write (5.37) for some $r \neq t$, subtract these two equalities, divide by $t - r$, integrate from 0 to s and pass with n to infinity we obtain

$$\lim_{t \rightarrow r} \int_0^s \frac{1}{r - t} \langle \mathbf{J}(\mathbf{E}(r)) - \mathbf{J}(\mathbf{E}(t)), \varphi \rangle = \int_0^s \langle \mathbf{z}(s), \varphi \rangle. \quad (5.38)$$

Thus,

$$\int_0^s \langle \partial_t \mathbf{J}(\mathbf{E}(s)), \varphi \rangle = \int_0^s \langle \mathbf{z}(s), \varphi \rangle$$

for any $\varphi \in \mathbf{C}_0^\infty(\Omega)$.

Using the last identity and rewriting (5.37) as follows

$$\langle \mathbf{j}_n(t), \varphi \rangle = \langle \mathbf{J}(\mathbf{E}_0), \varphi \rangle + \int_0^t \langle \partial_t \mathbf{j}_n(t), \varphi \rangle,$$

gives the desired convergence for any $\varphi \in \mathbf{C}_0^\infty(\Omega)$.

(vi)

We integrate the equation (5.11) in time and get

$$\langle \mathbf{j}_n(t), \varphi \rangle + \int_0^t (\nabla \times \bar{\mathbf{e}}_n, \nabla \times \varphi) = \langle \mathbf{j}_n(0), \varphi \rangle.$$

Taking arbitrary $\varphi \in \mathbf{C}_0^\infty(\Omega)$, passing to the limit for $n \rightarrow \infty$ and using (i)–(v) gives that \mathbf{E} satisfies (5.1) for any $\varphi \in \mathbf{C}_0^\infty(\Omega)$. The density of $\mathbf{C}_0^\infty(\Omega)$ in \mathbf{V}_0 guarantees, that \mathbf{E} satisfies (5.1) for all $\varphi \in \mathbf{V}_0$. \square

5.5 Error estimates

This section is devoted to the error estimates for the approximation scheme (5.6).

Theorem 5.12 *Suppose $\mathbf{E}_0 \in \mathbf{V}_0$. Then there exists a positive constant C such that*

$$\int_0^T \int_\Omega \left(|\bar{\mathbf{e}}_n|^{1-1/(2p)} - |\mathbf{E}|^{1-1/(2p)} \right)^2 + \left\| \int_0^T \nabla \times (\bar{\mathbf{e}}_n - \mathbf{E}) \right\|^2 \leq C\tau. \quad (5.39)$$

Proof First, we subtract (5.1) from (5.11) and integrate with respect to the time variable. Then we set $\varphi = \bar{\mathbf{e}}_n - \mathbf{E} \in \mathbf{V}_0$ and again integrate with respect to the time. We obtain

$$\begin{aligned} \int_0^T (\mathbf{J}(\bar{\mathbf{e}}_n) - \mathbf{J}(\mathbf{E}), \bar{\mathbf{e}}_n - \mathbf{E}) &+ \frac{1}{2} \left\| \int_0^T \nabla \times (\bar{\mathbf{e}}_n - \mathbf{E}) \right\|^2 \\ &= \int_0^T (\mathbf{J}(\bar{\mathbf{e}}_n) - \mathbf{j}_n, \bar{\mathbf{e}}_n - \mathbf{E}). \end{aligned}$$

For the first term on the left we use the Cauchy inequality and the relation (5.5) and we obtain

$$\int_0^T (\mathbf{J}(\bar{\mathbf{e}}_n) - \mathbf{J}(\mathbf{E}), \bar{\mathbf{e}}_n - \mathbf{E}) \geq C \int_0^T \int_{\Omega} \left(|\bar{\mathbf{e}}_n|^{1-1/(2p)} - |\mathbf{E}|^{1-1/(2p)} \right)^2.$$

Next, using (5.14) we deduce

$$\left| \int_0^T (\mathbf{J}(\bar{\mathbf{e}}_n) - \mathbf{j}_n, \bar{\mathbf{e}}_n - \mathbf{E}) \right| \leq C\tau \int_0^T \|\partial_t \mathbf{j}_n\|_{\mathbf{V}^*} \|\bar{\mathbf{e}}_n - \mathbf{E}\|_{\mathbf{V}} \leq C\tau.$$

Collecting all relations above we arrive at the statement of the theorem. \square

Remark 5.13 *Slodička in [61] discussed the problem (1.15), where the non-linearity is given by the modified power law (1.4). The vector field \mathbf{J} is then coercive, so better error estimate can be proven:*

$$\int_0^T \|\bar{\mathbf{e}}_n - \mathbf{E}\|^2 + \left\| \int_0^T \nabla \times (\bar{\mathbf{e}}_n - \mathbf{E}) \right\|^2 \leq C\tau. \quad (5.40)$$

Remark 5.14 *In [65] the authors derived optimal error estimates applicable to the problem (1.15) in case that the power law (1.5) is used. The vector field \mathbf{J} is then coercive and Lipschitz continuous and we have that*

$$\int_0^T \|\bar{\mathbf{e}}_n - \mathbf{E}\|^2 + \left\| \int_0^T \nabla \times (\bar{\mathbf{e}}_n - \mathbf{E}) \right\|^2 \leq C\tau^2. \quad (5.41)$$

5.6 Numerical experiments

The proposed numerical method is studied on several types of numerical examples. We check the efficiency of the method on problems with known exact solution.³ We will start with the problems where $p \in [1.2, 2]$. This does not coincide completely with the range of the power p as derived in Section 1.3, but for its lower demands on the calculation time, it serves as a good model example to show the dependence of the relative error on the problem parameters. Some

³This requires to impose some right-hand side and boundary condition to the problem (5.1) but it will repay with the known error of the method and therefore the possibility to study the behaviour of the method for different combinations of parameters.

examples are shown with the parameter $p = 1.2$ and $p = 1.143$. As the later problems seem to be rather computationally expensive, we compare our results with another known method in order to show which approach is more efficient.

In the experiments, the space discretization based on the Whitney edge elements is employed (Chapter 4).

Thereinafter the domain Ω —the region occupied by the superconductor—is the unit cube in \mathbb{R}^3 . We split this domain into a tetrahedral mesh. The basic mesh consists of 6 tetrahedra and thus 19 degrees of freedom (DOFs). One refinement of the basic mesh (using the bisection procedure introduced by Kossaczky [48]) leads to a tetrahedral mesh with 48 tetrahedra and 98 DOFs. The number of vertices, elements and degrees of freedom in the used meshes as well as the value of the mesh characteristic h defined by (4.4) can be found in Table 5.1. The mesh does not refine adaptively.

	# vertices	# tetrahedra	# DOFs	h
Basic mesh	8	6	19	$\sqrt{3}$
1 refinement	27	48	98	$\sqrt{3}/2$
2 refinements	125	384	604	$\sqrt{3}/4$
3 refinements	729	3072	4184	$\sqrt{3}/8$
4 refinements	4913	24576	31024	$\sqrt{3}/16$

Table 5.1: Some characteristics of the used meshes.

The time interval $[0, 1]$ is considered.

The nonlinear scheme (5.6) is solved by the Newton method (Appendix B), the standard tool to solve nonlinear PDEs.

The efficiency of the method is studied on the basis of the relative error calculated in a discrete $L_{2-1/p}((0, T), \mathbf{L}_{2-1/p}(\Omega))$ norm. That is

$$E_{rel} = \left[\sum_{i=1}^n \tau \frac{\sum_{\forall T} \det(T) \sum_{q=1}^Q w(x_q) |\mathbf{E}(x_q, t_i) - \bar{\mathbf{e}}_n(x_q, t_i)|^{2-1/p}}{\sum_{\forall T} \det(T) \sum_{q=0}^Q w(x_q) |\mathbf{E}(x_q, t_i)|^{2-1/p}} \right]^{p/(2p-1)}, \quad (5.42)$$

where $\det(T)$ denotes determinant of the tetrahedron T . Depending on the quadrature, it can be for example the volume of the tetrahedron. The parameter Q denotes the number of quadrature points x_q and the function $w(x_q)$ the weight of the quadrature point x_q .

Linear exact solution

First, we consider the problem (1.15) with given (non-zero) right-hand side and boundary condition \mathbf{G}_1 in such a way that the vector field $\mathbf{E}(\mathbf{x})$ given by

$$\begin{aligned} E_1(\mathbf{x}) &= x_3 - x_2 + t \\ E_2(\mathbf{x}) &= x_1 - x_3 + 4t \\ E_3(\mathbf{x}) &= x_2 - x_1 + t \end{aligned} \tag{5.43}$$

is its solution. The exact solution serves to compute the error of approximate solutions obtained by the approximation scheme (5.6).

The convergence of the method with diminishing τ agrees with our expectations and theoretical results. With decreasing length of the time step the relative error decreases (Tables 5.2 and 5.3).

For $p = 2$, the effect of the refinement of the mesh is not remarkable, as the linear exact solution can be fitted by the Whitney edge elements precisely. Therefore the number of DOFs should not influence the final error. The refinement of the mesh shows however some anomaly when the time step is big. If $\tau = 0.05$, the error does not decrease when a denser mesh is used. But if $\tau = 0.05$ the value of the error is that big, that we cannot speak about relevant results.

For $p \leq 1.2$, the density of the mesh plays a more important role (Table 5.3). The denser the mesh, the smaller the final error. If p is close to 1 the nonlinearity is very steep, therefore solving the nonlinear equation becomes more difficult and imprecise. In these circumstances, the denser mesh provides more information on the problem and therefore enhances the final error.

The influence of different values of $p \in (1.2, 2]$ is plotted on Figure 5.1. We observe again that the problem gets more complex when the parameter p approaches 1. Accurate choice of the discretization parameters—the length of the time step and the density of the mesh—leads to better results even for the values of p near 1.

If $p = 1.2$ or $p = 1.143$, a very small time step is needed in order to obtain quite reasonable precision. Consequently, the calculations take a long time.

τ		0.05	0.02	0.01	0.005	0.002
rel. error	98 DOFs	0.09837	0.04311	0.02334	0.01286	0.00607
	604 DOFs	0.10053	0.04239	0.02196	0.01144	0.00491

Table 5.2: The dependence of the relative error (5.42) of the scheme (5.6) on the choice of the time step τ and the mesh. The error decreases with decreasing τ . The linear exact solution (5.43) is considered and $p = 2$.

τ		0.0005	0.0002	0.0001	
rel. error	$p = 1.2$	98 DOFs	0.05410	0.04827	0.04538
		604 DOFs	0.02030	0.01624	0.01465
rel. error	$p = 1.143$	98 DOFs	0.08176	0.07402	0.06998
		604 DOFs	0.03121	0.02550	0.02317

Table 5.3: The relative error (5.42) of the scheme (5.6) increases if p approaches 1. The higher the number of DOFs the smaller the final error. The linear exact solution is considered.

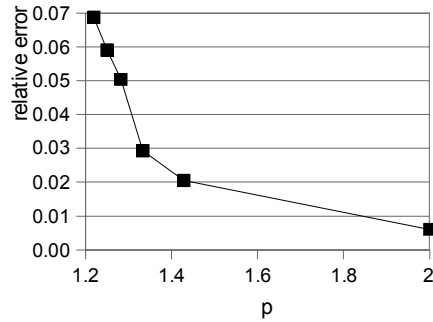


Figure 5.1: The relative error (5.42) of the approximation scheme (5.6) increases remarkably with p approaching 1.2. In this experiment the time step is $\tau = 0.002$, the linear exact solution (5.43) is considered and the mesh has only 98 DOFs.

Sinusoidal exact solution

Here, we consider the problem (1.15) with given (non-zero) right-hand side and boundary condition \mathbf{G}_1 in such a way that the vector field $\mathbf{E}(\mathbf{x})$ of the form

$$\begin{aligned} E_1(\mathbf{x}) &= 0.5 \sin(x_2) - 0.2 \sin(x_3) + t \\ E_2(\mathbf{x}) &= 0.5 \sin(x_3) - 0.5 \sin(x_1) + t \\ E_3(\mathbf{x}) &= 0.2 \sin(x_1) - 0.5 \sin(x_2) + t \end{aligned} \quad (5.44)$$

solves the BVP (1.15). The exact solution serves to compute the error of approximate solutions obtained by the approximation scheme (5.6).

The convergence of the method with diminishing τ agrees with our expectations and theoretical results. With decreasing length of the time step the relative error decreases (Tables 5.4 and 5.5). We can observe a bigger influence of the number of DOFs on the efficiency of the method because the sinusoidal solution (5.44) is more challenging to be fitted than the linear solution from the previous section. This effect is, however, more remarkable for smaller τ . This can be explained by less overall accuracy of the backward Euler method for big values of τ .

As the exponent p approaches 1 the problem gets more difficult to solve and the relative error (5.42) is higher (Figure 5.2). Better results even for p closer to 1 can be obtained by the choice of a smaller τ but this comes at the price of higher calculation time. Table 5.5 shows the results for the problem with sinusoidal exact solution (5.44) for $p = 1.2$, $p = 1.143$ and two different meshes. The precision of about 2% is obtained when a mesh with 604 DOFs is used and $\tau = 0.0002$. However, the computational time is in this case excessive.

τ		0.05	0.02	0.01	0.005	0.002
rel. error	98 DOFs	0.10910	0.05495	0.03924	0.03362	0.03161
	604 DOFs	0.10560	0.04738	0.02808	0.01984	0.01646

Table 5.4: The dependence of the relative error (5.42) of the scheme (5.6) on the choice of the length of the time step. The parameter $p = 2$ and the exact solution is given by (5.44).

		τ	0.0005	0.0002	0.0001
rel. error	$p = 1.2$	98 DOFs	0.04611	0.04561	0.04550
		604 DOFs	0.02027	0.01911	
rel. error	$p = 1.143$	98 DOFs	0.05092	0.05011	0.04991
		604 DOFs	0.02243	0.02053	

Table 5.5: The relative error (5.42) of the scheme (5.6) for two values of the exponent p : $p = 1.2$ and $p = 1.143$. Two different meshes are used: with 98 DOFs and with 604 DOFs. The method is extremely slow if p is close to 1. Some calculations were even not realized because of the unbearable time consumption. The sinusoidal exact solution is considered. (5.44).

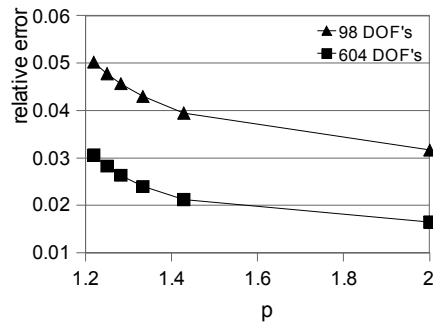


Figure 5.2: The dependence of the relative error (5.42) of the scheme (5.6) on the parameter p for two different meshes. The time step is $\tau = 0.002$ and the exact solution is given by (5.44).

H-formulation

Some authors suggest to compute the problem of field penetration in type-II superconductors in the \mathbf{H} -formulation [25, 73]. It means that they are looking for the magnetic field in place of the electric field. This gives rise to the following partial differential equation

$$\partial_t \mathbf{H} + \nabla \times \mathbf{E}(\nabla \times \mathbf{H}) = \mathbf{F} \quad \text{in } \Omega, \quad (5.45)$$

where the nonlinear function \mathbf{E} is given by $\mathbf{E}(\mathbf{x}) = |\mathbf{x}|^{n-1} \mathbf{x}$, according to the power law (1.2). Yin et al. [73] have studied only the well-posedness of the problem (5.45). No numerical examples were presented. Elliott et al. [25] have studied this type of problem in the form of variational inequality. They have proved the existence of a solution and convergence of the backward Euler method in the case of the power law, Bean's critical-state model and an extended Bean's critical-state model formulated using the subdifferential of a convex energy. Their model is a bit more complicated, but on the basis of their analysis I wrote a program calculating the following boundary value problem: For each $i = 1, \dots, n$ find \mathbf{H}_i such that

$$\frac{1}{\tau} \mathbf{H}_i + \nabla \times (|\nabla \times \mathbf{H}_i|^{n-1} \nabla \times \mathbf{H}_i) = \mathbf{F}(t_i) + \frac{1}{\tau} \mathbf{H}_{i-1} \quad \text{in } \Omega,$$

with the following nonlinear boundary condition

$$\boldsymbol{\nu} \times |\nabla \times \mathbf{H}_i|^{n-1} \nabla \times \mathbf{H}_i = \mathbf{G}_i \quad \text{on } \Gamma,$$

and initial condition

$$\mathbf{H}_0 = \mathbf{H}(0) = \mathbf{h}_0 \quad \text{in } \Omega.$$

The boundary condition as previously suggested seems probably artificial but it corresponds to the boundary condition (1.8) and makes the weak formulation of the problem easier, i.e.

$$\frac{1}{\tau} (\mathbf{H}_i, \boldsymbol{\varphi}) + (|\nabla \times \mathbf{H}_i|^{n-1} \nabla \times \mathbf{H}_i, \nabla \times \boldsymbol{\varphi}) + (\mathbf{G}_i, \boldsymbol{\varphi})_\Gamma = (\mathbf{F}(t_i), \boldsymbol{\varphi}) + \frac{1}{\tau} (\mathbf{H}_{i-1}, \boldsymbol{\varphi}). \quad (5.46)$$

This method shows several instabilities. The method converges sometimes very well but after a few time steps suddenly diverges quickly (Table 5.6). The error of the method is extremely small for some combinations of input parameters even for rough time steps and coarse mesh but for different combinations, the method diverges. A denser mesh does not always result in better results (Table 5.6). Neither a shorter time step assures more precise solution (Table 5.7).

			τ	0.02	0.01	0.005	0.002
rel. error	$n = 6$	604 DOFs	NAN	0.00753	0.00804	0.00795	
		4184 DOFs	0.01837	0.01906	0.01980	0.02069	
rel. error	$n = 8$	604 DOFs	0.10183	NAN	0.11067	0.11596	
		4184 DOFs	0.26059	0.26544	0.26219	0.26668	

Table 5.6: The relative error of the backward Euler method applied to the problem (5.45) with linear exact solution $\mathbf{H}=(5.43)$. We use $n = 6$ and $n = 8$ which corresponds to $p = 1.2$ and $p \doteq 1.143$ respectively. Two different meshes are used. We observe that a coarser mesh provides better results. The method diverges for some combinations of parameters (NAN).

			τ	0.5	0.25	0.02	0.005
rel. error	$n = 6$	98 DOFs	0.01993	0.02062	0.02153	0.02171	
		604 DOFs	0.00834	0.00910	0.01004	0.01012	
		4184 DOFs	0.00421	0.00461	0.00511	0.00515	
rel. error	$n = 8$	98 DOFs	0.03882	0.03782	0.03659	0.03696	
		604 DOFs	0.00884	0.00953	0.01038	0.01046	
		4184 DOFs	0.00423	0.00463	0.00512	0.00516	

Table 5.7: The relative error of the backward Euler method applied to the problem (5.45) with sinusoidal exact solution $\mathbf{H}=(5.44)$. We use $n = 6$ and $n = 8$ which corresponds to $p = 1.2$ and $p \doteq 1.143$ respectively. Three different meshes are used. We observe that a shorter time step does not always deliver better results.

5.7 Conclusions

The backward Euler method applied to the problem of the diffusion of the electric field in type-II superconductors has been studied theoretically and on numerical examples. The latter revealed that the method applied to the **H**-formulation gives faster and more precise results than the same method applied in the **E**-formulation. This can be caused by the inverse types of the nonlinearity in the two formulations. The powers in the nonlinearity in the formulation (5.45) are positive, so the derivative in zero is equal to zero. This is from numerical point of view a less troublesome problem than an unbounded derivative. The second aspect that has big influence on the speed of the method is the fact that Whitney's edge elements approximate the curl of a function by a piecewise constant. The nonlinearity term in the equation (5.46) is therefore calculated from one value on each tetrahedron and cannot be more precise if more values are used. On the contrary, the nonlinearity in the equation (1.15) changes in each tetrahedron markedly from point to point and thus makes the calculations much slower.

However, in comparison to the backward Euler method applied in the **H**-formulation, the same method applied to the **E**-formulation manifests more stability. The instabilities of the backward Euler method in **H**-formulation were not mentioned in the article by Elliott et al. [25]. Hence I suspect that the nonlinear boundary condition can be the cause.

6 FIXED-POINT METHOD

After the discretization in time, the time-dependent nonlinear problem (1.15) changes to the steady-state nonlinear problem of the form

$$(\mathbf{J}(\mathbf{E}), \varphi) + (\nabla \times \mathbf{E}, \nabla \times \varphi) = (\mathbf{F}, \varphi) \quad \forall \varphi \in \mathbf{W}. \quad (6.1)$$

As the problem (6.1) is nonlinear, the next step is to linearize it.

This chapter is based on our article [38], it is divided into four sections. Section 6.1 is devoted to the analysis of a new linearization scheme for the Lipschitz continuous case, i.e. the nonlinearity term \mathbf{J} defined by (1.5). In Section 6.2, the linearization scheme for the non-Lipschitz continuous case is studied, i.e. the nonlinearity given by (1.4). In both cases the function space \mathbf{W} is given by

$$\mathbf{W} := \mathbf{H}_0(\mathbf{curl}; \Omega).$$

This means that the boundary condition (1.14) is considered. We can also consider the boundary condition (1.13). Then $\mathbf{W} := \{\mathbf{w} \in \mathbf{H}(\mathbf{curl}; \Omega) \mid \nabla \times \mathbf{w} \times \boldsymbol{\nu} = 0\}$, but the weak formulation as well as the mathematical reasoning will be the same.

Both the Lipschitz continuous and the non-Lipschitz continuous case re-join in Section 6.3 on numerical experiments. An accurate combination of proposed schemes¹ leads to an effective numerical tool for calculation of nonlinear and degenerate PDE (6.1). The numerical experiments for both the Lipschitz and the non-Lipschitz continuous case are presented in Section 6.3. Conclusions are drawn in Section 6.4.

¹The convergence of the combined scheme follows directly from the convergence of each scheme separately.

Remark 6.1 In [37], we have studied a simpler variant of the problem (6.1). The nonlinearity \mathbf{J} was given by

$$\mathbf{J}(\mathbf{E}) = \mathbf{J} \begin{pmatrix} E_1 \\ E_2 \\ E_3 \end{pmatrix} = \begin{pmatrix} j(E_1) & 0 & 0 \\ 0 & j(E_2) & 0 \\ 0 & 0 & j(E_3) \end{pmatrix} \begin{pmatrix} E_1 \\ E_2 \\ E_3 \end{pmatrix}. \quad (6.2)$$

One could also consider different nonlinearities j for each component, but without loss of generality we assumed that they were of the same shape. First, we have designed a linearization scheme in case that the nonlinearity was a Lipschitz continuous function. Next, we have focused on the degenerate, non-Lipschitz continuous case. When the two proposed linearization schemes were combined carefully, a powerful tool to solve (6.1) arose, under assumption that \mathbf{J} was given by (6.2). This last constraint has been removed later in [38], where the generalization of the simpler formulation was considered. The analysis of the simplified model based on (6.2) is similar to that presented in this chapter. The details of the proofs and numerical experiments for the simplified model can be found in [37].

6.1 Iteration scheme in the Lipschitz continuous case

The nonlinearity (1.5) is used.

First, let us define an auxiliary function j given by the identity $\mathbf{J}(\mathbf{E}) = j(|\mathbf{E}|)\mathbf{E}$. If the vector field \mathbf{J} is given by (1.5), the function j has the following form

$$j(r) = \begin{cases} \alpha^{-1/p}, & 0 < r < \alpha, \\ r^{-1/p}, & \alpha \leq r \leq \beta, \\ \beta^{-1/p}, & \beta < r, \end{cases} \quad (6.3)$$

for some fixed positive constants $0 < \alpha < \beta$.

The following lemma states the well-posedness of the problem (6.1), if \mathbf{J} is given by (1.5).

Lemma 6.2 *The problem (6.1) admits one and only one solution $\mathbf{E} \in \mathbf{W}$.*

Proof We denote by \mathbf{W}^* the dual space to the Hilbert space \mathbf{W} . We introduce the nonlinear differential operator $\mathcal{J} : \mathbf{W} \rightarrow \mathbf{W}^*$ defined by

$$\langle \mathcal{J}(\mathbf{E}), \boldsymbol{\varphi} \rangle := (\mathbf{J}(\mathbf{E}), \boldsymbol{\varphi}) + (\nabla \times \mathbf{E}, \nabla \times \boldsymbol{\varphi}).$$

We will prove that the operator \mathcal{J} is monotone, continuous and coercive. The well-posedness of the problem (6.1) can be then proven using the theory of monotone operators [70].

Continuity of \mathcal{J} is straightforward.

The operator \mathcal{J} is monotone if for all $\mathbf{x}, \mathbf{y} \in \mathbf{W}$ holds that

$$\langle \mathcal{J}(\mathbf{x}) - \mathcal{J}(\mathbf{y}), \mathbf{x} - \mathbf{y} \rangle \geq 0.$$

Thus we study the following expression

$$(\mathbf{J}(\mathbf{x}) - \mathbf{J}(\mathbf{y}), \mathbf{x} - \mathbf{y}) + \|\nabla \times (\mathbf{x} - \mathbf{y})\|^2.$$

The second part is always nonnegative so we work further with the first part only. The Gâteaux differential of $\mathbf{J}(\mathbf{x})$ in the direction \mathbf{h} is equal to

$$D\mathbf{J}(\mathbf{x}, \mathbf{h}) = \begin{cases} \alpha^{-1/p}\mathbf{h}, & |\mathbf{x}| < \alpha, \\ -p^{-1}|\mathbf{x}|^{-2-1/p}(\mathbf{h} \cdot \mathbf{x})\mathbf{x} + |\mathbf{x}|^{-1/p}\mathbf{h}, & |\mathbf{x}| \in (\alpha, \beta), \\ \beta^{-1/p}\mathbf{h}, & |\mathbf{x}| > \beta. \end{cases}$$

In addition,

$$(D\mathbf{J}(\mathbf{x}, \mathbf{h}), \mathbf{h}) \geq \begin{cases} \alpha^{-1/p}|\mathbf{h}|^2, & |\mathbf{x}| < \alpha, \\ |\mathbf{x}|^{-1/p}|\mathbf{h}|^2(1 - p^{-1}), & |\mathbf{x}| \in (\alpha, \beta), \\ \beta^{-1/p}|\mathbf{h}|^2, & |\mathbf{x}| > \beta. \end{cases}$$

Therefore

$$|(D\mathbf{J}(\mathbf{x}, \mathbf{h}), \mathbf{h})| \geq \beta^{-1/p}(1 - p^{-1})|\mathbf{h}|^2 \quad \forall \mathbf{x} \in \mathbb{R}^3.$$

From the generalized Lagrange formula (see [70, Chapter 1]) and the previous inequality, we get that there exists a $\theta \in (0, 1)$ such that

$$(\mathbf{J}(\mathbf{x} + \mathbf{h}) - \mathbf{J}(\mathbf{x}), \mathbf{h}) = (D\mathbf{J}(\mathbf{x} + \theta\mathbf{h}, \mathbf{h}), \mathbf{h}) \geq \beta^{-1/p}(1 - p^{-1})|\mathbf{h}|^2. \quad (6.4)$$

This proves the monotonicity of \mathbf{J} as well as its coercivity. \square

Iteration scheme

For $k \in \mathbb{N}$ we introduce the following linear approximation scheme

$$L(\mathbf{E}_k, \boldsymbol{\varphi}) + (\nabla \times \mathbf{E}_k, \nabla \times \boldsymbol{\varphi}) = (\mathbf{F}, \boldsymbol{\varphi}) + L(\mathbf{E}_{k-1}, \boldsymbol{\varphi}) - (\mathbf{J}(\mathbf{E}_{k-1}), \boldsymbol{\varphi}) \quad (6.5)$$

for any $\varphi \in \mathbf{W}$. The parameter $L > 0$ will be specified later.

Problem (6.5) is linear and elliptic in \mathbf{W} . The existence and uniqueness of a weak solution in \mathbf{W} is guaranteed by the Lax–Milgram lemma.

Now, we introduce a real function $h(s) := j(s) - L$ and the vector field $\mathbf{H}(\mathbf{s}) := \mathbf{J}(\mathbf{s}) - L\mathbf{s}$. The equation (6.1) can be rewritten as follows

$$L(\mathbf{E}, \varphi) + (\nabla \times \mathbf{E}, \nabla \times \varphi) = (\mathbf{F}, \varphi) - (\mathbf{H}(\mathbf{E}), \varphi).$$

By subtracting this from (6.5) we get

$$L(\mathbf{E}_k - \mathbf{E}, \varphi) + (\nabla \times (\mathbf{E}_k - \mathbf{E}), \nabla \times \varphi) = (\mathbf{H}(\mathbf{E}) - \mathbf{H}(\mathbf{E}_{k-1}), \varphi).$$

Setting $\varphi = \mathbf{E}_k - \mathbf{E}$, we obtain the variational formulation for the error $\|\mathbf{E}_k - \mathbf{E}\|$

$$L\|\mathbf{E}_k - \mathbf{E}\|^2 + \|\nabla \times (\mathbf{E}_k - \mathbf{E})\|^2 = (\mathbf{H}(\mathbf{E}) - \mathbf{H}(\mathbf{E}_{k-1}), \mathbf{E}_k - \mathbf{E}). \quad (6.6)$$

6.1.1 Basic inequalities

The following lemmas play significant role in the error estimation.

Lemma 6.3 *For all $\mathbf{s}, \mathbf{t} \in \mathbb{R}^3$ the following inequality holds*

$$|\mathbf{H}(\mathbf{s}) - \mathbf{H}(\mathbf{t})| \leq M|\mathbf{s} - \mathbf{t}|,$$

where $M > 0$ depends on L and equals to

$$M = M(L) = \max\{|L - (1 - p^{-1})\beta^{-1/p}|, |L - \alpha^{-1/p}|\}.$$

Proof The scalar functions j and h are defined as previously. The first derivative of j is

$$j'(s) = \begin{cases} 0, & 0 < s < \alpha, \\ -p^{-1}s^{-1-1/p}, & \alpha < s < \beta, \\ 0, & \beta < s. \end{cases}$$

The first derivative of the scalar function $h(s)s$ is then

$$[h(s)s]' = \begin{cases} \alpha^{-1/p} - L, & 0 < s < \alpha, \\ (1 - p^{-1})s^{-1/p} - L, & \alpha < s < \beta, \\ \beta^{-1/p} - L, & \beta < s. \end{cases}$$

We plan to use the mean value theorem in the form

$$|h(r)r - h(q)q| \leq \sup_{s \geq 0} \{|[h(s)s]'\}| |r - q| \quad \forall r, q \geq 0,$$

so we have to find $\sup\{|[h(s)s]'\}|$ for all $s \geq 0$.

One can easily see that

$$\sup_{s \geq 0} \{|[h(s)s]'\}| = \max \left\{ |L - \alpha^{-1/p}|, |L - \beta^{-1/p}|, \max_{\alpha \leq s \leq \beta} \left\{ |L - (1 - p^{-1}) s^{-1/p}| \right\} \right\}.$$

As $\alpha < \beta$, we deduce that

$$L - (1 - p^{-1}) \alpha^{-1/p} \leq L - (1 - p^{-1}) s^{-1/p} \leq L - (1 - p^{-1}) \beta^{-1/p} \quad \forall s \in [\alpha, \beta].$$

Therefore

$$\begin{aligned} \max_{\alpha \leq s \leq \beta} \left\{ |L - (1 - p^{-1}) s^{-1/p}| \right\} \\ \leq \max \left\{ |L - (1 - p^{-1}) \alpha^{-1/p}|, |L - (1 - p^{-1}) \beta^{-1/p}| \right\}. \end{aligned}$$

The right-hand side of the previous inequality is plotted in red in Figure 6.1 as the function of L . Now, we use the notation

$$M = M(L) = \max \left\{ |L - (1 - p^{-1}) \beta^{-1/p}|, |L - \alpha^{-1/p}| \right\}$$

and we can deduce (check also Figure 6.1) that $\sup_{s \geq 0} \{|[h(s)s]'\}| = M$. Thus for all positive real numbers r and q holds

$$|h(r)r - h(q)q| \leq M|r - q|. \quad (6.7)$$

One can easily verify that for all $r > 0$

$$|h(r)| \leq \max \left\{ |L - \alpha^{-1/p}|, |L - \beta^{-1/p}| \right\} \leq M. \quad (6.8)$$

We proceed with the following algebraic identity valid for all vectors $\mathbf{s}, \mathbf{t} \in \mathbb{R}^3$

$$|\mathbf{H}(\mathbf{s}) - \mathbf{H}(\mathbf{t})|^2 = [h(|\mathbf{s}|)|\mathbf{s}| - h(|\mathbf{t}|)|\mathbf{t}|]^2 + 2h(|\mathbf{s}|)h(|\mathbf{t}|) [|\mathbf{s}||\mathbf{t}| - (\mathbf{s}, \mathbf{t})], \quad (6.9)$$

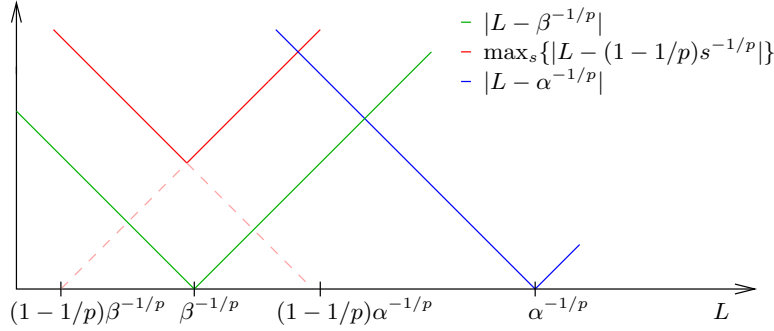
we use (6.7), (6.8) and the Cauchy inequality

$$|\mathbf{s}||\mathbf{t}| - (\mathbf{s}, \mathbf{t}) \geq 0$$

and from (6.9) we successively obtain

$$\begin{aligned} |\mathbf{H}(\mathbf{s}) - \mathbf{H}(\mathbf{t})|^2 &\leq M^2 |\mathbf{s}| - |\mathbf{t}||^2 + 2M^2 [|\mathbf{s}||\mathbf{t}| - (\mathbf{s}, \mathbf{t})] \\ &= M^2 |\mathbf{s} - \mathbf{t}|^2. \end{aligned}$$

This completes the proof. \square

Figure 6.1: Auxiliary figure to deduce the value of M in Lemma 6.3.

Lemma 6.4 *There exists $L > 0$ such that $M(L) < L$.*

Proof If $L \geq (\alpha^{-1/p} + (1 - p^{-1})\beta^{-1/p})/2$ then $M = L - (1 - p^{-1})\beta^{-1/p}$ and the statement of the lemma is fulfilled directly from the assumptions $\beta > 0$ and $p > 1$. Moreover, the inequality $M(L) < L$ is also valid for all L such that

$$\alpha^{-1/p}/2 < L < (\alpha^{-1/p} + (1 - p^{-1})\beta^{-1/p})/2,$$

what is easy to check. \square

Lemma 6.5 *For all $\mathbf{s}, \mathbf{t} \in \mathbb{R}^3$ holds*

$$(\mathbf{J}(\mathbf{s}) - \mathbf{J}(\mathbf{t}), \mathbf{s} - \mathbf{t}) \geq \beta^{-1/p}(1 - p^{-1})|\mathbf{s} - \mathbf{t}|^2, \quad (\text{coercivity})$$

and

$$|\mathbf{J}(\mathbf{s}) - \mathbf{J}(\mathbf{t})| \leq \alpha^{-1/p}|\mathbf{s} - \mathbf{t}|. \quad (\text{continuity})$$

Proof Coercivity of \mathbf{J} is proven by (6.4).

Continuity of \mathbf{J} can be shown similarly as its coercivity or using the technique from the proof of Lemma 6.3. The important facts are the following

$$|j(r)| \leq \alpha^{-1/p} \quad \forall r \in \mathbb{R}$$

and

$$|[j(r)r]'| \leq \alpha^{-1/p}.$$

\square

6.1.2 Error estimates and convergence

The proof of the convergence of the sequence $\{\mathbf{E}_k\}$ to the solution \mathbf{E} to the problem (6.1) is based on the Banach fixed-point theorem. Its assumptions are satisfied thanks to Lemma 6.4 and the following theorem:

Theorem 6.6 *If \mathbf{E}_k results from the iteration scheme (6.5) and \mathbf{E} is the solution to the problem (6.1), then*

$$\begin{aligned}\|\mathbf{E}_k - \mathbf{E}\| &\leq \left(\frac{M(L)}{L}\right)^k \|\mathbf{E}_0 - \mathbf{E}\|, \\ \|\nabla \times (\mathbf{E}_k - \mathbf{E})\| &\leq \sqrt{L} \left(\frac{M(L)}{L}\right)^k \|\mathbf{E}_0 - \mathbf{E}\|\end{aligned}$$

holds for any $k \in \mathbb{N}$.

Proof Applying the Cauchy inequality and Lemma 6.3 to the right-hand side of (6.6) we successively obtain

$$\begin{aligned}L\|\mathbf{E}_k - \mathbf{E}\|^2 + \|\nabla \times (\mathbf{E}_k - \mathbf{E})\|^2 &= (\mathbf{H}(\mathbf{E}) - \mathbf{H}(\mathbf{E}_{k-1}), \mathbf{E}_k - \mathbf{E}) \\ &\leq \|\mathbf{H}(\mathbf{E}) - \mathbf{H}(\mathbf{E}_{k-1})\| \|\mathbf{E}_k - \mathbf{E}\| \\ &\leq M\|\mathbf{E}_{k-1} - \mathbf{E}\| \|\mathbf{E}_k - \mathbf{E}\|.\end{aligned}\tag{6.10}$$

This directly implies

$$\|\mathbf{E}_k - \mathbf{E}\| \leq \frac{M}{L} \|\mathbf{E}_{k-1} - \mathbf{E}\|.$$

This is in fact a recursive formula, from which we can deduce that

$$\|\mathbf{E}_k - \mathbf{E}\| \leq \left(\frac{M}{L}\right)^k \|\mathbf{E}_0 - \mathbf{E}\|.$$

Using this last estimate in (6.10) we can write

$$\begin{aligned}\|\nabla \times (\mathbf{E}_k - \mathbf{E})\|^2 &\leq M\|\mathbf{E}_{k-1} - \mathbf{E}\| \|\mathbf{E}_k - \mathbf{E}\| \\ &\leq L \left(\frac{M}{L}\right)^{2k} \|\mathbf{E}_0 - \mathbf{E}\|^2,\end{aligned}$$

which concludes the proof. \square

Remark 6.7 (The optimal choice of the parameter L)

In order to assure fast convergence of the proposed iteration scheme, the value of the ratio $M(L)/L$ vis-à-vis L needs to be minimized.

Let us investigate the derivative of the ratio $M(L)/L$ as a function of L for $L > (\alpha^{-1/p} + (1 - p^{-1})\beta^{-1/p})/2$. Then $M(L) = L - (1 - p^{-1})\beta^{-1/p}$ and

$$\partial_L \left(\frac{M(L)}{L} \right) = (1 - p^{-1})\beta^{-1/p}/L^2 > 0.$$

Thus the minimal value is obtained for $L = (\alpha^{-1/p} + (1 - p^{-1})\beta^{-1/p})/2$.

Now, suppose $0 < L < (\alpha^{-1/p} + (1 - p^{-1})\beta^{-1/p})/2$, then $M(L) = \alpha^{-1/p} - L$ and

$$\partial_L \left(\frac{M(L)}{L} \right) = -\alpha^{-1/p}/L^2.$$

This is negative as α , β and L are positive. So the minimal value of the ratio $M(L)/L$ is obtained again for $L = (\alpha^{-1/p} + (1 - p^{-1})\beta^{-1/p})/2$.

We conclude that the optimal value of the parameter L is

$$L_0 = \left(\alpha^{-1/p} + (1 - p^{-1})\beta^{-1/p} \right) / 2$$

and the ratio $M(L_0)/L_0 = (\alpha^{-1/p} - (1 - p^{-1})\beta^{-1/p})/(\alpha^{-1/p} + \beta^{-1/p})$.

However, when we get back to the inequality (6.10) we realize that during the error analysis, the term $\|\nabla \times (\mathbf{E}_k - \mathbf{E})\|^2$ was neglected. But it is positive and therefore could help us to obtain better estimates and successively different optimal value of the parameter L . Unfortunately, there are no suitable estimates known for this particular problem.

Another aspect playing role in the optimal choice of the parameter L is the knowledge of the exact solution we are looking for. The slope of the nonlinearity \mathbf{J} varies in wide boundaries between $\alpha^{-1/p}$ for $|\mathbf{E}| \sim \alpha$ and $(1 - p^{-1})\beta^{-1/p}$ for $|\mathbf{E}| \sim \beta$ but if we knew that the exact solution achieves values in a limited interval only, we could pick L in such a way that it would track the slope of the nonlinearity \mathbf{J} in the considered region. The ambition to find the optimal L by numerical experiments can therefore end up with a misleading result as each experiment will be influenced by the nature of the exact solution.

Theorem 6.8 *The sequence of the solutions to the iteration scheme (6.5) converges for $k \rightarrow \infty$ to the solution to the problem (6.1) in the space \mathbf{W} .*

Proof The proof is a straightforward consequence of the Banach fixed-point theorem. Its assumptions are satisfied thanks to Lemma 6.4 and Theorem 7.4. \square

6.2 Iteration scheme in the non-Lipschitz continuous case

The nonlinearity (1.4) is used.

First, let us define an auxiliary function j given by the identity $\mathbf{J}(\mathbf{E}) = j(|\mathbf{E}|)\mathbf{E}$. If the vector field \mathbf{J} is given by (1.4), the function j has the following form

$$j(r) = \begin{cases} r^{-1/p}, & 0 \leq r \leq \beta, \\ \beta^{-1/p}, & \beta < r \end{cases} \quad (6.11)$$

for some $\beta \gg 1$.

The well-posedness of the problem (6.1) can be proven analogously as in the previous section (Lemma 6.2).

Iteration scheme

For $k \in \mathbb{N}$ we introduce the following linear approximation scheme

$$k(\mathbf{E}_k, \boldsymbol{\varphi}) + (\nabla \times \mathbf{E}_k, \nabla \times \boldsymbol{\varphi}) = (\mathbf{F}, \boldsymbol{\varphi}) + k(\mathbf{E}_{k-1}, \boldsymbol{\varphi}) - (\mathbf{J}_k(\mathbf{E}_{k-1}), \boldsymbol{\varphi}) \quad (6.12)$$

for any $\boldsymbol{\varphi} \in \mathbf{W}$. Here, the regularization \mathbf{J}_k of \mathbf{J} is defined by the identity $\mathbf{J}_k(\mathbf{E}) = j_k(|\mathbf{E}|)\mathbf{E}$, where j_k is defined by²

$$j_k(s) = \begin{cases} k & \text{for } |s| < k^{-p}, \\ |s|^{-1/p} & \text{for } k^{-p} \leq |s| \leq \beta, \\ \beta^{-1/p} & \text{for } |s| > \beta. \end{cases} \quad (6.13)$$

The vector field \mathbf{J}_k is Lipschitz continuous for any $k \in \mathbb{N}$ and one can easily check that

$$|\mathbf{J}_k(\mathbf{s}) - \mathbf{J}(\mathbf{s})| \leq C(p) k^{1-p}. \quad (6.14)$$

The coefficient $C(p)$ depends only on the parameter p .

The problem (6.12) is linear and elliptic in \mathbf{W} . The existence and uniqueness of a weak solution in \mathbf{W} is guaranteed by the Lax–Milgram lemma.

Now, the equation (6.1) is rewritten as follows

$$k(\mathbf{E}, \boldsymbol{\varphi}) + (\nabla \times \mathbf{E}, \nabla \times \boldsymbol{\varphi}) = (\mathbf{F}, \boldsymbol{\varphi}) + (k\mathbf{E} - \mathbf{J}_k(\mathbf{E}), \boldsymbol{\varphi}) + (\mathbf{J}_k(\mathbf{E}) - \mathbf{J}(\mathbf{E}), \boldsymbol{\varphi}).$$

²If $k < \beta^{-1/p}$, the definition of the function j_k is meaningless, but $k \geq \beta^{-1/p}$ for all $k \in \mathbb{N}$ as the parameter $\beta \gg 1$.

By subtracting this from (6.12) and introducing a real function $h_k(s) := j_k(s) - k$ and the vector field $\mathbf{H}_k(\mathbf{s}) := \mathbf{J}_k(\mathbf{s}) - k\mathbf{s}$, we get

$$k(\mathbf{E}_k - \mathbf{E}, \boldsymbol{\varphi}) + (\nabla \times (\mathbf{E}_k - \mathbf{E}), \nabla \times \boldsymbol{\varphi}) = (\mathbf{H}_k(\mathbf{E}) - \mathbf{H}_k(\mathbf{E}_{k-1}), \boldsymbol{\varphi}) + (\mathbf{J}(\mathbf{E}) - \mathbf{J}_k(\mathbf{E}), \boldsymbol{\varphi}).$$

We set $\boldsymbol{\varphi} = \mathbf{E}_k - \mathbf{E}$ and we obtain the variational formulation for the error $\|\mathbf{E}_k - \mathbf{E}\|$

$$k\|\mathbf{E}_k - \mathbf{E}\|^2 + \|\nabla \times (\mathbf{E}_k - \mathbf{E})\|^2 = (\mathbf{H}_k(\mathbf{E}) - \mathbf{H}_k(\mathbf{E}_{k-1}), \mathbf{E}_k - \mathbf{E}) + (\mathbf{J}(\mathbf{E}) - \mathbf{J}_k(\mathbf{E}), \mathbf{E}_k - \mathbf{E}). \quad (6.15)$$

We point out that Lemma 6.3 is valid for the vector field \mathbf{H}_k and $M = k - \beta^{-1/p}$.

6.2.1 Stability

We establish the a priori estimates for \mathbf{E} and \mathbf{E}_k in the space $\mathbf{L}_2(\Omega)$ that will play role in the proof of the convergence of the approximation scheme (6.12).

Lemma 6.9 *Let $\mathbf{F} \in \mathbf{L}_2(\Omega)$ and $\beta \in \mathbb{R}$ be fixed. The following estimates hold for the norm of the solution \mathbf{E} to the problem (6.1) and \mathbf{E}_k —the solution to the approximation scheme (6.12)—on each step $k \in \mathbb{N}$.*

$$\begin{aligned} \|\mathbf{E}\| &\leq \frac{\|\mathbf{F}\|}{\beta^{-1/p}}, \\ \|\mathbf{E}_k\| &\leq \frac{\|\mathbf{F}\|}{\beta^{-1/p}} + \|\mathbf{E}_0\|. \end{aligned}$$

Proof When we set $\boldsymbol{\varphi} = \mathbf{E}$ to the equation (6.1), we get

$$(\mathbf{J}(\mathbf{E}), \mathbf{E}) + \|\nabla \times \mathbf{E}\|^2 = (\mathbf{F}, \mathbf{E}).$$

For each vector $\mathbf{s} \in \mathbb{R}^3$ the following inequality holds

$$j(|\mathbf{s}|) \geq \beta^{-1/p}.$$

Hence

$$\beta^{-1/p}\|\mathbf{E}\|^2 + \|\nabla \times \mathbf{E}\|^2 \leq \|\mathbf{F}\| \|\mathbf{E}\|$$

and this completes the proof of the first estimate.

Now, by setting $\varphi = \mathbf{E}_k$ in the equation (6.12) we obtain

$$k\|\mathbf{E}_k\|^2 + \|\nabla \times \mathbf{E}_k\|^2 = (k\mathbf{E}_{k-1} - \mathbf{J}_k(\mathbf{E}_{k-1}), \mathbf{E}_k) + (\mathbf{F}, \mathbf{E}_k). \quad (6.16)$$

For each vector $\mathbf{s} \in \mathbb{R}^3$ we can prove that

$$|k\mathbf{s} - \mathbf{J}_k(\mathbf{s})| \leq |k - \beta^{-1/p}| |\mathbf{s}|,$$

thus

$$k\|\mathbf{E}_k\|^2 + \|\nabla \times \mathbf{E}_k\|^2 \leq \|\mathbf{F}\| \|\mathbf{E}_k\| + |k - \beta^{-1/p}| \|\mathbf{E}_{k-1}\| \|\mathbf{E}_k\|.$$

This leads to

$$\begin{aligned} \|\mathbf{E}_k\| &\leq \frac{1}{k} \|\mathbf{F}\| + \frac{k - \beta^{-1/p}}{k} \|\mathbf{E}_{k-1}\| \\ &\leq \frac{1}{k} \|\mathbf{F}\| + \frac{k - \beta^{-1/p}}{k} \|\mathbf{F}\| + \frac{(k - \beta^{-1/p})(k - 1 - \beta^{-1/p})}{k(k-1)} \|\mathbf{E}_{k-2}\| \\ &\leq \dots \\ &< \frac{1}{k} \|\mathbf{F}\| \left(1 - \frac{k - \beta^{-1/p}}{k}\right)^{-1} + \|\mathbf{E}_0\| \\ &< \frac{\|\mathbf{F}\|}{\beta^{-1/p}} + \|\mathbf{E}_0\|. \end{aligned} \quad (6.17)$$

This completes the proof. \square

6.2.2 Error estimates and convergence

The following error estimate proves the convergence of the proposed method in the space $\mathbf{L}_2(\Omega)$.

Theorem 6.10 *If \mathbf{E}_k results from the iteration scheme (6.12) and \mathbf{E} is the solution to (6.1), then for any $k \in \mathbb{N}$ holds*

$$\|\mathbf{E}_k - \mathbf{E}\| \leq C k^{-\min\{\beta^{-1/p}, p-1\}}. \quad (6.18)$$

Proof Applying Lemma 6.3, (6.14) and the Cauchy and Young inequalities to the right-hand side of (6.15), we obtain

$$\begin{aligned} k\|\mathbf{E}_k - \mathbf{E}\|^2 + \|\nabla \times (\mathbf{E}_k - \mathbf{E})\|^2 &\leq (k - \beta^{-1/p}) \|\mathbf{E}_{k-1} - \mathbf{E}\| \|\mathbf{E}_k - \mathbf{E}\| \\ &\quad + C(p) k^{1-p} \|\mathbf{E}_k - \mathbf{E}\|. \end{aligned} \quad (6.19)$$

This directly implies

$$\|\mathbf{E}_k - \mathbf{E}\| \leq \frac{k - \beta^{-1/p}}{k} \|\mathbf{E}_{k-1} - \mathbf{E}\| + C(p) k^{-p}.$$

It is a recursive formula. The rest of the proof follows from [63, Lemma 4.2]. \square

6.3 Numerical experiments

In this section we present some numerical examples to demonstrate the efficiency and robustness of the proposed linearization schemes (6.5) and (6.12).

In all examples, the domain Ω —the region occupied by the superconductor—is the unit cube in \mathbb{R}^3 . We split this domain into a tetrahedral mesh. The number of elements is chosen depending on the nature of the exact solution. The mesh consisting of 48 elements is used, if the exact solution can be fitted precisely by Whitney’s edge elements. A denser mesh is used for more complicated³ solutions. The convergence of the full discretized scheme and the dependence on the density of the mesh is discussed in Chapter 8.

During the experiments, different values of the parameter p are used, varying from 1.01 to 2. The approximate solutions are determined in an iterative way always starting from $\mathbf{E}_0 \equiv \mathbf{0}$.

6.3.1 Lipschitz continuous case

The nonlinearity (1.5) is used.

The nonlinear vector field \mathbf{J} is defined as follows

$$\mathbf{J}(\mathbf{E}) = \begin{cases} 0.01^{-1/p} \mathbf{E}, & 0 \leq |\mathbf{E}| < 0.01, \\ |\mathbf{E}|^{-1/p} \mathbf{E}, & 0.01 \leq |\mathbf{E}| \leq 100, \\ 100^{-1/p} \mathbf{E}, & 100 < |\mathbf{E}|. \end{cases} \quad (6.20)$$

First, we consider the problem with linear exact solution. Namely: Find $\mathbf{E} \in \mathbf{H}(\mathbf{curl}; \Omega)$ satisfying

$$\begin{aligned} \mathbf{J}(\mathbf{E}) + \nabla \times \nabla \times \mathbf{E} &= \mathbf{F} && \text{in } \Omega, \\ \nabla \times \mathbf{E} \times \boldsymbol{\nu} &= \mathbf{g} && \text{on } \Gamma, \end{aligned} \quad (6.21)$$

³By complicated solutions, we mean the vector field that cannot be fitted by Whitney’s elements precisely.

where the data functions \mathbf{F} and \mathbf{g} are defined in such a way, that the vector field $\mathbf{E}^l(\mathbf{x}) = (E_1^l(x_1, x_2, x_3), E_2^l(x_1, x_2, x_3), E_3^l(x_1, x_2, x_3))$ defined by

$$\begin{aligned} E_1^l(\mathbf{x}) &= 10(x_3 - x_2) \\ E_2^l(\mathbf{x}) &= 10(x_1 - x_3) \\ E_3^l(\mathbf{x}) &= 10(x_2 - x_1) \end{aligned} \quad (6.22)$$

solves (6.21). The vector field \mathbf{E}^l can be fitted exactly by Whitney's edge elements. Therefore, a very sparse mesh can be used for the calculations and the discretization error does not influence the results.

The second considered BVP has a sinusoidal exact solution. Namely: The data functions \mathbf{F} and \mathbf{g} in (6.21) are defined in such a way, that the vector field $\mathbf{E}^s = (E_1^s, E_2^s, E_3^s)$ with

$$\begin{aligned} E_1^s(\mathbf{x}) &= 10(\sin(x_2) - \sin(x_3)) \\ E_2^s(\mathbf{x}) &= 10(\sin(x_3) - \sin(x_1)) \\ E_3^s(\mathbf{x}) &= 10(\sin(x_1) - \sin(x_2)) \end{aligned} \quad (6.23)$$

solves (6.21).

The exact solution serves to compute the error of approximate solutions obtained by the linearization scheme. We employ the linear approximation scheme (6.5) to both defined BVPs. After the discretization in space, the problem (6.5) reduces to the system of linear equations. The matrix of the system is constant during the whole iterative process. Therefore, the method is quite fast even if the number of iterations is high. The iterations are stopped when the difference between two subsequent right-hand sides measured in the $\mathbf{L}_2(\Omega)$ -norm is smaller than a fixed threshold δ . We use $\delta = 10^{-6}$, as it leads to satisfactory results in convenient time.

The value of L for each $p \in \{1.01, 1.05, 1.1, 1.2\}$ was chosen in accordance with the reasoning in Remark 6.7. Even if this is probably not the optimal value of L , we did not want to influence the choice of L by the knowledge of the exact solution as we realized that the optimal L depends strongly on the exact solution itself. On the other hand, if one has some knowledge of the exact solution, the implementation of an adaptive adjustment of L can considerably speed up the computations.

If the parameter p approaches 1, more iterations are required in order to obtain the same accuracy. This can be seen already on a simple example with the linear exact solution (Table 6.1). It is not surprising, as the parameter p close to 1 means, that the nonlinearity j has a very steep slope. In other words,

p	L	# iterations	relative error	
			1 st iteration	last iteration
1.20	23	19	0.487381	0.000001
1.10	32	24	0.570234	0.000002
1.05	40	28	0.624109	0.000002
1.01	50	33	0.674966	0.000003

Table 6.1: The evolution of the relative error $\|\mathbf{E}_k - \mathbf{E}^l\|/\|\mathbf{E}^l\|$ of the linear approximation scheme (6.5). The nonlinearity is given by (6.20). The mesh consisting of 48 tetrahedral elements (98 DOFs) is used.

p	L	# iterations	relative error	
			1 st iteration	last iteration
1.20	23	2068	0.610293	0.017253
1.10	32	3652	0.670763	0.017591
1.05	40	5234	0.710496	0.017884
1.01	50	7352	0.748185	0.018249

Table 6.2: The evolution of the relative error $\|\mathbf{E}_k - \mathbf{E}^s\|/\|\mathbf{E}^s\|$ of the linear approximation scheme (6.5). The nonlinearity is given by (6.20). The mesh consisting of 3072 elements (4184 DOFs) is used.

(6.21) differs a lot from the linear problem, which is the simplest to calculate. This is also in accordance with the error estimates derived in Theorem 6.6. The same phenomenon is observed in the iteration process if the problem (6.21) with sinusoidal exact solution \mathbf{E}^s is considered (Table 6.2).

The change of the convergence rate is another aspect to be discussed. The convergence of the method is fast (its slope depends on p) until the error reaches some constant value (Figure 6.2). This phenomenon can be explained by splitting the total error $\|\mathbf{E}_k - \mathbf{E}\|$ into two parts. The error caused by linearization (estimated in Theorem 6.6), and the error due to the space discretization. If the mesh consisting of 3072 elements is used, the vector field \mathbf{E}^s can be fitted by Whitney's edge elements with the error of about 1.7%. The discretization error is the minimal error that can be reached. Thus we see that in a practical computation the (linear) iterations converge to the finite element solution of the nonlinear problem under consideration. Once this "limit" value is reached,

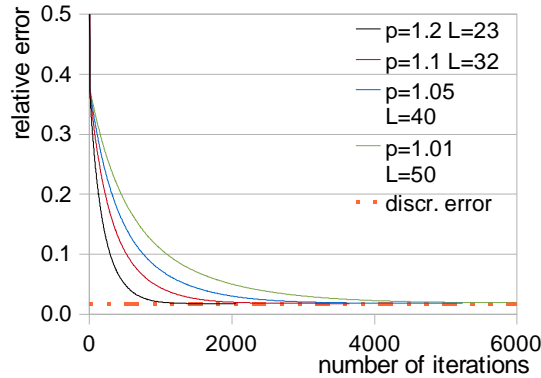


Figure 6.2: The relative error of the scheme (6.5) depending on the number of iterations. The nonlinear term is given by (6.20) and sinusoidal exact solution \mathbf{E}^s is considered. The mesh consists of 3072 elements (4184 DOFs). Hence, the vector field \mathbf{E}^s can be fitted by Whitney's edge elements with the error of 1.7377% also called discretization error. The discretization error is the minimal error that can be reached.

further iterations are no longer needed.

6.3.2 Non-Lipschitz continuous case

The nonlinearity (1.4) is used.

In this numerical experiment we will consider the nonlinear vector field \mathbf{J} defined as

$$\mathbf{J}(\mathbf{E}) = \begin{cases} |\mathbf{E}|^{-1/p} \mathbf{E}, & 0 \leq |\mathbf{E}| \leq 100, \\ 100^{-1/p} \mathbf{E}, & 100 < |\mathbf{E}|. \end{cases} \quad (6.24)$$

The problem (6.21) with sinusoidal exact solution \mathbf{E}^s is calculated using the numerical scheme (6.12). The mesh consisting of 3072 tetrahedral elements is used. The discretization error is of about 1.7%.

The error of about 1.8% is achieved after approximately 360 iterations if $p = 1.05$ (Table 6.3). A significantly lower number of iterations than in the previous example is needed to obtain approximately the same results in the same experimental conditions (compare Tables 6.3 and 6.2). This is due to a slight modification of the used linearization scheme (6.12). Properly, the iteration step k has to be changed successively after each calculation of the problem (6.12).

		relative error	
p	# iterations	1 st iteration	last iteration
1.20	167	0.316505	0.017245
1.10	262	0.326098	0.017570
1.05	361	0.330930	0.017840
1.01	503	0.334796	0.018154

Table 6.3: The evolution of the relative error $\|\mathbf{E}_k - \mathbf{E}^s\|/\|\mathbf{E}^s\|$ of the linear approximation scheme (6.12). The nonlinearity is given by (6.24). The mesh consisting of 3072 elements (4184 DOFs) is used.

But as the singularity of the problem appears for small values of \mathbf{E} and the exact solution (6.23) attains zero only in a quite small subdomain of Ω , the successive change of k would not be so helpful. Therefore, we decide to combine the two proposed linearization schemes (6.12) and (6.5), what considerably speeds up the convergence. First, we calculate the problem (6.12) only once. Then, we fix k and set $\mathbf{E}_k = \mathbf{E}_{k,0}$. Then the following scheme

$$k(\mathbf{E}_{k,i}, \boldsymbol{\varphi}) + (\nabla \times \mathbf{E}_{k,i}, \nabla \times \boldsymbol{\varphi}) = (\mathbf{F}, \boldsymbol{\varphi}) + k(\mathbf{E}_{k,i-1}, \boldsymbol{\varphi}) - (\mathbf{J}_k(\mathbf{E}_{k,i-1}), \boldsymbol{\varphi})$$

is computed for a fixed parameter k and a fixed vector field \mathbf{J}_k until the difference between the right-hand side of two subsequent iterations is sufficiently small, i.e.

$$\|k(\mathbf{E}_{k,i-1} - \mathbf{E}_{k,i}, \boldsymbol{\varphi}) - (\mathbf{J}_k(\mathbf{E}_{k,i-1}) - \mathbf{J}_k(\mathbf{E}_{k,i}), \boldsymbol{\varphi})\|_{L^2(\Omega)} < \delta.$$

Then we set $\mathbf{E}_{k,i} = \mathbf{E}_k$ and increase k . In the experiments, the value of δ equal to 10^{-6} is used.

As the convergence and the error estimates were proven for both iteration schemes (6.5) and (6.12), the convergence of its combination is straightforward.

We observe again, in accordance with the error estimates derived in Theorem 6.10, the dependence of the convergence rate on the parameter p . The use of the finite element approximation again causes the stabilization of the total relative error at about 1.8% what is approximately the value of the discretization error. The rate of the convergence remarkably decreases when the relative error approaches the discretization one (Figure 6.3).

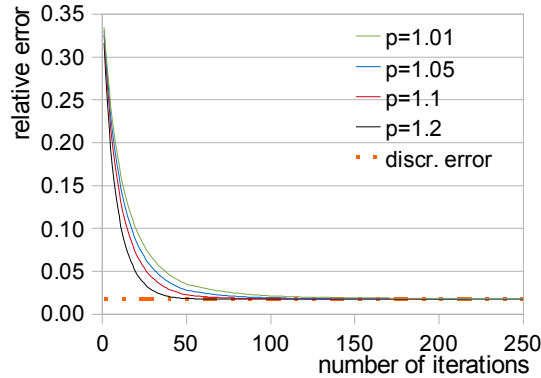


Figure 6.3: The relative error of the scheme (6.12) depending on the number of iterations. The nonlinear term is given by (6.24) and sinusoidal exact solution \mathbf{E}^s is considered. The mesh consists of 3072 elements. In these circumstances, the vector field \mathbf{E}^s can be fitted by Whitney's edge elements with the error of 1.7377% also called discretization error. The discretization error is the minimal error that can be reached.

6.4 Conclusions

In this chapter a 3D stationary state problem for current flow in type-II superconductors was studied. The study was based on the article [38].

Two new linearization schemes were proposed to calculate the nonlinear PDE (6.1), where \mathbf{J} is given by (1.5) and the nonlinear degenerate PDE (6.1), where \mathbf{J} is given by (1.4). The cut-off of \mathbf{J} for large values of electric field formed the crucial step in proving the convergence of the proposed linearization schemes. As both schemes are based on the fixed-point principle, one can expect that they will be very slow. However, a careful combination of the schemes (6.12) and (6.5) leads to a robust and efficient numerical tool to solve the degenerate problem (6.1) equipped with the modified power law (1.4).

The graphs in the numerical experiments have all the same character. The rapidly decreasing part at the beginning is followed by a relatively constant section. This is due to the fact that with an increasing number of iterations the initially dominant linearization error becomes subjacent to the discretization one. As the precision of the linearization schemes (6.5) and (6.12) is approximately equal to the discretization error, it can be improved by the choice of a

denser mesh. However, the consecutive increase of calculation time and memory consumption needs to be taken into account.

The computations can be speed up by implementation of an adaptive adjustment of parameter L . This “cosmetic” modification can lead to considerably faster results and therefore is, in our opinion, worth to try.

7 RELAXATION METHOD

The nonlinearity (1.5) is used¹.

The methods of solving nonlinear PDEs presented in the previous chapters are just few of several possible ways. In the nineties, Kačur and Jäger came out with a new idea to solve nonlinear parabolic equations numerically [34–36]: They proposed methods based on a nonstandard time discretization including relaxation functions. They focused on the diffusion problems with free boundary, degenerate parabolic equations and degenerate doubly nonlinear parabolic and parabolic-elliptic equations and systems [45,46]. All these results have their main application in porous media problems—PDEs involving the Laplace operator. We studied their approach and derived some basic modifications to the problems with applications in electromagnetism.

The fixed-point linearization schemes presented in the previous chapter are based on the choice of one fixed constant. This constant is the same for all three equations in the system (1.15) and does not depend on the space variable \mathbf{x} . The theoretical results presented in this chapter are based on the linearization by a *full*² matrix varying in space. The method is referred to as relaxation method because the nonlinear parabolic PDE is split into a system of equations. The linear elliptic PDE is coupled with a nonlinear equation involving no partial derivatives.

The suggested method involves a positive-definite linearization matrix which can be for example chosen as a Jacobi matrix (or a regularized Jacobi matrix) of

¹The results of this chapter can be straightforward derived also for the nonlinearity defined by (1.4).

²By *full* we mean that the matrix can have non-zero components out of the diagonal.

the nonlinearity. We show the convergence of this method to the solution to the problem (1.15) in the space $\mathbf{H}_0(\mathbf{curl}; \Omega)$ for the Lipschitz continuous nonlinear vector field \mathbf{J} (1.5). The proofs can be equally good repeated for the nonlinear vector field \mathbf{J} given by (1.4) as only the coercivity of the nonlinearity is required. The coercivity holds for both \mathbf{J} given by (1.4) or (1.5) (check (6.4)).

Approximation scheme

We use an equidistant time partitioning with a time step $\tau = T/n$ for any $n \in \mathbb{N}$, so we divide the time interval $[0, T]$ into $n \in \mathbb{N}$ subintervals $[t^{i-1}, t^i]$ for $t^i = i\tau$. We decided to put the index of the time step to the superscript as the subscript will be later used to denote the space component. For any function f , we introduce the notation

$$f^i = f(t^i), \quad \delta f^i = \frac{f^i - f^{i-1}}{\tau}.$$

Analogously to the approximation scheme proposed by Kačur in [44], we introduce the relaxation matrix $\mathbf{A}^i = \mathbf{A}^i(\mathbf{x})$ on each time step and solve the elliptic problem in $\boldsymbol{\theta}^i$

$$(\mathbf{A}^i(\boldsymbol{\theta}^i - \mathbf{e}^{i-1}), \boldsymbol{\varphi}) + \tau (\nabla \times \boldsymbol{\theta}^i, \nabla \times \boldsymbol{\varphi}) = 0 \quad \forall \boldsymbol{\varphi} \in \mathbf{H}_0(\mathbf{curl}; \Omega), \quad (7.1)$$

where for all $i = 1, \dots, n$ and $\mathbf{x} \in \Omega$, the matrix \mathbf{A}^i is a positive-definite matrix and there exist constants $\lambda^i, \Lambda^i > 0$ such that

$$\lambda^i |\boldsymbol{\xi}|^2 \leq (\mathbf{A}^i \boldsymbol{\xi}, \boldsymbol{\xi}) < \Lambda^i |\boldsymbol{\xi}|^2. \quad (7.2)$$

Then we define \mathbf{e}^i from the relation

$$(\mathbf{J}(\mathbf{e}^i), \boldsymbol{\varphi}) = (\mathbf{J}(\mathbf{e}^{i-1}), \boldsymbol{\varphi}) + (\mathbf{A}^i(\boldsymbol{\theta}^i - \mathbf{e}^{i-1}), \boldsymbol{\varphi}) \quad \forall \boldsymbol{\varphi} \in \mathbf{L}_2(\Omega). \quad (7.3)$$

Once the solutions $\boldsymbol{\theta}^i$ and \mathbf{e}^i on each time step are found, we construct the step-in-time vector fields $\overline{\boldsymbol{\theta}}^n$ and $\overline{\mathbf{e}}^n$ such that

$$\begin{aligned} \overline{\boldsymbol{\theta}}^n(0) &= \mathbf{E}^0, & \overline{\boldsymbol{\theta}}^n(t) &= \boldsymbol{\theta}^i \quad \text{for } t \in (t^{i-1}, t^i], \\ \overline{\mathbf{e}}^n(0) &= \mathbf{E}^0, & \overline{\mathbf{e}}^n(t) &= \mathbf{e}^i \quad \text{for } t \in (t^{i-1}, t^i] \end{aligned}$$

and an in time piecewise-linear vector field \mathbf{J}^n , given by

$$\begin{aligned} \mathbf{J}^n(0) &= \mathbf{J}(\mathbf{E}^0), \\ \mathbf{J}^n(t) &= \mathbf{J}(\mathbf{e}^{i-1}) + (t - t^{i-1})\delta [\mathbf{J}(\mathbf{e}^i)] \quad \text{for } t \in (t^{i-1}, t^i]. \end{aligned}$$

Employing this notation, the relation (7.3) can be rewritten as

$$\tau(\partial_t \mathbf{J}^n(t), \varphi) = (\mathbf{A}^i(\boldsymbol{\theta}^i - \mathbf{e}^{i-1}), \varphi) \quad \forall \varphi \in \mathbf{L}_2(\Omega). \quad (7.4)$$

Thus we can write that (7.1) is equivalent to

$$(\partial_t \mathbf{J}^n(t), \varphi) + \left(\nabla \times \bar{\boldsymbol{\theta}}^n(t), \nabla \times \varphi \right) = 0 \quad \forall \varphi \in \mathbf{H}_0(\mathbf{curl}; \Omega). \quad (7.5)$$

Our main goal is to prove the convergence of $\{\bar{\boldsymbol{\theta}}^n\}$ to the variational solution \mathbf{E} to (1.15) if \mathbf{J} is defined by (1.5).

7.1 Existence and uniqueness

The existence and uniqueness of the solution $\mathbf{E} \in L_2((0, T), \mathbf{H}_0(\mathbf{curl}; \Omega))$ to the problem (1.15) follows from the error estimate in Remark 5.14.

If $\mathbf{E}^0 \in \mathbf{L}_2(\Omega)$ and since \mathbf{J} is strictly monotone, there exists a unique solution $\mathbf{e}^i \in \mathbf{L}_2(\Omega)$ to (7.3) for all $i = 1, \dots, n$ and $n \in \mathbb{N}$. The inverse to \mathbf{J} is the following

$$\mathbf{J}^{-1}(\mathbf{z}) = \begin{cases} \alpha^{1/p} \mathbf{z}, & |\mathbf{z}| < \alpha^{1-1/p}, \\ |\mathbf{z}|^{\frac{1}{p-1}} \mathbf{z}, & \alpha^{1-1/p} \leq |\mathbf{z}| \leq \beta^{1-1/p}, \\ \beta^{1/p} \mathbf{z}, & |\mathbf{z}| > \beta^{1-1/p}. \end{cases}$$

The existence and uniqueness of the solution $\boldsymbol{\theta}^i \in \mathbf{H}_0(\mathbf{curl}; \Omega)$ to the problem (7.1) follows directly from the Lax–Milgram lemma.

7.2 The properties of the Jacobian of the vector field \mathbf{J}

Let $\text{Jac}[\mathbf{J}(\mathbf{u})]$ be the Jacobian of \mathbf{J} in \mathbf{u} . For $\alpha \leq |\mathbf{u}| \leq \beta$ holds

$$\text{Jac}[\mathbf{J}(\mathbf{u})] = p^{-1} |\mathbf{u}|^{-2-1/p} \begin{pmatrix} p|\mathbf{u}|^2 - u_1^2 & -u_1 u_2 & -u_1 u_3 \\ -u_1 u_2 & p|\mathbf{u}|^2 - u_2^2 & -u_2 u_3 \\ -u_1 u_3 & -u_2 u_3 & p|\mathbf{u}|^2 - u_3^2 \end{pmatrix}$$

and the eigenvalues of $\text{Jac}[\mathbf{J}(\mathbf{u})]$ are equal to $(1 - 1/p)|\mathbf{u}|^{-1/p}$ and $|\mathbf{u}|^{-1/p}$. For $|\mathbf{u}| > \beta$ is

$$\text{Jac}[\mathbf{J}(\mathbf{u})] = \beta^{-1/p} \mathbf{I}$$

with the only eigenvalue equal to $\beta^{-1/p}$. Finally, for $|\mathbf{u}| < \alpha$ is

$$\text{Jac}[\mathbf{J}(\mathbf{u})] = \alpha^{-1/p} \mathbf{I}$$

with the only eigenvalue equal to $\alpha^{-1/p}$.

Therefore, if $(1 - 1/p)\alpha^{-1/p} > \beta^{-1/p}$, then

$$(1 - 1/p)\beta^{-1/p}|\boldsymbol{\xi}|^2 \leq \text{Jac}[\mathbf{J}(\mathbf{u})]\boldsymbol{\xi} \cdot \boldsymbol{\xi} \leq \alpha^{-1/p}|\boldsymbol{\xi}|^2 \quad \forall \mathbf{u}, \boldsymbol{\xi} \in \mathbb{R}^3.$$

We denote by $\text{Jac}[\mathbf{J}^{-1}(\mathbf{z})]$ the Jacobian of \mathbf{J}^{-1} in \mathbf{z} and for $\alpha^{1-1/p} \leq |\mathbf{z}| \leq \beta^{1-1/p}$ holds that

$$\text{Jac}[\mathbf{J}^{-1}(\mathbf{z})] = \frac{|\mathbf{z}|^{-2+1/p'}}{p'} \begin{pmatrix} p'|\mathbf{z}|^2 + z_1^2 & z_1 z_2 & z_1 z_3 \\ z_1 z_2 & p'|\mathbf{z}|^2 + z_2^2 & z_2 z_3 \\ z_1 z_3 & z_2 z_3 & p'|\mathbf{z}|^2 + z_3^2 \end{pmatrix},$$

where the notation $p' = p - 1$ is used. For $|\mathbf{z}| < \alpha^{1-1/p}$ and $|\mathbf{z}| > \beta^{1-1/p}$, we easily derive that

$$\text{Jac}[\mathbf{J}^{-1}(\mathbf{z})] = \alpha^{1/p} \mathbf{I} \text{ and } \text{Jac}[\mathbf{J}^{-1}(\mathbf{z})] = \beta^{1/p} \mathbf{I}, \text{ respectively.}$$

As $(\text{Jac}[\mathbf{J}(\mathbf{u})])^{-1} = \text{Jac}[\mathbf{J}^{-1}(|\mathbf{u}|^{-1/p} \mathbf{u})]$, we deduce that

$$\alpha^{1/p}|\boldsymbol{\xi}|^2 \leq \text{Jac}[\mathbf{J}^{-1}(\mathbf{z})]\boldsymbol{\xi} \cdot \boldsymbol{\xi} \leq \frac{p}{p-1} \beta^{1/p}|\boldsymbol{\xi}|^2 \quad \forall \mathbf{z}, \boldsymbol{\xi} \in \mathbb{R}^3. \quad (7.6)$$

7.3 A priori estimates

Firstly, we define a function \mathcal{J} (see [2]) as follows

$$\mathcal{J}(\mathbf{u}) = \mathbf{J}(\mathbf{u}) \cdot \mathbf{u} - \int_0^1 \mathbf{J}(t\mathbf{u}) \cdot \mathbf{u} \, dt \quad \forall \mathbf{u} \in \mathbb{R}^3.$$

Following the definition of the function \mathbf{J} , we successively obtain for any \mathbf{u} such that $\alpha \leq |\mathbf{u}| \leq \beta$ that

$$\begin{aligned} \mathcal{J}(\mathbf{u}) &= |\mathbf{u}|^{2-1/p} - \int_0^1 t^{1-1/p} |\mathbf{u}|^{2-1/p} \, dt \\ &= |\mathbf{u}|^{2-1/p} \left(1 - \frac{p}{2p-1} \right) = \frac{p-1}{2p-1} |\mathbf{u}|^{2-1/p} \end{aligned}$$

and thus

$$\frac{\mathcal{J}(\mathbf{u})}{|\mathbf{u}|^2} = \frac{p-1}{2p-1} |\mathbf{u}|^{-1/p} \geq \frac{p-1}{2p-1} \beta^{-1/p}.$$

Hence, if $\alpha \leq |\mathbf{u}| \leq \beta$ then there exists $C > 0$ such that

$$\mathcal{J}(\mathbf{u}) \geq C|\mathbf{u}|^2.$$

Moreover, for any \mathbf{u} such that $|\mathbf{u}| > \beta$ holds

$$\begin{aligned} \mathcal{J}(\mathbf{u}) &= \beta^{-1/p} |\mathbf{u}|^2 - \int_0^{\beta/|\mathbf{u}|} t^{1-1/p} |\mathbf{u}|^{2-1/p} dt - \int_{\beta/|\mathbf{u}|}^1 t \beta^{-1/p} |\mathbf{u}|^2 dt \\ &= \beta^{-1/p} |\mathbf{u}|^2 - \frac{p}{2p-1} \beta^{2-1/p} - |\mathbf{u}|^2 \beta^{-1/p} \left(\frac{1}{2} - \frac{\beta^2}{2|\mathbf{u}|^2} \right) \\ &= \frac{1}{2} \beta^{-1/p} |\mathbf{u}|^2 - \frac{\beta^{2-1/p}}{4p-2} \end{aligned}$$

and similar identity is valid for $|\mathbf{u}| < \alpha$.

Therefore we can conclude that there exist $C_1, C_2 > 0$ such that for all \mathbf{u} holds

$$\mathcal{J}(\mathbf{u}) \geq C_1 |\mathbf{u}|^2 - C_2. \quad (7.7)$$

Next, we derive similar relation between $\mathcal{J}(\mathbf{u})$ and $|\mathbf{J}(\mathbf{u})|^2$. First, we see that for all \mathbf{u} such that $\alpha \leq |\mathbf{u}| \leq \beta$ holds

$$|\mathbf{J}(\mathbf{u})|^2 = |\mathbf{u}|^{2-2/p}.$$

Second, for all \mathbf{u} such that $|\mathbf{u}| > \beta$ we have that

$$|\mathbf{J}(\mathbf{u})|^2 = \beta^{-1/p} |\mathbf{u}|^2 = 2 \left(\mathcal{J}(\mathbf{u}) + \frac{\beta^{2-1/p}}{4p-2} \right) = 2\mathcal{J}(\mathbf{u}) + \frac{\beta^{2-1/p}}{2p-1}$$

and analogously for $|\mathbf{u}| < \alpha$.

Thus, there exist $C_3, C_4 > 0$ such that for all \mathbf{u} holds

$$\mathcal{J}(\mathbf{u}) \geq C_3 |\mathbf{J}(\mathbf{u})|^2 - C_4. \quad (7.8)$$

Lemma 7.1 *The following inequality holds true for all $\mathbf{u}, \mathbf{v} \in \mathbb{R}^3$.*

$$(\mathbf{J}(\mathbf{u}) - \mathbf{J}(\mathbf{v}), \mathbf{u}) \geq \int_{\Omega} \mathcal{J}(\mathbf{u}) - \int_{\Omega} \mathcal{J}(\mathbf{v}).$$

Proof In the proof, we will employ Lemma 5.3. The non-negative continuous function g is defined by

$$g(t) = \begin{cases} \alpha^{1/p}, & 0 \leq t < \alpha^{1-1/p}, \\ t^{1/(p-1)}, & \alpha^{1-1/p} \leq t \leq \beta^{1-1/p}, \\ \beta^{1/p}, & \beta^{1-1/p} < t. \end{cases}$$

The function Φ_G is given by

$$\Phi_G(s) = \int_0^s g(t) \cdot t \, dt = \begin{cases} \frac{1}{2} \left(\alpha^{1/p} s^2 - \frac{\alpha^{2-1/p}}{2p-1} \right), & 0 \leq s < \alpha^{1-1/p} \\ \frac{p-1}{2p-1} s^{\frac{2p-1}{p-1}}, & \alpha^{1-1/p} \leq s \leq \beta^{1-1/p}, \\ \frac{1}{2} \left(\beta^{1/p} s^2 - \frac{\beta^{2-1/p}}{2p-1} \right), & \beta^{1-1/p} < s. \end{cases}$$

We set $\mathbf{x} = \mathbf{J}(\mathbf{v})$ and $\mathbf{y} = \mathbf{J}(\mathbf{u})$ and apply Lemma 5.3 to get the inequality

$$\Phi_G(|\mathbf{J}(\mathbf{u})|) - \Phi_G(|\mathbf{J}(\mathbf{v})|) \leq g(|\mathbf{J}(\mathbf{u})|) \mathbf{J}(\mathbf{u}) \cdot (\mathbf{J}(\mathbf{u}) - \mathbf{J}(\mathbf{v})). \quad (7.9)$$

We proceed by the study of the right-hand side of this inequality. First we assume that \mathbf{u} is such that $\alpha \leq |\mathbf{u}| \leq \beta$. Then $|\mathbf{J}(\mathbf{u})| = |\mathbf{u}|^{1-1/p} \in [\alpha^{1-1/p}, \beta^{1-1/p}]$ and

$$g(|\mathbf{J}(\mathbf{u})|) \mathbf{J}(\mathbf{u}) = g(|\mathbf{u}|^{1-1/p}) |\mathbf{u}|^{-1/p} \mathbf{u} = \mathbf{u}.$$

If $|\mathbf{u}| > \beta$, then $|\mathbf{J}(\mathbf{u})| = \beta^{-1/p} |\mathbf{u}| > \beta^{1-1/p}$ and

$$g(|\mathbf{J}(\mathbf{u})|) \mathbf{J}(\mathbf{u}) = g(\beta^{-1/p} |\mathbf{u}|) \beta^{-1/p} |\mathbf{u}| = \mathbf{u}.$$

Analogously if $|\mathbf{u}| < \alpha$ then $g(|\mathbf{J}(\mathbf{u})|) \mathbf{J}(\mathbf{u}) = \mathbf{u}$.

Thus we deduce that

$$g(|\mathbf{J}(\mathbf{u})|) \mathbf{J}(\mathbf{u}) \cdot (\mathbf{J}(\mathbf{u}) - \mathbf{J}(\mathbf{v})) = \mathbf{u} \cdot (\mathbf{J}(\mathbf{u}) - \mathbf{J}(\mathbf{v})).$$

So the right-hand side of the inequality (7.9) after integration over Ω coincides with the left-hand side of the inequality to be proven.

After simple algebraic operations and careful analysis for different possible combinations of the norms of \mathbf{u} and \mathbf{v} , one can verify that

$$\Phi_G(|\mathbf{J}(\mathbf{u})|) - \Phi_G(|\mathbf{J}(\mathbf{v})|) = \mathcal{J}(\mathbf{u}) - \mathcal{J}(\mathbf{v}).$$

Thus we proved the statement of the lemma. \square

Lemma 7.2 Let $\mathbf{E}^0 \in \mathbf{L}_2(\Omega)$ and let for all $i = 1, \dots, n$ the matrix \mathbf{A}^i be a positive semidefinite matrix fulfilling (7.2), where λ^i and Λ^i are such that:

- (i) There exists $\lambda > 0$ such that $\lambda^i \geq \lambda$ for all $i = 1, \dots, n$ and all $n \in \mathbb{N}$.
- (ii) For all $i = 1, \dots, n$ and all $n \in \mathbb{N}$ holds

$$\Lambda^i \leq \frac{p-1}{p} \beta^{-1/p}. \quad (7.10)$$

Then the following estimates hold true uniformly for n :

$$\sum_{i=1}^n \|\mathbf{J}(\mathbf{e}^i) - \mathbf{J}(\mathbf{e}^{i-1})\|^2 + \sum_{i=1}^n \tau \|\nabla \times \boldsymbol{\theta}^i\|^2 \leq C, \quad (7.11)$$

$$\int_{\Omega} \mathcal{J}(\mathbf{e}^j) \leq C, \quad 1 \leq j \leq n, \quad (7.12)$$

$$\sum_{i=1}^n \|\mathbf{e}^i - \mathbf{e}^{i-1}\|^2 \leq C, \quad (7.13)$$

$$\|\mathbf{J}(\mathbf{e}^j)\|^2 \leq C, \quad \|\mathbf{e}^j\|^2 \leq C, \quad 1 \leq j \leq n, \quad (7.14)$$

$$\sum_{i=1}^n \|\boldsymbol{\theta}^i - \mathbf{e}^{i-1}\|^2 \leq C, \quad (7.15)$$

$$\|\boldsymbol{\theta}^j\|^2 \leq C, \quad 1 \leq j \leq n. \quad (7.16)$$

Proof We set $\boldsymbol{\varphi} = \boldsymbol{\theta}^i$ in (7.1) and sum it up for $i = 1, \dots, j$, $1 \leq j \leq n$. We employ the relation (7.3) and obtain

$$\sum_{i=1}^j (\mathbf{J}(\mathbf{e}^i) - \mathbf{J}(\mathbf{e}^{i-1}), \boldsymbol{\theta}^i) + \sum_{i=1}^j \tau \|\nabla \times \boldsymbol{\theta}^i\|^2 = 0.$$

We will focus on the first term in the previous equality in order to bound it from below.

Firstly, we rewrite it as follows

$$\begin{aligned} (\mathbf{J}(\mathbf{e}^i) - \mathbf{J}(\mathbf{e}^{i-1}), \boldsymbol{\theta}^i) &= (\mathbf{J}(\mathbf{e}^i) - \mathbf{J}(\mathbf{e}^{i-1}), \boldsymbol{\theta}^i - \mathbf{e}^{i-1}) + \\ &\quad (\mathbf{J}(\mathbf{e}^i) - \mathbf{J}(\mathbf{e}^{i-1}), \mathbf{e}^i) - (\mathbf{J}(\mathbf{e}^i) - \mathbf{J}(\mathbf{e}^{i-1}), \mathbf{e}^i - \mathbf{e}^{i-1}) \end{aligned}$$

and we denote the three terms on the left-hand side by J_1 , J_2 and $-J_3$ respectively. As a result of (7.3) and (7.2) we have

$$\begin{aligned} J_1 &= \left(\mathbf{J}(\mathbf{e}^i) - \mathbf{J}(\mathbf{e}^{i-1}), (\mathbf{A}^i)^{-1} (\mathbf{J}(\mathbf{e}^i) - \mathbf{J}(\mathbf{e}^{i-1})) \right) \\ &\geq \frac{1}{\Lambda^i} \|\mathbf{J}(\mathbf{e}^i) - \mathbf{J}(\mathbf{e}^{i-1})\|^2. \end{aligned}$$

Further, using Lemma 7.1 we obtain

$$J_2 \geq \int_{\Omega} \mathcal{J}(\mathbf{e}^i) - \int_{\Omega} \mathcal{J}(\mathbf{e}^{i-1}).$$

The last term is estimated using the mean-value theorem and the estimate (7.6).

$$\begin{aligned} J_3 &= (\mathbf{J}(\mathbf{e}^i) - \mathbf{J}(\mathbf{e}^{i-1}), \mathbf{J}^{-1}(\mathbf{J}(\mathbf{e}^i)) - \mathbf{J}^{-1}(\mathbf{J}(\mathbf{e}^{i-1}))) \\ &= (\text{Jac}[\mathbf{J}^{-1}(\mathbf{z})] (\mathbf{J}(\mathbf{e}^i) - \mathbf{J}(\mathbf{e}^{i-1})), \mathbf{J}(\mathbf{e}^i) - \mathbf{J}(\mathbf{e}^{i-1})) \\ &\leq \frac{p\beta^{1/p}}{p-1} \|\mathbf{J}(\mathbf{e}^i) - \mathbf{J}(\mathbf{e}^{i-1})\|^2. \end{aligned}$$

Thus

$$\begin{aligned} (\mathbf{J}(\mathbf{e}^i) - \mathbf{J}(\mathbf{e}^{i-1}), \boldsymbol{\theta}^i) &\geq \left(\frac{1}{\Lambda^i} - \frac{p}{p-1} \beta^{1/p} \right) \|\mathbf{J}(\mathbf{e}^i) - \mathbf{J}(\mathbf{e}^{i-1})\|^2 \\ &\quad + \int_{\Omega} \mathcal{J}(\mathbf{e}^i) - \int_{\Omega} \mathcal{J}(\mathbf{e}^{i-1}). \end{aligned}$$

Due to the proposition (7.10) we can directly conclude the estimates (7.11) and (7.12).

From the coercivity of the vector field \mathbf{J} (6.4) and the Cauchy-Schwartz inequality, we successively obtain

$$\begin{aligned} \beta^{-1/p}(1-1/p) \|\mathbf{e}^i - \mathbf{e}^{i-1}\|^2 &\leq (\mathbf{J}(\mathbf{e}^i) - \mathbf{J}(\mathbf{e}^{i-1}), \mathbf{e}^i - \mathbf{e}^{i-1}) \\ &\leq \|\mathbf{J}(\mathbf{e}^i) - \mathbf{J}(\mathbf{e}^{i-1})\| \|\mathbf{e}^i - \mathbf{e}^{i-1}\|. \end{aligned}$$

Hence the estimate (7.13) follows from the estimate (7.11).

We easily derive (7.14) from (7.7)–(7.8) and the estimate (7.12).

We proceed to the proof of the estimate (7.15). We set $\boldsymbol{\varphi} = \boldsymbol{\theta}^i - \mathbf{e}^{i-1}$ in the relation (7.3) and derive

$$(\mathbf{J}(\mathbf{e}^i) - \mathbf{J}(\mathbf{e}^{i-1}), \boldsymbol{\theta}^i - \mathbf{e}^{i-1}) = (\mathbf{A}^i(\boldsymbol{\theta}^i - \mathbf{e}^{i-1}), \boldsymbol{\theta}^i - \mathbf{e}^{i-1}).$$

The use of the Cauchy-Schwartz inequality and relation (7.2) leads to

$$\|\mathbf{J}(\mathbf{e}^i) - \mathbf{J}(\mathbf{e}^{i-1})\| \|\boldsymbol{\theta}^i - \mathbf{e}^{i-1}\| \geq \lambda^i \|\boldsymbol{\theta}^i - \mathbf{e}^{i-1}\|^2.$$

Thus

$$\|\boldsymbol{\theta}^i - \mathbf{e}^{i-1}\| \leq \frac{1}{\lambda^i} \|\mathbf{J}(\mathbf{e}^i) - \mathbf{J}(\mathbf{e}^{i-1})\|.$$

The desired estimate follows now directly from (i) and (7.11).

Combining (7.14) and (7.15) gives the estimate (7.16). \square

Lemma 7.3 *Assume that $\mathbf{E}_0 \in \mathbf{L}_2(\Omega)$. Then there exists a positive C such that*

$$\sum_{i=1}^n \|\delta\mathbf{J}(\mathbf{e}^i)\|_{\mathbf{H}_0^*(\mathbf{curl};\Omega)}^2 \tau \leq C.$$

Proof We remind the definition of the norm in $\mathbf{H}_0^*(\mathbf{curl};\Omega)$

$$\|\mathbf{z}\|_{\mathbf{H}_0^*(\mathbf{curl};\Omega)} = \sup_{\boldsymbol{\varphi} \in \mathbf{H}_0(\mathbf{curl};\Omega)} \frac{|\langle \mathbf{z}, \boldsymbol{\varphi} \rangle|}{\|\boldsymbol{\varphi}\|_{\mathbf{H}_0(\mathbf{curl};\Omega)}}.$$

Further we can write for any $\boldsymbol{\varphi} \in \mathbf{H}_0(\mathbf{curl};\Omega)$

$$(\delta\mathbf{J}(\mathbf{e}^i), \boldsymbol{\varphi}) = -(\nabla \times \boldsymbol{\theta}^i, \nabla \times \boldsymbol{\varphi}).$$

Applying the Cauchy inequality, we deduce that

$$|(\delta\mathbf{J}(\mathbf{e}^i), \boldsymbol{\varphi})| \leq \|\nabla \times \boldsymbol{\theta}^i\| \|\nabla \times \boldsymbol{\varphi}\|$$

and

$$\|\delta\mathbf{J}(\mathbf{e}^i)\|_{\mathbf{H}_0^*(\mathbf{curl};\Omega)} = \sup_{\boldsymbol{\varphi} \in \mathbf{H}_0(\mathbf{curl};\Omega)} \frac{|(\delta\mathbf{J}(\mathbf{e}^i), \boldsymbol{\varphi})|}{\|\boldsymbol{\varphi}\|_{\mathbf{H}_0(\mathbf{curl};\Omega)}} \leq \|\nabla \times \boldsymbol{\theta}^i\|.$$

The rest of the proof readily follows from previous lemma. \square

7.4 Convergence

We can proceed to the convergence of the proposed approximation scheme. In the following theorem, we will employ the Minty-Browder method (see, e.g. [26]). The convergence is valid for the subsequences denoted by the same symbol as the whole sequence. As the problem (1.15) admits a unique solution (Lemma 6.2), the convergence of the whole sequences can be deduced.

Theorem 7.4 *Suppose $\mathbf{J}(\mathbf{E}_0) \in \mathbf{L}_2(\Omega)$. Then there exists a vector field \mathbf{e} such that*

- (i) $\bar{\mathbf{e}}^n \rightharpoonup \mathbf{e}$ in $L_2((0, T), \mathbf{L}_2(\Omega))$,
- (ii) $\bar{\boldsymbol{\theta}}^n \rightharpoonup \boldsymbol{\theta}$ in $L_2((0, T), \mathbf{L}_2(\Omega))$,
- (iii) $\nabla \times \bar{\boldsymbol{\theta}}^n \rightharpoonup \nabla \times \boldsymbol{\theta}$ in $L_2((0, T), \mathbf{L}_2(\Omega))$,
- (iv) $\mathbf{J}(\bar{\mathbf{e}}^n) \rightharpoonup \mathbf{J}(\mathbf{e})$ in $L_2((0, T), \mathbf{L}_2(\Omega))$,
- (v) \mathbf{e} is a weak solution of (1.15).

Proof The proof is worked out in steps.

(i) and (ii)

Thanks to the a priori estimates (7.14), (7.16) and the reflexivity of the space $L_2((0, T), \mathbf{L}_2(\Omega))$, there exist weakly convergent subsequences of $\{\bar{\mathbf{e}}^n\}$ and $\{\bar{\boldsymbol{\theta}}^n\}$. We denote their limits by \mathbf{e} and $\boldsymbol{\theta}$ respectively. Furthermore holds that

$$\begin{aligned}
 \int_0^T |(\mathbf{e} - \boldsymbol{\theta}, \boldsymbol{\varphi})| &= \lim_{n \rightarrow \infty} \int_0^T |(\bar{\mathbf{e}}^n - \bar{\boldsymbol{\theta}}^n, \boldsymbol{\varphi})| = \lim_{n \rightarrow \infty} \sum_{i=1}^n \tau |(\mathbf{e}^i - \boldsymbol{\theta}^i, \boldsymbol{\varphi})| \\
 &\leq \lim_{n \rightarrow \infty} \sum_{i=1}^n \tau |(\mathbf{e}^i - \mathbf{e}^{i-1}, \boldsymbol{\varphi})| + \lim_{n \rightarrow \infty} \sum_{i=1}^n \tau |(\mathbf{e}^{i-1} - \boldsymbol{\theta}^i, \boldsymbol{\varphi})| \\
 &\leq \tau \|\boldsymbol{\varphi}\| \left(\lim_{n \rightarrow \infty} \sum_{i=1}^n \|\mathbf{e}^i - \mathbf{e}^{i-1}\| + \lim_{n \rightarrow \infty} \sum_{i=1}^n \|\mathbf{e}^{i-1} - \boldsymbol{\theta}^i\| \right) \\
 &\leq C\tau. \tag{7.17}
 \end{aligned}$$

The last inequality follows from the a priori estimates (7.13) and (7.15). Hence, $\mathbf{e} = \boldsymbol{\theta}$.

(iii)

Using the a priori estimate (7.11), the proof of this part of the theorem follows the proof of part (ii) of Theorem 5.7.

(iv)

From the estimate (7.14) and the reflexivity of the space $L_2((0, T), \mathbf{L}_2(\Omega))$, we deduce that there exists $\mathbf{w} \in L_2((0, T), \mathbf{L}_2(\Omega))$ such that $\mathbf{J}^n \rightharpoonup \mathbf{w}$ in

$L_2((0, T), \mathbf{L}_2(\Omega))$. We integrate (7.5) twice over the time and we pass to the limit for $n \rightarrow \infty$. We obtain

$$\int_0^t (\mathbf{w}, \boldsymbol{\varphi}) + \int_0^t \left(\int_0^s \nabla \times \mathbf{e}, \nabla \times \boldsymbol{\varphi} \right) = \int_0^t (j(|\mathbf{E}_0|)\mathbf{E}_0, \boldsymbol{\varphi}) \quad (7.18)$$

for any $\boldsymbol{\varphi} \in \mathbf{H}_0(\mathbf{curl}; \Omega)$ and $s, t \in [0, T]$.

Further for all $\boldsymbol{\varphi} \in \mathbf{H}_0(\mathbf{curl}; \Omega)$ holds that

$$\int_0^T (\mathbf{J}^n(t), \boldsymbol{\varphi}) = \int_0^T (\mathbf{J}(\bar{\boldsymbol{\epsilon}}^n(t)), \boldsymbol{\varphi}) + \int_0^T (t - t_{i-1} - \tau) (\delta \mathbf{J}(\bar{\boldsymbol{\epsilon}}^n(t)), \boldsymbol{\varphi}). \quad (7.19)$$

We use Cauchy-Schwartz's and Young's inequalities to deduce that

$$\begin{aligned} \left| \int_0^T (t - t_{i-1} - \tau) (\delta \mathbf{J}(\bar{\boldsymbol{\epsilon}}^n(t)), \boldsymbol{\varphi}) \right| &\leq \int_0^T \tau \|\delta \mathbf{J}(\bar{\boldsymbol{\epsilon}}^n(t))\|_{\mathbf{H}_0^*(\mathbf{curl}; \Omega)} \|\boldsymbol{\varphi}\|_{\mathbf{H}(\mathbf{curl}; \Omega)} \\ &\leq C \int_0^T \tau \left(\|\delta \mathbf{J}(\bar{\boldsymbol{\epsilon}}^n(t))\|_{\mathbf{H}_0^*(\mathbf{curl}; \Omega)}^2 + \|\boldsymbol{\varphi}\|_{\mathbf{H}(\mathbf{curl}; \Omega)}^2 \right) \xrightarrow{n \rightarrow \infty} 0. \end{aligned}$$

Employing Lemma 7.3 and passing to the limit with $n \rightarrow \infty$ in (7.19) gives

$$\lim_{n \rightarrow \infty} \int_0^T (\mathbf{J}^n(t), \boldsymbol{\varphi}) = \lim_{n \rightarrow \infty} \int_0^T (\mathbf{J}(\bar{\boldsymbol{\epsilon}}^n(t)), \boldsymbol{\varphi}) \quad \forall \boldsymbol{\varphi} \in \mathbf{H}_0(\mathbf{curl}; \Omega).$$

Thus for all $\boldsymbol{\varphi} \in \mathbf{H}_0(\mathbf{curl}; \Omega)$

$$\lim_{n \rightarrow \infty} \int_0^T (\mathbf{J}(\bar{\boldsymbol{\epsilon}}^n(t)), \boldsymbol{\varphi}) = \int_0^T (\mathbf{w}, \boldsymbol{\varphi}). \quad (7.20)$$

We remind that (3.4) holds for any weakly convergent sequence. This fact allows us to successively deduce

$$\begin{aligned}
\lim_{n \rightarrow \infty} \int_0^T (\mathbf{J}(\bar{\mathbf{e}}^n), \bar{\boldsymbol{\theta}}^n) &= \lim_{n \rightarrow \infty} \left[\int_0^T (\mathbf{J}(\mathbf{E}_0), \bar{\boldsymbol{\theta}}^n) - \int_0^T \left(\int_0^t \nabla \times \bar{\boldsymbol{\theta}}^n, \nabla \times \bar{\boldsymbol{\theta}}^n \right) \right] \\
&= \int_0^T (\mathbf{J}(\mathbf{E}_0), \mathbf{e}) - \frac{1}{2} \lim_{n \rightarrow \infty} \left\| \int_0^T \nabla \times \bar{\boldsymbol{\theta}}^n \right\|^2 \\
&\leq \int_0^T (\mathbf{J}(\mathbf{E}_0), \mathbf{e}) - \frac{1}{2} \left\| \int_0^T \nabla \times \mathbf{e} \right\|^2 \\
&= \int_0^T (\mathbf{J}(\mathbf{E}_0), \mathbf{e}) - \int_0^T \left(\int_0^t \nabla \times \mathbf{e}, \nabla \times \mathbf{e} \right) \\
&\stackrel{(7.18)}{=} \int_0^T (\mathbf{w}, \mathbf{e}). \tag{7.21}
\end{aligned}$$

The nonlinear operator \mathbf{J} is monotone in $L_2((0, T), \mathbf{L}_2(\Omega))$, hence

$$\int_0^T (\mathbf{J}(\bar{\mathbf{e}}^n) - \mathbf{J}(\mathbf{u}), \bar{\mathbf{e}}^n - \mathbf{u}) \geq 0 \quad \forall \mathbf{u} \in L_2((0, T), \mathbf{L}_2(\Omega)).$$

We rewrite the previous inequality as follows

$$\int_0^T (\mathbf{J}(\bar{\mathbf{e}}^n) - \mathbf{J}(\mathbf{u}), \bar{\mathbf{e}}^n - \bar{\boldsymbol{\theta}}^n) + \int_0^T (\mathbf{J}(\bar{\mathbf{e}}^n) - \mathbf{J}(\mathbf{u}), \bar{\boldsymbol{\theta}}^n - \mathbf{u}) \geq 0.$$

Taking the limit for $n \rightarrow \infty$, the first term on the left-hand side tends to 0 due to the estimates (7.11), (7.15) and (7.17). On the second term we use (7.20) and (7.21) and in the limit we obtain that for all $\mathbf{u} \in L_2((0, T), \mathbf{L}_2(\Omega))$

$$\int_0^T (\mathbf{w} - \mathbf{J}(\mathbf{u}), \mathbf{e} - \mathbf{u}) \geq 0.$$

By substituting $\mathbf{u} = \mathbf{e} + \varepsilon \mathbf{v}$ for any \mathbf{v} and $\varepsilon > 0$ we obtain

$$\int_0^T (\mathbf{w} - \mathbf{J}(\mathbf{e} + \varepsilon \mathbf{v}), \mathbf{v}) \leq 0.$$

Considering the limit case $\varepsilon \rightarrow 0$, we see that

$$\int_0^T (\mathbf{w} - \mathbf{J}(\mathbf{e}), \mathbf{v}) \leq 0.$$

Finally we put $\mathbf{v} = \mathbf{w} - \mathbf{J}(\mathbf{e})$ and we can deduce that

$$\mathbf{w} = \mathbf{J}(\mathbf{e}) \quad \text{in } L_2((0, T), \mathbf{L}_2(\Omega)).$$

(v)

This step of the proof follows directly the proof of the part (iv) of Theorem 5.7. Therefore it will be omitted. \square

7.5 Choice of the linearization matrix

The best choice of the linearization matrix \mathbf{A}^i is essential in order to obtain an efficient numerical method. Here follow some suggestions.

If the Lipschitz continuous nonlinearity (1.5) is considered, the linearization matrix can be chosen as a multiple of the Jacobi matrix of the nonlinear vector field \mathbf{J} in the solution \mathbf{e}^{i-1} from the previous time step. Indeed, the matrix $s_i \text{Jac}\mathbf{J}(\mathbf{e}^{i-1})$ is a real positive-definite matrix. The multiple s_i has to be chosen in such a way that the conditions of Lemma 7.2 are satisfied, i.e. there exists $s > 0$ such that

$$0 < s \leq s_i \leq \frac{p-1}{p} \alpha^{1/p} \beta^{-1/p}.$$

If the non-Lipschitz continuous but coercive nonlinearity (1.4) is considered, the linearization matrix has to be chosen more carefully. One possibility is a regularized Jacobi matrix of \mathbf{J} , namely

$$\mathbf{A}^i = \begin{cases} s_i \text{diag}\{\alpha_i^{-1/p}\}, & |\mathbf{e}^{i-1}| < \alpha_i, \\ s_i \text{Jac}[\mathbf{J}(\mathbf{e}^{i-1})], & \alpha_i \leq |\mathbf{e}^{i-1}| \leq \beta, \\ s_i \text{diag}\{\beta^{-1/p}\}, & |\mathbf{e}^{i-1}| > \beta. \end{cases}$$

The multiple s_i and the cut-off value α_i have to be again chosen in such a way that the conditions of Lemma 7.2 are satisfied, i.e. there exists $s > 0$ such that

$$0 < s \leq s_i \leq \frac{p-1}{p} \alpha_i^{1/p} \beta^{-1/p}.$$

7.6 Conclusions

The new theoretical results presented in this chapter should serve as preliminaries to the further study of relaxation methods applied in electromagnetism.

A lot of potential future work is bounded with this chapter: implementation of presented theoretical results and study of their accuracy on numerical experiments. The best choice of the linearization matrix has to be studied deeply too. One can expect the matrix to be close to the Jacobi matrix of the nonlinearity but then the method would perform effectively only for small time steps. Another possibility to determine the matrix is by an iterative process. The *secant* iterative method introduced by Kačur [46] works well even for large time steps. However, the method is designed for 1D problems only and thus forms a challenging issue for 3D modifications.

Performing the inverse to \mathbf{J} can lead to inaccuracy if large time step is used. Inspired by the article of Kačur [46], we suggest that the scheme should work more efficiently if the coupling (7.3) is replaced by a convergence criterion in the form of an inequality, for example

$$|(\mathbf{A}^i(\boldsymbol{\theta}^i - \mathbf{e}^{i-1}), \boldsymbol{\varphi}) - (\mathbf{J}(\mathbf{e}^i) - \mathbf{J}(\mathbf{e}^{i-1}), \boldsymbol{\varphi})| \leq \tau^d \int_{\Omega} \sum_{l=1}^3 (\boldsymbol{\theta}_l^i - \mathbf{e}_l^{i-1}) \sum_{k=1}^3 \varphi_k, \quad (7.22)$$

with $d > 0$ the parameter of the method. The proof of the convergence should not differ much from the one presented in this chapter, thanks to the factor τ^d . Nevertheless, the main difference between the scheme based on (7.22) and the one presented in this chapter is based on the fact that now, the matrix \mathbf{A}^i is also unknown. How to construct a matrix such that the convergence criterion is satisfied stays an open problem. However, based on the reported performance of relaxation method [46], I believe that this problem is worth an effort to resolve.

8 FULL DISCRETIZATION

In this chapter, we combine previous partial results into one complete problem involving discretization in time and space, and linearization. In other words, we propose fully-discrete linear computational methods for solving a nonlinear (degenerate) PDE (1.15). We suppose that the domain Ω is a polygonal domain.

The backward Euler method is employed for the discretization in time. This standard method was for the first time rigorously analysed in the case of the diffusion of the electric field in type-II superconductors by Slodička in [61]. The nonlinearity defined by (1.4) was considered. The complete mathematical analysis of the backward Euler method in case the constitutive relation (1.3) is employed is carried out in Chapter 5 of this thesis. If the problem (1.15) equipped with the constitutive relation (1.5) is considered, the error estimates from Remark 5.14 are applicable.

For the linearization and discretization in space, we develop a linear computational scheme based on the fixed-point principle and Whitney's edge elements. We derive error estimates that insure the convergence of the proposed fully-discrete linear numerical scheme and express the dependence of the error on the choice of the discretization parameters.

This chapter is organized as follows. In the first section, we study the problem (1.15) with constitutive relation (1.5). We refer to this case as to a Lipschitz continuous case (the same as in Chapter 6). In the second section, the problem (1.15) equipped with the constitutive relation (1.4) is analysed (non-Lipschitz continuous case). Both sections have the following structure. We first suggest a linear computational scheme and we show that the scheme is well-posed. Then we derive error estimates, on basis of which the convergence is proven. The ef-

efficiency of the method and the real convergence rates are studied on numerical examples at the end of each section. Some of the results of this chapter were presented on the conference ACOMEN 2008 [39].

8.1 Full discretization in the Lipschitz continuous case

The nonlinearity (1.5) is used.

We propose a new computational method—linear and discrete in time and space—to find an approximate solution to the problem (1.15), where \mathbf{J} is defined by (1.5). Slodička et al. [65] derived the error estimates for the backward Euler method for the Lipschitz continuous type of nonlinearity. Based on these results, the problem (1.15) equipped with the constitutive relation (1.5) can be considered in some sense equivalent to the problem (5.6) equipped with (1.5). The solution \mathbf{e}^i of the latter problem will therefore be frequently used as an intermedium in the error analysis.

8.1.1 Computational scheme

The finite dimensional space \mathbf{W}^h based on the Whitney edge elements is defined by (4.9). The integer n denotes the number of time steps (see Section 5.1).

The following computational scheme is proposed:

First $\mathbf{u}_0 = \mathcal{P}_h \mathbf{E}_0$. Then for each $i = 1, \dots, n$ and $k > 0$ we define $\mathbf{u}_{i,k}^h \in \mathbf{W}^h$ as the solution of the following boundary value problem

$$\begin{aligned} L(\mathbf{u}_{i,k}^h, \boldsymbol{\varphi}^h) + \tau (\nabla \times \mathbf{u}_{i,k}^h, \nabla \times \boldsymbol{\varphi}^h) &= L(\mathbf{u}_{i,k-1}^h, \boldsymbol{\varphi}^h) - (\mathbf{J}(\mathbf{u}_{i,k-1}^h), \boldsymbol{\varphi}^h) \\ &\quad + (\mathbf{J}(\mathbf{u}_{i-1}^h), \boldsymbol{\varphi}^h) \end{aligned} \quad (8.1)$$

for all $\boldsymbol{\varphi}^h \in \mathbf{W}^h$. We set $\mathbf{u}_{i,k_i}^h =: \mathbf{u}_i^h$ if and only if

$$\|\mathbf{u}_{i,k_i}^h - \mathbf{u}_{i,k_i-1}^h\| \leq \tau^\eta. \quad (8.2)$$

The parameters $L, \eta > 0$ are the parameters of the method, which will be specified later. The index $k_i > 0$ changes depending on i because the number of iterations needed during two different time steps can differ.

For the sake of simplicity, we introduce the notation $b := (1 - 1/p)\beta^{-1/p}$.

We denote by \mathcal{P}^h the orthogonal projection onto \mathbf{W}^h defined by scalar product in $\mathbf{H}(\mathbf{curl}; \Omega)$. That is for any \mathbf{E} holds

$$(\mathbf{E} - \mathcal{P}^h \mathbf{E}, \boldsymbol{\varphi}^h) + (\nabla \times (\mathbf{E} - \mathcal{P}^h \mathbf{E}), \nabla \times \boldsymbol{\varphi}^h) = 0 \quad \forall \boldsymbol{\varphi}^h \in \mathbf{W}^h. \quad (8.3)$$

As in Section 6.1, we define an auxiliary vector field \mathbf{H} as $\mathbf{H}(\mathbf{E}) = \mathbf{J}(\mathbf{E}) - L\mathbf{E}$.

8.1.2 Auxiliary problem

We introduce a sequence of auxiliary problems. If the sequence $\{\mathbf{u}_{i,k}^h\}$ converges for $k \rightarrow \infty$ to the solution to the auxiliary problem, then the sequence $\{\mathbf{u}_{i,k}^h\}$ is a Cauchy sequence and therefore the stopping criterion (8.2) makes sense.

The auxiliary problems are defined as follows:

First $\mathbf{v}_0^h = \mathbf{u}_0^h = \mathcal{P}_h \mathbf{E}_0$. Then for $i = 1, \dots, n$ we define \mathbf{v}_i as a unique solution to the next problem: Find $\mathbf{v}_i^h \in \mathbf{W}^h$ such that for all $\boldsymbol{\varphi}^h \in \mathbf{W}^h$ holds

$$(\mathbf{J}(\mathbf{v}_i^h), \boldsymbol{\varphi}^h) + \tau (\nabla \times \mathbf{v}_i^h, \nabla \times \boldsymbol{\varphi}^h) = (\mathbf{J}(\mathbf{u}_{i-1}^h), \boldsymbol{\varphi}^h). \quad (8.4)$$

By similar reasoning as in the proof of Lemma 6.2, one can prove that there exists a unique \mathbf{v}_i solving (8.4).

8.1.3 Convergence to the auxiliary problem

Theorem 8.1 *For any $k > 0$, $n > 1$, $i = 1, \dots, n$ and $\tau < 1$ the following estimates hold*

$$\|\mathbf{v}_i^h - \mathbf{u}_{i,k}^h\| \leq \left(\frac{M}{L}\right)^k \|\mathbf{u}_{i,0}^h - \mathbf{v}_i^h\|, \quad (8.5)$$

$$\|\nabla \times (\mathbf{u}_{i,k}^h - \mathbf{v}_i^h)\| \leq \left(\frac{L}{\tau}\right)^{1/2} \left(\frac{M}{L}\right)^k \|\mathbf{u}_{i,0}^h - \mathbf{v}_i^h\|. \quad (8.6)$$

Proof We rewrite the equation (8.4) as follows

$$L(\mathbf{v}_i^h, \boldsymbol{\varphi}^h) + \tau (\nabla \times \mathbf{v}_i^h, \nabla \times \boldsymbol{\varphi}^h) = L(\mathbf{v}_i^h, \boldsymbol{\varphi}^h) - (\mathbf{J}(\mathbf{v}_i^h), \boldsymbol{\varphi}^h) + (\mathbf{J}(\mathbf{u}_{i-1}^h), \boldsymbol{\varphi}^h)$$

and subtract this from (8.1). We obtain

$$L(\mathbf{u}_{i,k}^h - \mathbf{v}_i^h, \boldsymbol{\varphi}^h) + \tau (\nabla \times (\mathbf{u}_{i,k}^h - \mathbf{v}_i^h), \nabla \times \boldsymbol{\varphi}^h) = (\mathbf{H}(\mathbf{v}_i^h) - \mathbf{H}(\mathbf{u}_{i,k-1}^h), \boldsymbol{\varphi}^h).$$

By setting $\boldsymbol{\varphi}^h = \mathbf{u}_{i,k}^h - \mathbf{v}_i^h$ we get

$$L \|\mathbf{u}_{i,k}^h - \mathbf{v}_i^h\|^2 + \tau \|\nabla \times (\mathbf{u}_{i,k}^h - \mathbf{v}_i^h)\|^2 = (\mathbf{H}(\mathbf{v}_i^h) - \mathbf{H}(\mathbf{u}_{i,k-1}^h), \mathbf{u}_{i,k}^h - \mathbf{v}_i^h). \quad (8.7)$$

Employing Lemma 6.3 (p. 71), Cauchy-Schwartz inequality, the fact that

$$\|\nabla \times (\mathbf{u}_{i,k}^h - \mathbf{v}_i^h)\|^2 > 0$$

and dividing by $L \|\mathbf{u}_{i,k}^h - \mathbf{v}_i^h\|$, we end up with the recurrent relation

$$\|\mathbf{u}_{i,k}^h - \mathbf{v}_i^h\| \leq \frac{M}{L} \|\mathbf{u}_{i,k-1}^h - \mathbf{v}_i^h\|. \quad (8.8)$$

Thus

$$\|\mathbf{u}_{i,k}^h - \mathbf{v}_i^h\| \leq \left(\frac{M}{L}\right)^k \|\mathbf{u}_{i,0}^h - \mathbf{v}_i^h\|. \quad (8.9)$$

This completes the proof of the estimate (8.5).

Let us now get back to the equality (8.7). Using Lemma 6.3, Cauchy-Schwartz inequality, the fact that

$$\|\mathbf{u}_{i,k}^h - \mathbf{v}_i^h\|^2 > 0$$

and the estimate (8.8), we obtain the recurrent relation

$$\|\nabla \times (\mathbf{u}_{i,k}^h - \mathbf{v}_i^h)\|^2 \leq \frac{M}{\tau} \|\mathbf{u}_{i,k-1}^h - \mathbf{v}_i^h\| \|\mathbf{u}_{i,k}^h - \mathbf{v}_i^h\| \leq \frac{M^2}{\tau L} \|\mathbf{u}_{i,k-1}^h - \mathbf{v}_i^h\|^2.$$

Finally, using the inequality (8.9) squared, we get

$$\|\nabla \times (\mathbf{u}_{i,k}^h - \mathbf{v}_i^h)\|^2 \leq \frac{L}{\tau} \left(\frac{M}{L}\right)^{2k} \|\mathbf{u}_{i,0}^h - \mathbf{v}_i^h\|^2,$$

which completes the proof. \square

By employing Lemma 6.4 to the results of the previous theorem, we conclude that there exists L such that the sequence $\{\mathbf{u}_{i,k}^h\}$ is convergent for $k \rightarrow \infty$. Thus the stopping criterion (8.2) makes sense. This fact, together with Lax-Milgram lemma, induces the well-posedness of the scheme (8.1)–(8.2).

8.1.4 Error estimates and convergence to the time-space problem

Let us rewrite the equation (8.1) as follows

$$(\mathbf{J}(\mathbf{u}_{i,k}^h) - \mathbf{J}(\mathbf{u}_{i,k-1}^h), \boldsymbol{\varphi}^h) + \tau (\nabla \times \mathbf{u}_{i,k}^h, \nabla \times \boldsymbol{\varphi}^h) = (\mathbf{H}(\mathbf{u}_{i,k}^h) - \mathbf{H}(\mathbf{u}_{i,k-1}^h), \boldsymbol{\varphi}^h).$$

Sum it up for $i = 1, \dots, j$ and set $k = k_i$. Then

$$\begin{aligned} (\mathbf{J}(\mathbf{u}_j^h), \boldsymbol{\varphi}^h) + \sum_{i=1}^j \tau (\nabla \times \mathbf{u}_i^h, \nabla \times \boldsymbol{\varphi}^h) &= \sum_{i=1}^j (\mathbf{H}(\mathbf{u}_{i,k_i}^h) - \mathbf{H}(\mathbf{u}_{i,k_i-1}^h), \boldsymbol{\varphi}^h) \\ &\quad + (\mathbf{J}(\mathbf{u}_0^h), \boldsymbol{\varphi}^h). \end{aligned}$$

We sum also the equation (5.6) for $i = 1, \dots, j$ we set $\varphi = \varphi^h$, we subtract the two obtained equations from each other and we get

$$\begin{aligned} (\mathbf{J}(\mathbf{e}_j) - \mathbf{J}(\mathbf{u}_j^h), \varphi^h) + \sum_{i=1}^j \tau (\nabla \times (\mathbf{e}_i - \mathbf{u}_i^h), \nabla \times \varphi^h) \\ = \sum_{i=1}^j (\mathbf{H}(\mathbf{u}_{i,k_i-1}^h) - \mathbf{H}(\mathbf{u}_{i,k_i}^h), \varphi^h) + (\mathbf{J}(\mathbf{e}_0) - \mathbf{J}(\mathbf{u}_0^h), \varphi^h). \end{aligned} \quad (8.10)$$

By setting $\varphi^h = \tau(\mathcal{P}^h \mathbf{e}_j - \mathbf{u}_j^h)$ and using (8.3) we have

$$\begin{aligned} (\mathbf{J}(\mathcal{P}^h \mathbf{e}_j) - \mathbf{J}(\mathbf{u}_j^h), \mathcal{P}^h \mathbf{e}_j - \mathbf{u}_j^h) \tau + \sum_{i=1}^j \tau^2 (\nabla \times (\mathcal{P}^h \mathbf{e}_i - \mathbf{u}_i^h), \nabla \times (\mathcal{P}^h \mathbf{e}_j - \mathbf{u}_j^h)) \\ = \sum_{i=1}^j \tau (\mathbf{H}(\mathbf{u}_{i,k_i}^h) - \mathbf{H}(\mathbf{u}_{i,k_i-1}^h), \mathcal{P}^h \mathbf{e}_j - \mathbf{u}_j^h) + (\mathbf{J}(\mathbf{e}_0) - \mathbf{J}(\mathbf{u}_0^h), \mathcal{P}^h \mathbf{e}_j - \mathbf{u}_j^h) \tau \\ + (\mathbf{J}(\mathcal{P}^h \mathbf{e}_j) - \mathbf{J}(\mathbf{e}_j), \mathcal{P}^h \mathbf{e}_j - \mathbf{u}_j^h) \tau + \sum_{i=1}^j \tau^2 (\mathbf{e}_i - \mathcal{P}^h \mathbf{e}_i, \mathcal{P}^h \mathbf{e}_j - \mathbf{u}_j^h). \end{aligned}$$

The first term on the left-hand side can be estimated using Lemma 6.5 (*coercivity*). The right-hand side is estimated using Cauchy-Schwartz inequality, stopping criterion (8.2) and Lemmas 6.3 and 6.5 what leads to

$$\begin{aligned} \tau b \|\mathcal{P}^h \mathbf{e}_j - \mathbf{u}_j^h\|^2 + \sum_{i=1}^j \tau^2 (\nabla \times (\mathcal{P}^h \mathbf{e}_i - \mathbf{u}_i^h), \nabla \times (\mathcal{P}^h \mathbf{e}_j - \mathbf{u}_j^h)) \\ \leq \left[CM\tau^\eta + \alpha^{-1/p}\tau \|\mathbf{e}_0 - \mathbf{u}_0^h\| + \alpha^{-1/p}\tau \|\mathcal{P}^h \mathbf{e}_j - \mathbf{e}_j\| \right. \\ \left. + \sum_{i=1}^j \tau^2 \|\mathbf{e}_i - \mathcal{P}^h \mathbf{e}_i\| \right] \|\mathcal{P}^h \mathbf{e}_j - \mathbf{u}_j^h\|. \end{aligned}$$

By Young inequality we obtain for some small fixed $\epsilon > 0$

$$\begin{aligned} \tau(b - \epsilon) \|\mathcal{P}^h \mathbf{e}_j - \mathbf{u}_j^h\|^2 + \sum_{i=1}^j \tau^2 (\nabla \times (\mathcal{P}^h \mathbf{e}_i - \mathbf{u}_i^h), \nabla \times (\mathcal{P}^h \mathbf{e}_j - \mathbf{u}_j^h)) \\ \leq C_\epsilon \left[M^2 \tau^{2\eta-1} + \alpha^{-2/p}\tau \|\mathbf{e}_0 - \mathbf{u}_0^h\|^2 + \alpha^{-2/p}\tau \|\mathcal{P}^h \mathbf{e}_j - \mathbf{e}_j\|^2 \right. \\ \left. + \sum_{i=1}^j \tau^3 \|\mathbf{e}_i - \mathcal{P}^h \mathbf{e}_i\|^2 \right]. \end{aligned}$$

We sum it up for $j = 1, \dots, n$. After the summation, the second term on the left-hand side is positive. This can be proven by employing the algebraic identity (5.10) for $a_j = \sum_{i=1}^j \nabla \times_s (\mathcal{P}^h \mathbf{e}_i - \mathbf{u}_i^h)$ and $a_0 = 0$. Here $\nabla \times_s$ denotes the s -th vector component of the curl. We use the fact that $\mathbf{u}_0^h = \mathcal{P}^h \mathbf{e}_0$ and the triangle inequality to conclude that

$$\begin{aligned} \sum_{j=1}^n \tau \|\mathbf{e}_j - \mathbf{u}_j^h\|^2 &\leq C_\epsilon \left[\tau^{2\eta-2} + \sum_{j=1}^n \tau \|\mathbf{e}_0 - \mathcal{P}^h \mathbf{e}_0\|^2 \right. \\ &\quad \left. + \sum_{j=1}^n \tau \|\mathcal{P}^h \mathbf{e}_j - \mathbf{e}_j\|^2 + \sum_{j=1}^n \tau^2 \|\mathbf{e}_j - \mathcal{P}^h \mathbf{e}_j\|^2 \right] \\ &\leq C_\epsilon \left[\tau^{2\eta-2} + \|\mathbf{e}_0 - \mathcal{P}^h \mathbf{e}_0\|^2 + \sum_{j=1}^n \tau \|\mathbf{e}_j - \mathcal{P}^h \mathbf{e}_j\|^2 \right]. \end{aligned}$$

Rewriting this result in the notation introduced in Section 5.3 and using continuous norms we deduce that

$$\int_0^T \|\bar{\mathbf{e}}_n - \bar{\mathbf{u}}_n^h\|^2 \leq C \left(\tau^{2\eta-2} + \int_0^T \|\bar{\mathbf{e}}_n - \mathcal{P}^h \bar{\mathbf{e}}_n\|^2 + \|\mathbf{e}_0 - \mathcal{P}^h \mathbf{e}_0\|^2 \right).$$

Using the triangle inequality, the continuity of the projection \mathcal{P}^h and the estimate from [65, Theorem 3.1], we conclude that

$$\int_0^T \|\bar{\mathbf{u}}_n^h - \mathbf{E}\|^2 \leq C \left(\tau^2 + \tau^{2\eta-2} + \int_0^T \|\mathbf{E} - \mathcal{P}^h \mathbf{E}\|^2 + \|\mathbf{E}_0 - \mathcal{P}^h \mathbf{E}_0\|^2 \right). \quad (8.11)$$

In order to assure the convergence of the method, the parameter L has to fulfil the condition $M < L$ (see Lemma 6.4 and Remark 6.7), the parameter η has to fulfil $\eta > 1$ and the difference $\|\mathbf{E} - \mathcal{P}^h \mathbf{E}\|$ has to be estimated.

If the regularity of the solution \mathbf{E} is high enough, we can combine estimate (8.11) with the theorems from Section 4.5 in order to obtain the following theorem.

Theorem 8.2 *If $\mathbf{E} \in \mathbf{L}^2((0, T), \mathbf{W}^{1,s}(\Omega) \cap \mathbf{W}^{2,2}(\Omega))$ and $\mathbf{E}_0 \in \mathbf{W}^{1,s}(\Omega) \cap \mathbf{W}^{2,2}(\Omega)$ for $s > 2$ then*

$$\int_0^T \|\bar{\mathbf{u}}_n^h - \mathbf{E}\|^2 \leq C (\tau^2 + \tau^{2\eta-2} + h^2).$$

If $\mathbf{E} \in \mathbf{L}^2((0, T), \mathbf{H}^s(\mathbf{curl}; \Omega))$ and $\mathbf{E}_0 \in \mathbf{H}^s(\mathbf{curl}; \Omega)$ for $s \in \mathbb{N}$ then

$$\int_0^T \|\bar{\mathbf{u}}_n^h - \mathbf{E}\|^2 \leq C \left(\tau^2 + \tau^{2\eta-2} + h^{2\min\{2, s\}} \right)$$

holds.

Supposing that $\mathbf{E} \in \mathbf{L}^2((0, T), \mathbf{H}^s(\mathbf{curl}; \Omega))$ and $\mathbf{E}_0 \in \mathbf{H}^s(\mathbf{curl}; \Omega)$ for some $s \in (0.5, 1]$ then

$$\int_0^T \|\bar{\mathbf{u}}_n^h - \mathbf{E}\|^2 \leq C \left(\tau^2 + \tau^{2\eta-2} + h^{2s} \right)$$

is true.

Proof We use the fact that the orthogonal projection \mathcal{P}^h generates the best approximation of any vector $\mathbf{v} \in \mathbf{H}(\mathbf{curl}; \Omega)$ in the norm of the space $\mathbf{H}(\mathbf{curl}; \Omega)$. Thus holds for any $\mathbf{v} \in \mathbf{H}(\mathbf{curl}; \Omega)$ that

$$\|\mathbf{v} - \mathcal{P}^h \mathbf{v}\| \leq \|\mathbf{v} - \mathcal{P}^h \mathbf{v}\|_{\mathbf{H}(\mathbf{curl}; \Omega)} \leq \|\mathbf{v} - r_h \mathbf{v}\|_{\mathbf{H}(\mathbf{curl}; \Omega)}. \quad (8.12)$$

Then the first estimate from the statement of the theorem follows from the estimate (8.11) and Theorem 4.6.

The second estimate follows for $s = 1$ from Theorems 4.7 and 4.8. For $s \geq 2$ it is a consequence of Theorems 4.6 and 4.8.

The last estimate is a result of Theorems 4.7 and 4.8. \square

Theorem 8.3 *If $\eta > 1$, $L > \alpha^{-1/p}/2$ and the solution \mathbf{E} to the problem (1.15) satisfies one of the assumptions of Theorem 8.2 then the solutions to the computational scheme (8.1)–(8.2) converge to \mathbf{E} in $\mathbf{L}_2((0, T), \mathbf{L}_2(\Omega))$ for $\tau \rightarrow 0$ and $h \rightarrow 0$.*

8.1.5 Numerical experiments

In this section, we investigate the dependence of the relative error of the scheme (8.1)–(8.2) on the parameters p , η , τ and h . We denote $\mathbf{L}_2((0, 1), \mathbf{L}_2(\Omega))$ by \mathbf{K} and express the error in the norm of this space (see also (5.42)).

The domain Ω —the region occupied by the superconductor—is the unit cube in \mathbb{R}^3 . We split this domain into a tetrahedral mesh. The number of elements varies from 6 to 24 576, depending on the nature of the exact solution. The mesh consisting of 6 elements is used if the exact solution can be fitted precisely by Whitney's edge elements.

The parameter L is chosen in accordance with the reasoning in Remark 6.7 (Table 6.1).

The dependence of the error $\|\bar{\mathbf{u}}_n^h - \mathbf{E}\|_{\mathbf{L}_2((0,1),\mathbf{L}_2(\Omega))}$ on the parameters τ , p , η and γ is studied on the following problem:

$$\partial_t(\mathbf{J}(\mathbf{E})) + \nabla \times \nabla \times \mathbf{E} = \mathbf{F} \quad \text{in } \Omega \times [0, 1], \quad (8.13)$$

$$\nabla \times \mathbf{E} \times \boldsymbol{\nu} = \mathbf{G} \quad \text{on } \Gamma \times [0, 1],$$

$$\mathbf{E}(0) = \mathbf{E}_0 \quad \text{in } \Omega, \quad (8.14)$$

with \mathbf{J} given by (6.20) and a known exact solution

$$\mathbf{E}^l(\mathbf{x}) = (E_1^l(x_1, x_2, x_3), E_2^l(x_1, x_2, x_3), E_3^l(x_1, x_2, x_3))$$

given by

$$\mathbf{E}^l(\mathbf{x}) = (10x_3 - 10x_2 + t, 10x_1 - 10x_3 + t, 10x_2 - 10x_1 + t).$$

The vector field \mathbf{E}^l can be fitted precisely by Whitney's edge elements independently of the mesh density. Thus, the mesh consisting of only 6 elements ($h = \sqrt{3}$) is used what results in faster calculations.

As $p \rightarrow \infty$ corresponds to the linear problem, the higher the exponent p in the nonlinearity \mathbf{J} , the faster and more precise the computation of the problem. The evolution of the relative error $\|\bar{\mathbf{u}}_i^h - \mathbf{E}(t_i)\|_{\mathbf{L}_2(\Omega)}$ in time (for $i = 1, \dots, n$ and thus $t_i = 0, \tau, \dots, (n-1)\tau, 1$) is plotted on Figure 8.1.

The influence of the parameter η on the relative error of the method is plotted on Figure 8.2. The value of $\eta = 4$ gives reasonable results in a short computational time. Higher values of η result in very long iterative process and do not remarkably enhance the final error.

The dependence of the relative error on the length of the time step τ can be fitted by the function of the type $f(\tau) = C\tau^{1.2}$ (Figure 8.3). This is slightly better result than the one obtained by theoretical analysis of the method, but it is possible that it is influenced by the choice of the exact solution.

In order to study the dependence of the method on the used mesh, we compute the problem (8.13) with the exact solution

$$\mathbf{E}^s(\mathbf{x}) = (\sin(x_2) - \sin(x_3) + t, \sin(x_3) - \sin(x_1) + t, \sin(x_1) - \sin(x_2) + t).$$

The vector field \mathbf{E}^s is regular enough in order to satisfy the assumptions of Theorem 8.3, but can be interpolated by Whitney's elements only with precision reported in Table 8.1 as discretization error. The relative error of the

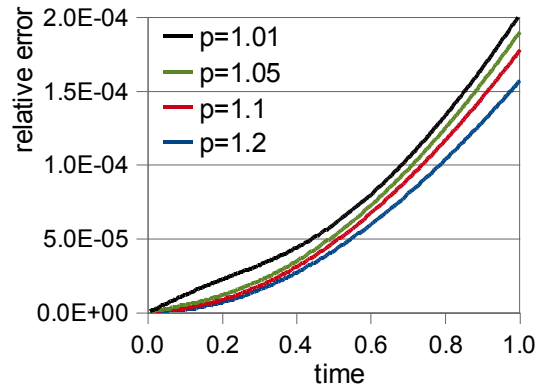


Figure 8.1: The evolution of the relative error $\|\bar{\mathbf{u}}_n^h - \mathbf{E}^l\|$ of the scheme (8.1)–(8.2) in time for different values of p . As p approaches 1, the solution of the scheme (8.1)–(8.2) becomes more imprecise. We consider $h = \sqrt{3}$, $\tau = 0.005$, $\eta = 4$ and the linear exact solution \mathbf{E}^l .

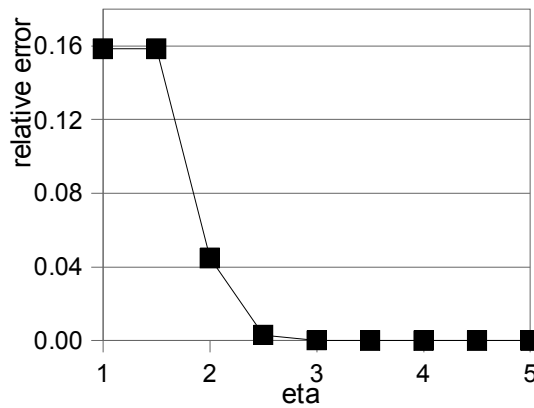


Figure 8.2: Considering the following parameters fixed: $h = \sqrt{3}$, $p = 1.2$, $\tau = 0.005$ and the linear exact solution \mathbf{E}^l , we observe that the total relative error $\|\bar{\mathbf{u}}_n^h - \mathbf{E}^l\|_{\mathbf{K}} / \|\mathbf{E}^l\|_{\mathbf{K}}$ of the scheme (8.1)–(8.2) can be decreased by choosing $\eta \geq 3$.

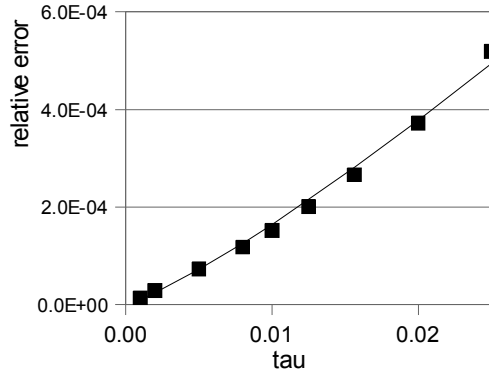


Figure 8.3: The dependence of the relative error $\|\bar{\mathbf{u}}_n^h - \mathbf{E}^l\|_{\mathbf{K}} / \|\mathbf{E}^l\|_{\mathbf{K}}$ of the scheme (8.1)–(8.2) on τ . We use $h = \sqrt{3}$, $p = 1.2$, $\eta = 4$ and the linear exact solution \mathbf{E}^l . The experimentally obtained data can be fitted by the function $f(\tau) = 0.0413\tau^{1.2}$ (—).

h	discr.error	relative error
$\sqrt{3}$	0.050331	0.049466
$\sqrt{3}/2$	0.061503	0.062957
$\sqrt{3}/4$	0.033977	0.033976
$\sqrt{3}/8$	0.017377	0.017250

Table 8.1: The relative error of the scheme (8.1)–(8.2) for different values of h . We use $p = 1.2$, $\tau = 0.005$, $\eta = 4$ and the exact solution \mathbf{E}^s . The dependence of the relative error on the parameter h tracks the values of the discretization error $\|\mathbf{E}_0 - r_h \mathbf{E}_0\|$. No smaller error than the discretization error can be reached on the mesh with characteristic h . Too few DOFs (large h) mislead the results if the non-linear exact solution is considered (compare the discretization error for $h = \sqrt{3}$ with the one for $h = \sqrt{3}/2$).

method seems to track the discretization error, it means that it is proportional to h^2 .¹ However, it is difficult to study this phenomenon closer, as a very dense mesh leads to extremely slow computations and only the meshes with the characteristic $h = \sqrt{3}/2^k$ are allowed by our software. This is due to the strong dependence of h on the strategy of mesh-refinement (Table 5.1), which is a legacy of ALBERT [59].

8.2 Full discretization in the non-Lipschitz continuous case

The nonlinearity (1.4) is used.

A new computational method—linear and discrete in time and space—is proposed to find an approximate solution to the problem (1.15), where \mathbf{J} is defined by (1.4). Once the result of Slodička [61] is known, the problem (1.15) can be considered equivalent to the problem (5.6). The solution \mathbf{e}^i to this problem will be therefore frequently used as an intermedium in the error estimates. The integer n denotes the number of time steps (see Section 5.1).

8.2.1 Computational scheme

First, we introduce $L_\tau = \tau^{-\gamma}$, where the parameter $\gamma > 0$ is a parameter of the method and will be specified later. Next, we define auxiliary vector fields \mathbf{J}_τ and \mathbf{H}_τ as

$$\mathbf{J}_\tau(\mathbf{E}) = \begin{cases} L_\tau \mathbf{E}, & |\mathbf{E}| < L_\tau^{-p}, \\ |\mathbf{E}|^{-1/p} \mathbf{E}, & L_\tau^{-p} \leq |\mathbf{E}| \leq \beta, \\ \beta^{-1/p} \mathbf{E}, & |\mathbf{E}| > \beta \end{cases}$$

and

$$\mathbf{H}_\tau(\mathbf{E}) = \mathbf{J}_\tau(\mathbf{E}) - L_\tau \mathbf{E}.$$

The space \mathbf{W}^h is defined as in the previous section by (4.9).

The following discrete linear approximation scheme is proposed:

First $\mathbf{u}_0 = \mathcal{P}^h \mathbf{E}_0$. Then for each $i = 1, \dots, n$ and $k > 0$, $\mathbf{u}_{i,k}^h \in \mathbf{W}^h$ is the solution of the following boundary value problem

$$\begin{aligned} L_\tau(\mathbf{u}_{i,k}^h, \varphi^h) + \tau(\nabla \times \mathbf{u}_{i,k}^h, \nabla \times \varphi^h) &= L_\tau(\mathbf{u}_{i,k-1}^h, \varphi^h) - (\mathbf{J}_\tau(\mathbf{u}_{i,k-1}^h), \varphi^h) \\ &\quad + (\mathbf{J}_\tau(\mathbf{u}_{i-1}^h), \varphi^h) \end{aligned} \quad (8.15)$$

¹The fact that the relative error of the method is sometimes slightly smaller than the discretization one is due to the use of the discrete norm for the calculation of the discretization error.

for all $\varphi^h \in \mathbf{W}^h$. We set $\mathbf{u}_{i,k_i}^h =: \mathbf{u}_i^h$ if

$$\|\mathbf{u}_{i,k_i}^h - \mathbf{u}_{i,k_i-1}^h\| \leq \tau^\eta. \quad (8.16)$$

The parameter $\eta > 0$ is the parameter of the method. It will be specified later. The *stopping index* $k_i > 0$ depends on i .

The existence and uniqueness of the solution to the equation (8.15) follows directly from Lax–Milgram lemma. The well-posedness of the stopping criterion (8.16) will be proven later by showing that the sequence $\{\mathbf{u}_{i,k}^h\}$ is convergent for $k \rightarrow \infty$. First some basic properties of the functions \mathbf{H}_τ , \mathbf{J}_τ and \mathbf{J} have to be mentioned.

Basic inequalities

The proofs of the following lemmas are similar to those of Lemmas 6.3–6.5 and therefore will be omitted.

Lemma 8.4 *For all $\mathbf{s}, \mathbf{t} \in \mathbb{R}^3$ holds that*

$$|\mathbf{H}_\tau(\mathbf{s}) - \mathbf{H}_\tau(\mathbf{t})| \leq M_\tau |\mathbf{s} - \mathbf{t}|,$$

where $M_\tau > 0$ depends on L_τ and equals to

$$M_\tau = L_\tau - (1 - 1/p)\beta^{-1/p}.$$

Lemma 8.5 *There exists $C > 0$ depending only on p such that for all $\mathbf{s} \in \mathbb{R}^3$*

$$|\mathbf{J}_\tau(\mathbf{s}) - \mathbf{J}(\mathbf{s})| \leq C(p)L_\tau^{1-p}.$$

Lemma 8.6 *For all $\mathbf{s}, \mathbf{t} \in \mathbb{R}^3$ holds*

$$(\mathbf{J}(\mathbf{s}) - \mathbf{J}(\mathbf{t}), \mathbf{s} - \mathbf{t}) \geq \beta^{-1/p}(1 - 1/p)|\mathbf{s} - \mathbf{t}|^2, \quad (\text{coercivity})$$

and

$$|\mathbf{J}_\tau(\mathbf{s}) - \mathbf{J}_\tau(\mathbf{t})| \leq L_\tau |\mathbf{s} - \mathbf{t}|. \quad (\text{boundedness})$$

Again, $b := (1 - 1/p)\beta^{-1/p}$ and \mathcal{P}^h denotes orthogonal projection onto \mathbf{W}^h defined by scalar product in $\mathbf{H}(\mathbf{curl}; \Omega)$.

8.2.2 Auxiliary problem

We follow the same line as in the previous section and we introduce a sequence of auxiliary problems solutions of which are defined in terms of $\mathbf{u}_{i,k}^h$ in the following way.

First $\mathbf{v}_0 = \mathbf{u}_0 = \mathcal{P}^h \mathbf{E}_0$. Then for $i = 1, \dots, n$, we define \mathbf{v}_i^h as a unique solution to the problem: Find $\mathbf{v}_i^h \in \mathbf{W}^h$ such that for all $\boldsymbol{\varphi}^h \in \mathbf{W}^h$ holds

$$(\mathbf{J}_\tau(\mathbf{v}_i^h), \boldsymbol{\varphi}^h) + \tau (\nabla \times \mathbf{v}_i^h, \nabla \times \boldsymbol{\varphi}^h) = (\mathbf{J}_\tau(\mathbf{u}_{i-1}^h), \boldsymbol{\varphi}^h). \quad (8.17)$$

The auxiliary problem will be used to show that the sequence $\{\mathbf{u}_{i,k}^h\}$ is convergent for $k \rightarrow \infty$ and therefore the stopping criterion (8.16) is meaningful.

8.2.3 Convergence to the auxiliary problem

Theorem 8.7 *For any $k > 0$, $n > 1$, $i = 1, \dots, n$ and $\tau < 1$ the following estimates hold*

$$\|\mathbf{u}_{i,k}^h - \mathbf{v}_i^h\| \leq (\tau^{-\gamma} - b)^k \tau^{k\gamma} \|\mathbf{u}_{i,0}^h - \mathbf{v}_i^h\|, \quad (8.18)$$

$$\|\nabla \times (\mathbf{u}_{i,k}^h - \mathbf{v}_i^h)\| \leq (\tau^{-\gamma} - b)^{k-1/2} \tau^{k\gamma-1/2} \|\mathbf{u}_{i,0}^h - \mathbf{v}_i^h\|. \quad (8.19)$$

Proof We rewrite the equation (8.17) as follows

$$\begin{aligned} L_\tau(\mathbf{v}_i^h, \boldsymbol{\varphi}^h) + \tau (\nabla \times \mathbf{v}_i^h, \nabla \times \boldsymbol{\varphi}^h) &= L_\tau(\mathbf{v}_i^h, \boldsymbol{\varphi}^h) - (\mathbf{J}_\tau(\mathbf{v}_i^h), \boldsymbol{\varphi}^h) \\ &\quad + (\mathbf{J}_\tau(\mathbf{u}_{i-1}^h), \boldsymbol{\varphi}^h) \end{aligned}$$

and subtract this from (8.15). We obtain

$$\begin{aligned} L_\tau(\mathbf{u}_{i,k}^h - \mathbf{v}_i^h, \boldsymbol{\varphi}^h) + \tau (\nabla \times (\mathbf{u}_{i,k}^h - \mathbf{v}_i^h), \nabla \times \boldsymbol{\varphi}^h) \\ = (\mathbf{H}_\tau(\mathbf{v}_i^h) - \mathbf{H}_\tau(\mathbf{u}_{i,k-1}^h), \boldsymbol{\varphi}^h). \end{aligned}$$

By setting $\boldsymbol{\varphi}^h = \mathbf{u}_{i,k}^h - \mathbf{v}_i^h$ we get

$$L_\tau \|\mathbf{u}_{i,k}^h - \mathbf{v}_i^h\|^2 + \tau \|\nabla \times (\mathbf{u}_{i,k}^h - \mathbf{v}_i^h)\|^2 = (\mathbf{H}_\tau(\mathbf{v}_i^h) - \mathbf{H}_\tau(\mathbf{u}_{i,k-1}^h), \mathbf{u}_{i,k}^h - \mathbf{v}_i^h). \quad (8.20)$$

Employing Lemma 8.4, Cauchy-Schwartz inequality, the fact that

$$\|\nabla \times (\mathbf{u}_{i,k}^h - \mathbf{v}_i^h)\|^2 > 0$$

and dividing by $L_\tau \|\mathbf{u}_{i,k}^h - \mathbf{v}_i^h\|$, we end up with a recurrent relation

$$\|\mathbf{u}_{i,k}^h - \mathbf{v}_i^h\| \leq \frac{M_\tau}{L_\tau} \|\mathbf{u}_{i,k-1}^h - \mathbf{v}_i^h\|.$$

From Lemma 8.4 we know that $M_\tau/L_\tau = (\tau^{-\gamma} - b)\tau^\gamma < 1$, thus

$$\|\mathbf{u}_{i,k}^h - \mathbf{v}_i^h\| \leq (\tau^{-\gamma} - b)^k \tau^{k\gamma} \|\mathbf{u}_{i,0}^h - \mathbf{v}_i^h\|,$$

what completes the proof of the estimate (8.18)

Let us now get back to (8.20). Using Lemma 8.4, Cauchy-Schwartz inequality, the fact that

$$\|\mathbf{u}_{i,k}^h - \mathbf{v}_i^h\|^2 > 0$$

and the estimate (8.18), we obtain the recurrent relation

$$\begin{aligned} \|\nabla \times (\mathbf{u}_{i,k}^h - \mathbf{v}_i^h)\|^2 &\leq \frac{\tau^{-\gamma} - b}{\tau} \|\mathbf{u}_{i,k-1}^h - \mathbf{v}_i^h\| \|\mathbf{u}_{i,k}^h - \mathbf{v}_i^h\| \\ &\leq \frac{(\tau^{-\gamma} - b)^2}{\tau^{1-\gamma}} \|\mathbf{u}_{i,k-1}^h - \mathbf{v}_i^h\|^2. \end{aligned}$$

Therefore

$$\|\nabla \times (\mathbf{u}_{i,k}^h - \mathbf{v}_i^h)\|^2 \leq (\tau^{-\gamma} - b)^{2k+1} \tau^{2k\gamma-1} \|\mathbf{u}_{i,0}^h - \mathbf{v}_i^h\|^2,$$

which completes the proof. \square

The previous theorem guarantees that the sequence $\{\mathbf{u}_{i,k}^h\}$ is convergent for $k \rightarrow \infty$ and therefore it is a Cauchy sequence. Thus the stopping criterion (8.16) makes sense.

8.2.4 Error estimates and convergence to the time-space problem

Let us rewrite equation (8.15) as follows

$$\begin{aligned} (\mathbf{J}(\mathbf{u}_{i,k}^h) - \mathbf{J}(\mathbf{u}_{i-1}^h), \boldsymbol{\varphi}^h) + \tau (\nabla \times \mathbf{u}_{i,k}^h, \nabla \times \boldsymbol{\varphi}^h) &= (\mathbf{H}_\tau(\mathbf{u}_{i,k}^h) - \mathbf{H}_\tau(\mathbf{u}_{i,k-1}^h), \boldsymbol{\varphi}^h) \\ &\quad + (\mathbf{J}(\mathbf{u}_{i,k}^h) - \mathbf{J}_\tau(\mathbf{u}_{i,k}^h), \boldsymbol{\varphi}^h) \\ &\quad + (\mathbf{J}_\tau(\mathbf{u}_{i-1}^h) - \mathbf{J}(\mathbf{u}_{i-1}^h), \boldsymbol{\varphi}^h). \end{aligned}$$

Sum it up for $i = 1, \dots, j$ and set $k = k_i$ then

$$\begin{aligned} (\mathbf{J}(\mathbf{u}_j^h), \varphi^h) + \sum_{i=1}^j \tau (\nabla \times \mathbf{u}_i^h, \nabla \times \varphi^h) &= \sum_{i=1}^j (\mathbf{H}_\tau(\mathbf{u}_{i,k_i}^h) - \mathbf{H}_\tau(\mathbf{u}_{i,k_i-1}^h), \varphi^h) \\ &\quad + (\mathbf{J}(\mathbf{u}_j^h) - \mathbf{J}_\tau(\mathbf{u}_j^h), \varphi^h) \\ &\quad + (\mathbf{J}_\tau(\mathbf{u}_0^h) - \mathbf{J}(\mathbf{u}_0^h), \varphi^h) \\ &\quad + (\mathbf{J}(\mathbf{u}_0^h), \varphi^h). \end{aligned}$$

We use a similar procedure for the equation (5.6), we subtract the two obtained equations from each other and we get

$$\begin{aligned} (\mathbf{J}(\mathbf{e}_j) - \mathbf{J}(\mathbf{u}_j^h), \varphi^h) + \sum_{i=1}^j \tau (\nabla \times (\mathbf{e}_i - \mathbf{u}_i^h), \nabla \times \varphi^h) \\ = \sum_{i=1}^j (\mathbf{H}_\tau(\mathbf{u}_{i,k_i-1}^h) - \mathbf{H}_\tau(\mathbf{u}_{i,k_i}^h), \varphi^h) + (\mathbf{J}(\mathbf{e}_0) - \mathbf{J}(\mathbf{u}_0^h), \varphi^h) \\ \quad + (\mathbf{J}_\tau(\mathbf{u}_j^h) - \mathbf{J}(\mathbf{u}_j^h), \varphi^h) + (\mathbf{J}(\mathbf{u}_0^h) - \mathbf{J}_\tau(\mathbf{u}_0^h), \varphi^h). \end{aligned}$$

By setting $\varphi^h = \tau(\mathcal{P}^h \mathbf{e}_j - \mathbf{u}_j^h)$ and using (8.3) we have

$$\begin{aligned} (\mathbf{J}(\mathcal{P}^h \mathbf{e}_j) - \mathbf{J}(\mathbf{u}_j^h), \mathcal{P}^h \mathbf{e}_j - \mathbf{u}_j^h) \tau + \sum_{i=1}^j \tau^2 (\nabla \times (\mathcal{P}^h \mathbf{e}_i - \mathbf{u}_i^h), \nabla \times (\mathcal{P}^h \mathbf{e}_j - \mathbf{u}_j^h)) \\ = \sum_{i=1}^j \tau (\mathbf{H}_\tau(\mathbf{u}_{i,k_i-1}^h) - \mathbf{H}_\tau(\mathbf{u}_{i,k_i}^h), \mathcal{P}^h \mathbf{e}_j - \mathbf{u}_j^h) + (\mathbf{J}(\mathbf{e}_0) - \mathbf{J}(\mathbf{u}_0^h), \mathcal{P}^h \mathbf{e}_j - \mathbf{u}_j^h) \tau \\ \quad + (\mathbf{J}_\tau(\mathbf{u}_j^h) - \mathbf{J}(\mathbf{u}_j^h), \mathcal{P}^h \mathbf{e}_j - \mathbf{u}_j^h) \tau + (\mathbf{J}(\mathbf{u}_0^h) - \mathbf{J}_\tau(\mathbf{u}_0^h), \mathcal{P}^h \mathbf{e}_j - \mathbf{u}_j^h) \tau \\ \quad + (\mathbf{J}(\mathcal{P}^h \mathbf{e}_j) - \mathbf{J}(\mathbf{e}_j), \mathcal{P}^h \mathbf{e}_j - \mathbf{u}_j^h) \tau + \sum_{i=1}^j \tau^2 (\mathbf{e}_i - \mathcal{P}^h \mathbf{e}_i, \mathcal{P}^h \mathbf{e}_j - \mathbf{u}_j^h). \end{aligned}$$

The first term on the left-hand side is estimated using Lemma 8.6 (*coercivity*). The right-hand side is estimated using Cauchy-Schwartz inequality,

stopping criterion (8.16) and Lemmas 8.4–8.6 what leads to

$$\begin{aligned} & \tau b \|\mathcal{P}^h \mathbf{e}_j - \mathbf{u}_j^h\|^2 + \sum_{i=1}^j \tau^2 (\nabla \times (\mathcal{P}^h \mathbf{e}_i - \mathbf{u}_i^h), \nabla \times (\mathcal{P}^h \mathbf{e}_j - \mathbf{u}_j^h)) \\ & \leq \left[CM_\tau \tau^\eta + C\tau^{(p-1)\gamma+1} + \tau^{1-\gamma} \|\mathbf{e}_0 - \mathbf{u}_0^h\| + \tau^{1-\gamma} \|\mathcal{P}^h \mathbf{e}_j - \mathbf{e}_j\| \right. \\ & \quad \left. + \sum_{i=1}^j \tau^2 \|\mathbf{e}_i - \mathcal{P}^h \mathbf{e}_i\| \right] \|\mathcal{P}^h \mathbf{e}_j - \mathbf{u}_j^h\|. \end{aligned}$$

By Young inequality we obtain for some small fixed $\epsilon > 0$

$$\begin{aligned} & \tau(b - \epsilon) \|\mathcal{P}^h \mathbf{e}_j - \mathbf{u}_j^h\|^2 + \sum_{i=1}^j \tau^2 (\nabla \times (\mathcal{P}^h \mathbf{e}_i - \mathbf{u}_i^h), \nabla \times (\mathcal{P}^h \mathbf{e}_j - \mathbf{u}_j^h)) \\ & \leq C_\epsilon \left[M_\tau^2 \tau^{2\eta-1} + \tau^{2(p-1)\gamma+1} + \tau^{-2\gamma} \|\mathbf{e}_0 - \mathbf{u}_0^h\|^2 + \tau^{-2\gamma} \|\mathcal{P}^h \mathbf{e}_j - \mathbf{e}_j\|^2 \right. \\ & \quad \left. + \sum_{i=1}^j \tau^3 \|\mathbf{e}_i - \mathcal{P}^h \mathbf{e}_i\|^2 \right]. \end{aligned}$$

We sum it up for $j = 1, \dots, n$. After the summation, the second term on the left-hand side is again positive (for detailed reasoning see Section 8.1.4). We use the fact that $\mathbf{u}_0^h = \mathcal{P}^h \mathbf{e}_0$ and the triangle inequality to conclude that

$$\begin{aligned} \sum_{j=1}^n \tau \|\mathbf{e}_j - \mathbf{u}_j^h\|^2 & \leq C_\epsilon \left[\tau^{2\eta-2\gamma-2} + \tau^{2(p-1)\gamma} + \tau^{-2\gamma} \sum_{j=1}^n \tau \|\mathbf{e}_0 - \mathcal{P}^h \mathbf{e}_0\|^2 \right. \\ & \quad \left. + \tau^{-2\gamma} \sum_{j=1}^n \tau \|\mathcal{P}^h \mathbf{e}_j - \mathbf{e}_j\|^2 + \sum_{j=1}^n \tau^2 \|\mathbf{e}_j - \mathcal{P}^h \mathbf{e}_j\|^2 \right] \\ & \leq C_\epsilon \left[\tau^{2 \min\{\eta-\gamma-1, (p-1)\gamma\}} + \tau^{-2\gamma} \|\mathbf{e}_0 - \mathcal{P}^h \mathbf{e}_0\|^2 \right. \\ & \quad \left. + \tau^{-2\gamma} \sum_{j=0}^n \tau \|\mathbf{e}_j - \mathcal{P}^h \mathbf{e}_j\|^2 \right]. \end{aligned} \quad (8.21)$$

We can now proceed to the statement of the following theorem.

Theorem 8.8 *Let us suppose that Ω is an open bounded set in \mathbb{R}^3 with Lipschitz continuous boundary Γ . We define*

$$\bar{\mathbf{u}}_n^h(0) = \mathcal{P}^h \mathbf{E}_0, \quad \bar{\mathbf{u}}_n^h(t) = \mathbf{u}_i^h \quad \text{for } t \in (t_{i-1}, t_i], \quad i = 1, \dots, n,$$

where \mathbf{u}_i^h is the solution of the approximation scheme (8.15)–(8.16).

We denote by

$$m = \min\{2\eta - 2\gamma - 2, 2(p-1)\gamma, 1 - 2\gamma\}.$$

Then the following estimate holds

$$\int_0^T \|\bar{\mathbf{u}}_n^h - \mathbf{E}\|^2 \leq C \left(\tau^m + \tau^{-2\gamma} \|\mathbf{E}_0 - \mathcal{P}^h \mathbf{E}_0\|^2 + \tau^{-2\gamma} \int_0^T \|\mathbf{E} - \mathcal{P}^h \mathbf{E}\|^2 \right). \quad (8.22)$$

If $\mathbf{E} \in \mathbf{L}_2((0, T), \mathbf{W}^{2,2}(\Omega))$ and $\mathbf{E}_0 \in \mathbf{W}^{2,2}(\Omega)$ then holds that

$$\int_0^T \|\bar{\mathbf{u}}_n^h - \mathbf{E}\|^2 \leq C (\tau^m + \tau^{-2\gamma} h^2). \quad (8.23)$$

If $\mathbf{E} \in \mathbf{L}_2((0, T), \mathbf{H}^2(\mathbf{curl}; \Omega))$ and $\mathbf{E}_0 \in \mathbf{H}^2(\mathbf{curl}; \Omega)$ then

$$\int_0^T \|\bar{\mathbf{u}}_n^h - \mathbf{E}\|^2 \leq C (\tau^m + \tau^{-2\gamma} h^4) \quad (8.24)$$

is true.

Proof Rewriting the relation (8.21) in the appropriate notation and using continuous norms, we deduce that

$$\begin{aligned} \int_0^T \|\bar{\mathbf{e}}_n - \bar{\mathbf{u}}_n^h\|^2 &\leq C \left(\tau^{2 \min\{\eta - \gamma - 1, (p-1)\gamma\}} + \tau^{-2\gamma} \|\mathbf{e}_0 - \mathcal{P}^h \mathbf{e}_0\|^2 \right. \\ &\quad \left. + \tau^{-2\gamma} \int_0^T \|\bar{\mathbf{e}}_n - \mathcal{P}^h \bar{\mathbf{e}}_n\|^2 \right). \end{aligned}$$

Using the triangle inequality on both sides of the previous inequality and employing the estimate (5.40), we conclude that (8.22) is valid.

Employing the relation (8.12) together with the second part of the Theorem 4.6, we deduce directly the estimate (8.23). The estimate (8.24) follows from Theorem 4.8. \square

Remark 8.9 Several variations of the estimate (8.23) can be obtained based on the use of different approximation results for Whitney's edge elements, depending on the regularity of the solution \mathbf{E} to the problem (1.15) (see Section 4.5).

Thanks to the estimate (8.23), the solution to the computational scheme (8.15)–(8.16) converges to the solution \mathbf{E} to the problem (1.7)–(1.10) in the space $L_2((0, T), \mathbf{L}_2(\Omega))$ when the regularity of \mathbf{E} is high enough and the parameters η, γ, τ and h fulfil these conditions:

$$\min\{2\eta - 2\gamma - 2, 2(p - 1)\gamma, 1 - 2\gamma\} > 0, \quad (8.25)$$

$$h\tau^{-\gamma} \longrightarrow 0 \text{ if } h, \tau \longrightarrow 0 \text{ (or } h^2\tau^{-\gamma} \longrightarrow 0 \text{ if } h, \tau \longrightarrow 0). \quad (8.26)$$

8.2.5 Numerical experiments

In this section, we investigate the dependence of the relative error of the proposed method (8.15)–(8.16) on the parameters p, η, γ, τ and h . We denote again $\mathbf{L}_2((0, 1), \mathbf{L}_2(\Omega))$ by \mathbf{K} and express the error in the norm of this space.

The domain Ω —the region occupied by the superconductor—is the unit cube in \mathbb{R}^3 . We split this domain into a tetrahedral mesh. The number of elements varies from 6 to 24 576, depending on the nature of the exact solution. The mesh consisting of 6 elements is used, if the exact solution can be fitted precisely by Whitney’s edge elements.

The dependence on τ, p, η and γ has been studied on the following problem:

$$\begin{aligned} \partial_t (\mathbf{J}(\mathbf{E})) + \nabla \times \nabla \times \mathbf{E} &= \mathbf{F} && \text{in } \Omega \times [0, 1], \\ \nabla \times \mathbf{E} \times \boldsymbol{\nu} &= \mathbf{G} && \text{on } \Gamma \times [0, 1], \\ \mathbf{E}(0, \mathbf{x}) &= \mathbf{E}_0(\mathbf{x}) && \text{in } \Omega, \end{aligned} \quad (8.27)$$

with \mathbf{J} given by (6.24) and the known exact solution $\mathbf{E}^l(\mathbf{x}) = \mathbf{E}^l(x_1, x_2, x_3)$ given by

$$\mathbf{E}^l(\mathbf{x}) = (x_3 - x_2 + t, x_1 - x_3 + t, x_2 - x_1 + t).$$

The vector field \mathbf{E}^l is regular enough in order to neglect the error of the space discretization. Therefore the mesh consisting of only 6 elements ($h = \sqrt{3}$) can be used. This results in extremely fast computations.

After numerous experiments, we picked the reference values of the parameters of the method which are the most favourable in order to speed up the computations without loss of accuracy. The length $\tau = 0.005$ of the time step gives reasonable results in short computational time. The higher the exponent p in the nonlinearity \mathbf{J} , the faster and more precise the computation of the problem. This follows from the condition (8.25) and the fact that $p \rightarrow \infty$ corresponds to the linear problem (non-superconducting metal). Therefore, $p = 1.2$ is used as reference value. From the condition (8.26) it follows that γ close to zero will result in faster convergence of the method. But from (8.25) we deduce that in

order to minimize the error, the parameter γ cannot be too close to zero and $\gamma < 0.5$ must hold. Nevertheless, the experiments show that the combination of $\gamma = 0.75$ with $\eta = 4$ is also applicable. This indicates that the estimate (5.40) is probably not optimal and is also valid for higher powers of τ . Some new results in [65] sustain this hypothesis. After several experiments (Fig. 8.4) we decided to choose the pair $\gamma = 0.4$ and $\eta = 4$ which gives fast (as γ is near 0) and stable (as $\eta > 1 + \gamma$) results. Once the reference values are known, the evolution of the relative error $\|\bar{\mathbf{u}}_n^h - \mathbf{E}\|_{\mathbf{K}}/\|\mathbf{E}\|_{\mathbf{K}}$ for different values of the parameters can be studied.

If γ is close to zero, the auxiliary vector field \mathbf{J}_τ differs from the non-Lipschitz continuous vector field \mathbf{J} in a remarkably wide area. For $\gamma = 0.002$, $p = 1.2$ and $\tau = 0.005$ we get

$$\mathbf{J}(\mathbf{E}^l) - \mathbf{J}_\tau(\mathbf{E}^l) = \begin{cases} (|\mathbf{E}^l|^{-1/p} - \tau^{-\gamma}) \mathbf{E}^l, & |\mathbf{E}^l| < \tau^{p\gamma} = 0.005^{1.2 \times 0.002} \doteq 0.987, \\ 0, & |\mathbf{E}^l| \geq \tau^{p\gamma} \doteq 0.987. \end{cases}$$

On the other hand, if $\gamma = 0.4$ the 'cut-off' value is equal to $\tau^{p\gamma} \doteq 0.079$. Logically, the error of the method increases, if the norm of the exact solution lies between 0 and L_τ^{-p} (in the considerable part of the domain) (Figure 8.5). The black cross on Figure 8.5 represents the moment in time, when the norm of the exact solution \mathbf{E}^l exceeds 0.987. Thanks to the fixed-point principle, which ensures the robustness of the method, the error starts to decrease already before the exact solution leaves the "problematic" region completely. This is also in agreement with the theoretically obtained condition (8.25).

Experimentally obtained dependence of the relative error on the exponent p is even better than that predicted by Theorem 8.8 as it can be fitted by a function of the form $f(p) = C_1 \tau^{k\gamma(p-1)} + C_2$ for $k > 1$ (Figure 8.6).

The relative error decreases linearly with decreasing length τ of the time step (Figure 8.7). This is again a better result than the one obtained by the theoretical analysis of the method.

In order to study the dependence of the method on the used mesh, we study the problem (8.27) with the exact solution

$$\mathbf{E}^s(\mathbf{x}) = (\sin(x_2) - \sin(x_3) + t, \sin(x_3) - \sin(x_1) + t, \sin(x_1) - \sin(x_2) + t).$$

The vector field \mathbf{E}^s belongs to $\mathbf{H}^2(\mathbf{curl}; \Omega)$ but cannot be interpolated by Whitney's elements precisely. The precision of the interpolation is plotted on Figure 8.8 by \blacktriangle (in $\mathbf{L}_2((0, 1), \mathbf{L}_2(\Omega))$ -norm). The relative error of the method decreases proportionally to h^2 as predicted in Theorem 8.8. This phenomenon

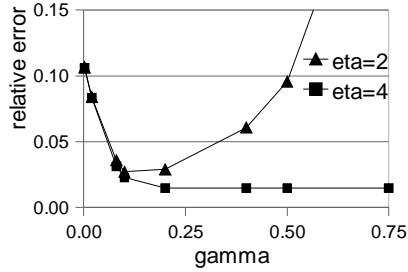


Figure 8.4: The relative error $\|\bar{\mathbf{u}}_n^h - \mathbf{E}^l\|_{\mathbf{K}} / \|\mathbf{E}^l\|_{\mathbf{K}}$, where $\bar{\mathbf{u}}_n^h$ is the solution to the scheme (8.15)–(8.16). Considering the following parameters fixed: $h = \sqrt{3}$, $p = 1.2$ and $\tau = 0.005$, we observed that the computational speed can be increased by choosing small γ and small η . However, this comes at the price of an increased relative error.

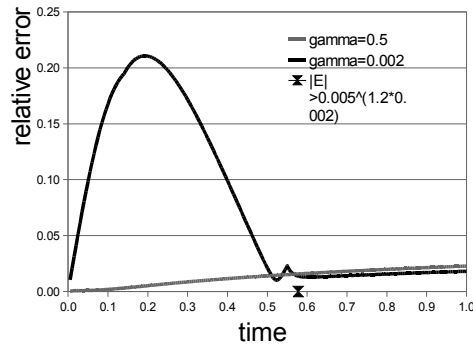


Figure 8.5: The influence of the parameter γ on the evolution of the relative error $\|\bar{\mathbf{u}}_n^h - \mathbf{E}^l\| / \|\mathbf{E}^l\|$ in time. $\bar{\mathbf{u}}_n^h$ is the solution to the scheme (8.15)–(8.16). We consider $h = \sqrt{3}$, $p = 1.2$, $\tau = 0.005$ and $\eta = 4$. The black cross represents the moment in time when everywhere in the domain the norm of the exact solution exceeds the value of L_{τ}^{-p} ($\gamma = 0.002$).

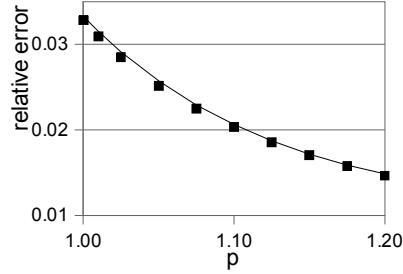


Figure 8.6: The relative error $\|\bar{\mathbf{u}}_n^h - \mathbf{E}^l\|_{\mathbf{K}} / \|\mathbf{E}^l\|_{\mathbf{K}}$, where $\bar{\mathbf{u}}_n^h$ is the solution to the scheme (8.15)–(8.16). We use $h = \sqrt{3}$, $\tau = 0.005$, $\eta = 4$, $\gamma = 0.4$ and the linear exact solution. Experimentally obtained dependence of the relative error on the exponent p (■) can be fitted by the function $f(p) = \tau^{3.7\gamma(p-1)}/43 + 0.01$ (—).

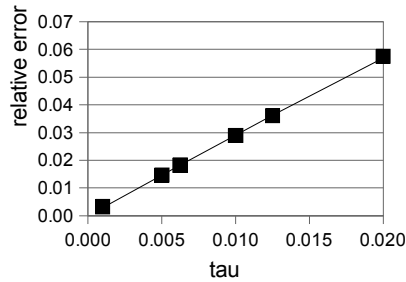


Figure 8.7: The relative error $\|\bar{\mathbf{u}}_n^h - \mathbf{E}^l\|_{\mathbf{K}} / \|\mathbf{E}^l\|_{\mathbf{K}}$ depends linearly on the length τ of the time step. Here, $\bar{\mathbf{u}}_n^h$ is the solution to the scheme (8.15)–(8.16). We use $h = \sqrt{3}$, $p = 1.2$, $\eta = 4$ and $\gamma = 0.4$.

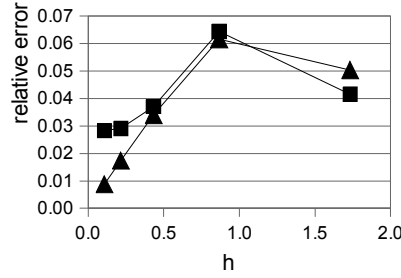


Figure 8.8: The dependence of the relative error $\|\bar{\mathbf{u}}_n^h - \mathbf{E}^s\|_{\mathbf{K}}/\|\mathbf{E}^s\|_{\mathbf{K}}$ on the parameter h (■) seems to be of the second order. Here, $\bar{\mathbf{u}}_n^h$ is the solution to the scheme (8.15)–(8.16). The discretization error $\|\mathbf{E}_0 - r_h \mathbf{E}_0\|_{\mathbf{K}}$ (▲) is the lowest eligible error to be obtained on the mesh with characteristic h . The computations are not reliable if h is too large. Too few DOFs mislead the results if the non-linear exact solution is considered. We use $p = 1.2$, $\tau = 0.005$, $\eta = 4$ and $\gamma = 0.4$.

is however very difficult to study deeply as the computations are slow for small h and only the values $h = \sqrt{3}/2^k$ are allowed by our software.

8.3 Conclusions

We have proven theoretically and tested on numerical examples that the proposed linear approximation schemes (8.1)–(8.2) and (8.15)–(8.16) converge to the solution of the nonlinear PDE describing the diffusion of the electric field in type-II superconductors. Yet, the error of the approximation scheme (8.15)–(8.16) converges to zero only if the length τ of the time step tends to zero slower than the characteristic h of the mesh.

The convergence of the approximation schemes seems to be even faster than predicted by theoretical analysis. However, the numerical experiments can be influenced by the choice of the exact solution. Therefore, before one tries to improve the error estimate, more extensive numerical experiments should be worked out. As the method is based on the fixed-point principle, it is not fast. Several hundreds of internal iterations are needed in order to reach the stopping criterion (8.16). The fixed-point principle however implies robustness and stability of the method.

APPENDIX

A. Basic algebraic inequalities

Here follows a list of some vector identities frequently used in the proofs. We suppose that $p, q \geq 1$ and

$$\frac{1}{p} + \frac{1}{q} = 1.$$

Hölder's inequality

$$(f, g) \leq \|f\|_p \|g\|_q$$

Cauchy-Schwartz's inequality

$$(f, g) \leq \|f\| \|g\|$$

Young's inequality

$$fg \leq \frac{f^p}{p} + \frac{g^q}{q}$$

Inequality without name

$$(a + b)^\alpha \leq \max\{1, 2^{\alpha-1}\} (a^\alpha + b^\alpha), \quad \alpha \geq 1$$

Abel's summation

$$\sum_{i=1}^m b_i(a_i - a_{i-1}) = b_m a_m - b_0 a_0 - \sum_{i=1}^m a_{i-1}(b_i - b_{i-1})$$

Vector identity without name

$$(\mathbf{a} \times \mathbf{b}) \times \mathbf{c} = (\mathbf{a} \cdot \mathbf{c})\mathbf{b} - (\mathbf{a} \cdot \mathbf{b})\mathbf{c}$$

B. Newton's method

Newton's method [67, p.269] is a well known tool to solve nonlinear equations of the form

$$F(x) = 0, \quad x \in X.$$

It is an iterative process. One starts with an initial guess x_0 , which has to be close enough to the solution x , then computes d_0 as a solution of linear equation

$$DF(x_0)d_0 = F(x_0), \quad d_0 \in X$$

and sets $x_1 = x_0 - d_0$. Here $DF(x)d$ denotes the derivative of the operator F in the point x and direction d . The method proceeds for each $k > 0$ by finding $d_k \in X$ such that

$$DF(x_k)d_k = F(x_k)$$

and setting $x_{k+1} = x_k - d_k$ until residual d_k is small enough.

LIST OF FIGURES

1.1	The dependence of the resistivity on the temperature for a non-superconducting metal and a superconductor.	2
1.2	The current-voltage characteristic: for a non-superconducting metal defined by the Ohm's law, for a superconductor defined by Bean's critical-state model or the power law.	4
1.3	The sketch of the dependence of the current density \mathbf{J} on the electric field \mathbf{E} used in our model.	6
1.4	Overview of results.	12
4.1	How to compute the scalar product $\nabla w_0 \cdot \boldsymbol{\tau}_e$	34
5.1	The relative error of the approximation scheme (5.6) increases remarkably with p approaching 1.2. ($\tau = 0.002$, the linear exact solution is considered and the mesh has 98 DOFs)	62
5.2	The dependence of the relative error of the scheme (5.6) on the parameter p for two different meshes. ($\tau = 0.002$ and the exact solution is given by (5.44)).	64
6.1	Auxiliary figure to deduce the value of M in Lemma 6.3.	73
6.2	The relative error of the scheme (6.5) depending on the number of iterations. The nonlinear term is given by (6.20) and sinusoidal exact solution is considered. (4184 DOFs)	82

6.3	The relative error of the scheme (6.12) depending on the number of iterations. The nonlinear term is given by (6.24) and the sinusoidal exact solution is considered. (4184 DOFs)	84
8.1	The evolution of the relative error of the scheme (8.1)–(8.2) in time for different values of p . ($h = \sqrt{3}$, $\tau = 0.005$, $\eta = 4$ and the linear exact solution is considered.)	108
8.2	The relative error of the scheme (8.1)–(8.2) for different values of η . ($h = \sqrt{3}$, $p = 1.2$, $\tau = 0.005$ and the linear exact solution is considered.)	108
8.3	The dependence of the relative error of the scheme (8.1)–(8.2) on τ . ($h = \sqrt{3}$, $p = 1.2$, $\eta = 4$ and the linear exact solution is considered.)	109
8.4	The relative error of the scheme (8.15)–(8.16) for different values of η and γ . ($h = \sqrt{3}$, $p = 1.2$ and $\tau = 0.005$ and the linear exact solution is considered.)	119
8.5	The influence of γ on the evolution of the relative error of the scheme (8.15)–(8.16). ($h = \sqrt{3}$, $p = 1.2$, $\tau = 0.005$, $\eta = 4$ and the linear exact solution is considered.)	119
8.6	The relative error of the scheme (8.15)–(8.16) for different values of p . ($h = \sqrt{3}$, $\tau = 0.005$, $\eta = 4$, $\gamma = 0.4$ and the linear exact solution is considered.)	120
8.7	The relative error of the scheme (8.15)–(8.16) depends linearly on the length τ of the time step. ($h = \sqrt{3}$, $p = 1.2$, $\eta = 4$, $\gamma = 0.4$ and the linear exact solution is considered.)	120
8.8	The dependence of the relative error of the scheme (8.15)–(8.16) on h seems to be of second order. ($p = 1.2$, $\tau = 0.005$, $\eta = 4$, $\gamma = 0.4$ and sinusoidal exact solution is considered.)	121

LIST OF TABLES

5.1	Some characteristics of the used meshes.	60
5.2	The dependence of the relative error of the scheme (5.6) on the choice of the time step τ and the mesh. The error decreases with decreasing length of the time step. ($p = 2$ and the linear exact solution (5.43) is considered.)	62
5.3	The relative error of the scheme (5.6) increases if p approaches 1. The higher the number of DOFs the smaller the final error. The linear exact solution is considered.	62
5.4	The dependence of the relative error of the scheme (5.6) on the choice of the length of the time step. ($p = 2$ and the exact solution is given by (5.44))	63
5.5	The relative error of the scheme (5.6) for two values of the exponent p : $p = 1.2$ and $p = 1.143$. Two different meshes are used: with 98 DOFs and with 604 DOFs. The method is extremely slow if p is close to 1. Some calculations were even not realized because of the unbearable time consumption. The sinusoidal exact solution is considered.	64
5.6	The relative error of the backward Euler method applied to the problem (5.45) with linear exact solution. Coarser mesh provides better results. The method diverges for some combinations of parameters. ($n = 6$ and $n = 8$ which corresponds to $p = 1.2$ and $p = 1.143$, and two different meshes are used)	66

5.7	The relative error of the backward Euler method applied to the problem (5.45) with sinusoidal exact solution. Shorter time step does not always deliver better results. ($n = 6$ and $n = 8$ which corresponds to $p = 1.2$ and $p = 1.143$, and three different meshes are used.	66
6.1	The evolution of the relative error of the linear approximation scheme (6.5) employed to the problem (6.21) with the linear exact solution depending on the number of iterations. The nonlinearity is given by (6.20). (98 DOFs)	81
6.2	The evolution of the relative error of the linear approximation scheme (6.5) employed to the problem (6.21) with sinusoidal exact solution (6.23) depending on the number of iterations. The nonlinearity is given by (6.20). (4184 DOFs)	81
6.3	The evolution of the relative error of the linear approximation scheme (6.12) to the problem (6.21) with sinusoidal exact solution (6.23) depending on the number of iterations. The nonlinearity is given by (6.24). (4184 DOFs)	83
8.1	The dependence of the relative error of the scheme (8.1)–(8.2) on h . ($p = 1.2$, $\tau = 0.005$, $\eta = 4$ and the sinusoidal exact solution is considered.)	109

INDEX

- Abel's summation, 44, **122**
- backward Euler method, **40**
- Bean's model, **4**
- Céa's lemma*, **29**
- convergence
 - strong, **21**
 - weak, **21**
- curl, **22**
- De Rham diagram, 36
- div-curl lemma*
 - steady-state, **49**
 - time-dependent, **51**
- finite elements, 27, 28, **30**
 - conforming, 27, **31**
 - Lagrange's, 28
 - unisolvant, **30**
 - Whitney's, 26, **31**
- Galerkin method, **29**
- inequalities
 - Cauchy-Schwartz, **122**
- Hölder, **122**
- Young, **122**
- interpolation operator, 29, **30**
- Kronecker's delta, **19**
- Lax–Milgram lemma*, **29**
- Maxwell's equations (eddy current version), **5**
- Meissner–Ochsenfeld effect, **2**
- Newton's method, **123**
- operator
 - coercive, **21**
 - Lipschitz continuous, 7, **20**
 - monotone, **21**
 - strictly monotone, **21**
- power law, **5**, 6
- space, 19
 - $\mathbf{H}^\alpha(\mathbf{curl}; \Omega)$, **23**
 - $\mathbf{H}(\mathbf{curl}; \Omega)$, **22**
 - \mathbf{V} , **23**

-
- dual, **19**
 - Lebesgue, **20**
 - Sobolev, **20**
 - superconductors, **1**
 - high-temperature, 3
 - type-I, 3
 - type-II, 3
-

BIBLIOGRAPHY

- [1] R.A. Adams. *Sobolev Spaces*. Pure and Applied Mathematics. Academic Press, New York, 1975.
- [2] W.H. Alt and S. Luckhaus. Quasilinear elliptic-parabolic differential equations. *Math. Z.*, 183:311–341, 1983.
- [3] J.F. Annett. *Superconductivity, Superfluids and Condensates*. Oxford Master Series in Condensed Matter Physics, Oxford University Press, 2004. ISBN-13: 978-0-19-850756-7.
- [4] C. Armouche, C. Bernardi, M. Dauge, and V. Girault. Vector potentials in three-dimensional non-smooth domains. *Math. Meth. Appl. Sci.*, 21:823–864, 1998.
- [5] G. Barnes, M. McCulloch, and D. Dew-Hughes. Computer modelling of type II superconductors in applications. *Supercond. Sci. Technol.*, 12:518–522, 1999.
- [6] J.W. Barrett and L. Prigozhin. Bean’s critical-state model as the $p \rightarrow \infty$ limit of an evolutionary p -Laplacian equation. *Nonlinear Anal., Theory Methods Appl.*, 42A(6):977–993, 2000.
- [7] Ľ. Bañas. *On dynamical micromagnetism with magnetostriction*. UGent, 2005. <http://www.ma.hw.ac.uk/~lubomir/pubs/thesis.pdf>.
- [8] C.P. Bean. Magnetization of high-field superconductors. *Rev. Mod. Phys.*, 36:31–39, 1964.
- [9] J.G. Bednorz and K.A. Müller. Possible high T_c superconductivity in the Ba-La-Cu-O systems. *Z. Phys. B - Condensed matter*, 64:189–193, 1986.
- [10] F. L. Bokose. *Optimized design of switched reluctance motors*. UGent, 2008. Phd thesis.
- [11] A. Bossavit. Numerical modelling of superconductors in three dimensions: a model and a finite element method. *IEEE Trans. Magn.*, 30:3363–3366, 1994.

-
- [12] A. Bossavit. *Computational electromagnetism. Variational formulations, complementarity, edge elements*, volume XVIII of *Electromagnetism*. Academic Press, Orlando, FL., 1998.
- [13] E.H. Brandt. Superconductors of finite thickness in a perpendicular magnetic field: strips and slabs. *Phys. Rev. B.*, 54:4246–4264, 1996.
- [14] E.H. Brandt. Universality of flux creep in superconductors with arbitrary shape and current-voltage law. *Physical Review Letters*, 76(21):40304033, 1996.
- [15] A. Buffa and P. Ciarlet Jr. On traces for functional spaces related to Maxwell’s equation. Part I: An integration by parts formula in Lipschitz polyhedra. *Math. Meth. Appl. Sci.*, 24(1):9–30, 2001.
- [16] S.J. Chapman. *Macroscopic Models of Superconductivity*. D. Phil. thesis. Oxford University, 1991. <http://www2.maths.ox.ac.uk/~chapman/>.
- [17] S.J. Chapman. A hierarchy of models for type-II superconductors. *SIAM Rev.*, 42(4):555–598, 2000.
- [18] S.J. Chapman. A hierarchy of models for superconducting thin films. *SIAM J. Appl. Math.*, 63(6):2087–2127, 2003.
- [19] P.G. Ciarlet. *The Finite Element Method for Elliptic Problems*, volume 4 of *Studies in Mathematics and its Applications*. North-Holland, New York, 1978.
- [20] P. Ciarlet Jr. and Zou Jun. Fully discrete finite element approaches for time-dependent Maxwell’s equations. *Numer. Math.*, 82:193–219, 1999.
- [21] I. Cimrák. *On the Landau–Lifshitz equation of ferromagnetism*. UGent, 2005. <http://cage.ugent.be/~cimo/thesis/thesis.pdf>.
- [22] C.W. Crowley, P.P. Silvester, and H. Hurwitz. Covariant projection elements for 3D vector field problems. *IEEE Transactions on Magnetics*, 24:397–400, 1988.
- [23] L. Demkowicz. *Computing with hp-adaptive finite elements*, volume 2 of *Thèse de l’Ecole Polytechnique*. Chapman & Hall/CRC Applied Mathematics and Nonlinear Science Series. Boca Raton, FL: Chapman & Hall/CRC., 2007.
- [24] J. Duron et al. Modelling the E – J relation of the high- T_c superconductors in an arbitrary current range. *Physica C*, 401:231–235, 2004.
- [25] Ch. Elliott and Y. Kashima. A finite-element analysis of critical-state models for type-II superconductivity in 3D. *IMA J Numer Anal*, 27:293–331, April 2007.
- [26] L. C. Evans. *Partial differential equations*, volume 19 of *Graduate Studies in Mathematics*. American Mathematical Society, 1998.
- [27] L.C. Evans. *Weak convergence methods for nonlinear partial differential equations*, volume 74 of *Conference Board of the Mathematical Sciences. Regional Conference Series in Mathematics*. American Mathematical Society, Providence, RI, 1990. ISBN 0-8218-0724-2.
-

-
- [28] D. Gilbarg and N. S. Trudinger. *Elliptic partial differential equations of second order*, volume 224 of *Grundlehren der Mathematischen Wissenschaften*. Springer, 1977.
- [29] V. Girault. Incompressible finite element method for Navier–Stokes equations with nonstandard boundary conditions in \mathbb{R}^3 . *Math. Comp.*, 51:55–74, 1988.
- [30] V. Girault and P.A. Raviart. *Finite Element Methods for Navier–Stokes Equations*. Springer, New York, 1986.
- [31] F. Grilli et al. Finite-element method modeling of superconductors: from 2-D to 3-D. *IEEE Trans. Appl. Supercond.*, 15:17–25, 2005.
- [32] A. Gurevich and M. Friesen. Nonlinear transport current flow in superconductors with planar obstacles. *Physical Review B*, 62(6):4004–4025, 1 August 2000-II.
- [33] B. Heise. Analysis of a fully discrete finite element method for a nonlinear magnetic field problem. *SIAM Journal on Numerical Analysis*, 31(3):745–759, 1994.
- [34] W. Jäger and J. Kačur. Approximation of degenerate elliptic-parabolic problems by nondegenerate elliptic and parabolic problems. *University Heidelberg*, 1991. Preprint.
- [35] W. Jäger and J. Kačur. Solution of porous medium systems by linear approximation scheme. *Numer. Math.*, 60:407–427, 1991. Proc. 2nd World Congress of Nonlinear Analysts.
- [36] W. Jäger and J. Kačur. Solution of doubly nonlinear and degenerate parabolic problems by relaxation schemes. *Nonlinear Analysis Theory, Methods & Applications*, 29(5):605–627, 1995.
- [37] E. Janíková and M. Slodička. Fix-point linearization schemes for nonlinear steady-state eddy current problems. *Mathematical Methods in the Applied Sciences*, 30(14):1697–1704, 2007.
- [38] E. Janíková and M. Slodička. A robust linearization scheme for nonlinear diffusion in type-II superconductors. *Applied Mathematical Modelling*, 32(10):1933–1940, 2007. doi: 10.1016/j.apm.2007.06.023.
- [39] E. Janíková and M. Slodička. Fully discrete linear approximation scheme for electric field diffusion in type-II superconductors. In *ACOMEN*, 2008.
- [40] E. Janíková and M. Slodička. Variations of div-curl lemma in nonlinear electromagnetism. In *NumAn*, 2008.
- [41] J. Jost. *Partial Differential Equations*, volume 214 of *Graduate Texts in Mathematics*. Springer–Verlag, New York, 2002.
- [42] H. Kamerlingh Onnes. Further experiments with liquid helium. on the change of the electrical resistance of pure metal at very low temperatures. *Leiden Comm.* 120b:3–5, April 1911.
-

-
- [43] J. Kačur. *Method of Rothe in evolution equations*, volume 80 of *Teubner Texte zur Mathematik*. Teubner, Leipzig, 1985.
- [44] J. Kačur. Solution of degenerate parabolic systems by relaxation schemes. *Nonlinear Analysis Theory, Methods & Applications*, 30(7):4629–4636, 1997. Proc. 2nd World Congress of Nonlinear Analysts.
- [45] J. Kačur. Solution of some free boundary problems by relaxation schemes. *SIAM J. Numer. Anal.*, 36(1):290–316, 1999.
- [46] J. Kačur. Solution to strongly nonlinear parabolic problems by a linear approximation scheme. *IMA Journal of Numerical Analysis*, 19:119–145, 1999.
- [47] J. Kačur and S. Luckhaus. Approximation of degenerate parabolic systems by nondegenerate elliptic and parabolic systems. *Applied Numerical Mathematics*, 26:307–326, 1998.
- [48] I. Kossaczky. A recursive approach to local mesh refinement in two and three dimensions. *J. Comput. Appl. Math.*, 55:275–288, 1994.
- [49] A. Kufner, O. John, and S. Fučík. *Function Spaces*. Monographs and textbooks on mechanics of solids and fluids. Noordhoff International Publishing, Leyden, 1977.
- [50] G. Lousberg, M. Ausloos, C. Geuzaine, P. Dular, and B. Vanderheyden. Simulation of the highly non linear properties of bulk superconductors: finite element approach with a backward Euler method and a single time step. In *ACOMEN*, 2008.
- [51] I.D. Mayergoyz. *Nonlinear diffusion of electromagnetic fields with applications to eddy currents and superconductivity*. Academic Press, San Diego, 1998.
- [52] P. Monk. Analysis of a finite element method for Maxwell’s equations. *SIAM J. Numer. Anal.*, 29(3):714–729, 1992.
- [53] P. Monk. *Finite element methods for Maxwell’s equations*. Numerical Mathematics and Scientific Computation. Clarendon Press, Oxford, 2003.
- [54] F. Murat. Compacité par compensation. *Ann. Sc. Norm. Super. Pisa, Cl. Sci., IV. Ser.* 5, pages 489–507, 1978.
- [55] J.C. Nédélec. Mixed finite elements in \mathbb{R}^3 . *Numer. Math.*, 35:315–341, 1980.
- [56] L. Prigozhin. The Bean model in superconductivity: Variational formulation and numerical solution. *J. Comput. Phys.*, 129(1):190–200, 1996.
- [57] Hiptmair R. Finite elements in computational electromagnetism. *Acta Numerica*, 11:237–339, 2002.
- [58] J. Rhyner. Magnetic properties and AC losses of superconductors with power-law current-voltage characteristics. *Physica C*, 212:292–300, 1993.
-

-
- [59] A. Schmidt and K.G. Siebert. *Design of Adaptive Finite Element Software, the Finite Element Toolbox ALBERTA*, volume 42 of *Lecture Notes in Computational Science and Engineering*. Springer, Berlin, 2005.
- [60] M. Sjöström. *Hysteresis modelling of high temperature superconductors*. Swiss Federal Institute of Technology Lausanne. Lausanne, EPFL, 2001. Thesis No 2372.
- [61] M. Slodička. Nonlinear diffusion in type-II superconductors. *Journal of Computational and Applied Mathematics*, 215(2):568–576, 1 June 2008. doi:10.1016/j.cam.2006.03.055.
- [62] M. Slodička. A robust and efficient linearization scheme for doubly nonlinear and degenerate parabolic problems arising in flow in porous media. *SIAM J.Sci.Comput.*, 23:1593–1614, 2002.
- [63] M. Slodička. A robust linearisation scheme for a nonlinear elliptic boundary value problem: Error estimates. *ANZIAM J.*, 46:449–470, 2005.
- [64] M. Slodička. A time discretization scheme for a non-linear degenerate eddy current model for ferromagnetic materials. *IMA Journal of Numerical Analysis*, 26:173–187, 2006.
- [65] M. Slodička and J. Buša, Jr. Error estimates for the time discretization for nonlinear maxwell’s equations. *Journal of Computational Mathematics*, 2008. Accepted for publication.
- [66] M. Slodička and E. Janíková. Convergence of the backward Euler method for type-II superconductors. *J. Math. Anal. Appl.*, 342(2):1026–1037, 15 June 2008. doi:10.1016/j.jmaa.2007.12.043.
- [67] J. Stoer and R. Bulirsch. *Introduction to numerical analysis*, volume 12 of *Texts in applied mathematics*. Springer, 1993. second edition.
- [68] L. Tartar. Compensated compactness and applications to partial differential equations. Nonlinear analysis and mechanics: Heriot-Watt Symp., Vol. 4, Edinburgh 1979, Res. Notes Math. 39, 136–212 (1979).
- [69] I. Terrasse. *Résolution mathématique et numérique des équations de Maxwell stationnaires par une méthode de potentiels retardés*. Thèse de l’Ecole Polytechnique. CMAP, 91128 Palaiseau Cedex, France, 1993.
- [70] M.M. Vajnberg. *Variational method and method of monotone operators in the theory of nonlinear equations*. John Wiley & Sons, Chichester, 1973.
- [71] J. Šouc, F. Gömöry, and E. Janíková. I – V curve of Bi-2223/Ag tapes in overload conditions determined from AC transport data. *Physica C*, 401:75–79, 2004.
- [72] H. Whitney. *Geometric integration theory*. Princeton University Press, 1957.
- [73] H.-M. Yin, B.Q. Li, and J. Zou. A degenerate evolution system modeling Bean’s critical-state type-II superconductors. *Discrete Conti. Dyn. Syst.*, 8:781–794, 2002.
-

- [74] K. Yosida. *Functional Analysis*. Springer-Verlag, Berlin-Heidelberg, 1965.
-